INFORMATION TO USERS

This manuscript has been reproduced from the microfilm master. UMI films the text directly from the original or copy submitted. Thus, some thesis and dissertation copies are in typewriter face, while others may be from any type of computer printer.

The quality of this reproduction is dependent upon the quality of the copy submitted. Broken or indistinct print, colored or poor quality illustrations and photographs, print bleedthrough, substandard margins, and improper alignment can adversely affect reproduction.

In the unlikely event that the author did not send UMI a complete manuscript and there are missing pages, these will be noted. Also, if unauthorized copyright material had to be removed, a note will indicate the deletion.

Oversize materials (e.g., maps, drawings, charts) are reproduced by sectioning the original, beginning at the upper left-hand corner and continuing from left to right in equal sections with small overlaps.

Photographs included in the original manuscript have been reproduced xerographically in this copy. Higher quality 6" x 9" black and white photographic prints are available for any photographs or illustrations appearing in this copy for an additional charge. Contact UMI directly to order.

Bell & Howell Information and Learning
300 North Zeeb Road, Ann Arbor, MI 48106-1346 USA
800-521-0600

Methylation of the p16 CpG Island During Neoplastic Progression

David J. S. Wong

A dissertation submitted in partial fulfillment of the requirements for the degree of

Doctor of Philosophy

University of Washington

2000

Molecular and Cellular Biology Program

UMI Number: 9995453

Bell & Howell Information and Learning Company
300 North Zeeb Road
P.O. Box 1346
Ann Arbor, MI 48106-1346

In presenting this dissertation in partial fulfillment of the requirements for the Doctoral degree at the University of Washington, I agree that the Library shall make its copies freely available for inspection. I further agree that extensive copying of the dissertation is allowable only for scholarly purposes, consistent with "fair use" as prescribed in the U.S. Copyright Law. Requests for copying or reproduction of this dissertation may be referred to Bell and Howell Information and Learning, 300 North Zeeb Road, Ann Arbor, MI 48106-1346, to whom the author has granted "the right to reproduce and sell (a) copies of the manuscript in microform and/or (b) printed copies of the manuscript made from microform."

Signature 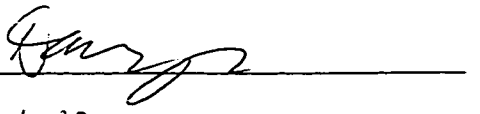

Date Sept. 22, 2000

University of Washington
Graduate School

This is to certify that I have examined this copy of a doctoral dissertation by

David J. S. Wong

and have found that it is complete and satisfactory in all respects,
and that any and all revisions required by the final
examining committee have been made.

Chair of Supervisory Committee:

Brian J. Reid

Reading Committee

Brian J. Reid

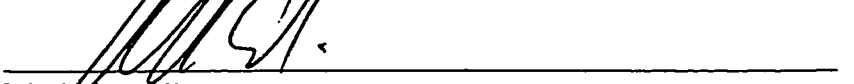

Mark Groudine

Maynard Olson

Date: 21 Sept 00

University of Washington

Abstract

Methylation of the p16 CpG Island During Neoplastic Progression

David J. S. Wong

Chairperson of the Supervisory Committee:
Professor Brian J. Reid
Departments of Genetics and Medicine

Genetic errors that alter the primary nucleotide sequence of the genome, such as mutations and deletions, are a common, but not the only, etiologic cause for the development of neoplasia. Epigenetic alterations, in particular the methylation of CpG islands, have been increasingly found to play a major role in the pathogenesis of neoplasia by transcriptionally silencing tumor suppressor genes.

$p16^{INK4a}$ is a tumor suppressor gene located on 9p21 whose protein product regulates the cell cycle and replicative senescence. Loss of heterozygosity (LOH) at 9p21 is one of the most prevalent genetic alterations in esophageal adenocarcinoma, but p16 mutations were detected in only a minority of the patients with 9p21 LOH. The majority of patients with 9p21 LOH but no p16 mutation were found to have p16 CpG island methylation, demonstrating that p16 is highly selected for inactivation in esophageal adenocarcinoma. In addition, by following the clonal evolution of neoplastic cell lineages in the premalignant Barrett's esophageal epithelium, early progenitor clones were found to have p16 inactivation (LOH and either methylation or mutation), and p16 nullizygous clones that also acquire p53 inactivation (LOH and mutation) can progress to develop ploidy abnormalities, other non-random LOH events, and cancer.

To investigate the dynamic process of de novo methylation, senescence at mortality stage 0 (M0) in primary human mammary epithelial cells (HMECs) was analyzed. The subpopulation of cells that escaped M0 were found to have methylation of the p16 CpG island and a dramatic decrease in p16 mRNA and protein levels. Analysis of the temporal development of the methylation demonstrated that the de novo methylation process is region specific and progressive. Methylation initially appeared at a subset of sites in three discrete regions of the p16 CpG island and gradually increased in density and expanded across the CpG island.

p16 lesions (methylation, mutation, and LOH) were found to be the earliest known somatic genetic/epigenetic abnormalities in the neoplastic progression of Barrett's esophagus. Barrett's epithelium was composed of p16 hemizygous cell populations that gave rise to p16 nullizygous cell populations. Both cell populations clonally expanded to occupy extensive regions of the esophagus.

TABLE OF CONTENTS

Page

List of Figures..... ii

List of Tables..... iv

List of Abbreviations..... v

Introduction..... 1

Chapter 1: $p16^{INK4a}$ CpG Island is Hypermethylated at a High Frequency in Esophageal Adenocarcinomas..... 14

Chapter 2: Evolution of Neoplastic Cell Lineages in Barrett's Esophagus..... 27

Chapter 3: Inactivation of $p16^{INK4a}$ in Human Mammary Epithelial Cells by CpG Island Methylation..... 42

Chapter 4: Progressive Region-Specific De Novo Methylation of the $p16^{INK4a}$ CpG Island in Primary Human Mammary Epithelial Cells..... 73

Chapter 5: $p16^{INK4a}$ Hemizygous Cell Populations Arise Early and Expand Clonally in Premalignant Metaplastic Esophageal (Barrett's) Epithelium..... 99

Bibliography..... 126

Appendix: DNA Methylation Analysis Flow Chart..... 145

Vita..... 146

LIST OF FIGURES

Number Page

0.1 Cell cycle regulatory mechanism of p16 and p15 11

0.2 Genomic structure and RNA processing of the $p15^{INK4b}$, $p14^{ARF}$, and $p16^{INK4a}$ genes at human chromosomal region 9p21 12

0.3 Cell cycle regulatory mechanism of $p14^{ARF}$ 13

1.1 Methylation-specific PCR analysis of the p16 CpG island in patients with Barrett's esophagus 25

2.1 Clonal evolution in patients with Barrett's esophagus *in vivo* 36

2.2 Multiple genetic routes to cancer in Barrett's esophagus 40

3.1 Analysis of different E7 proteins for their abilities to allow M0 bypass in HMEC 66

3.2 Western blots for cell cycle-related proteins in HMEC9 67

3.3 Expression of p16 in HMEC1 and HMEC3 before and after M0 68

3.4 Expression and methylation-specific PCR analyses of p16 in HMECs 69

3.5 Methylation-specific PCR analysis of p16 in E7 and E6/E7-expressing HMECs 70

4.1 Genomic map of the 5' CpG island of the p16 gene 93

4.2 Development of methylation in the p16 CpG island of HMEC9 94

4.3 Expression of p16 in HMEC9 95

4.4 Development of methylation in the p16 CpG island of HMEC4 and HMEC6 96

4.5 Individual epigenotypes at the p16 CpG island 97

5.1 Prevalence of p16 lesions in patients with Barrett's esophagus relative to histologic grade 117

5.2. p16 abnormalities and Barrett's segment length in patients without cancer..... 118

5.3. p16 abnormalities in the premalignant Barrett's epithelium from "mapped" endoscopic biopsies in patients without cancer..... 119

LIST OF TABLES

Number Page

1.1 p16 promoter region methylation in aneuploid cell populations from premalignant Barrett's epithelium and adenocarcinoma..... 26

2.1 Clonal orders in Barrett's esophagus..... 41

3.1 Effects of E6 and E7 on proliferation of HMEC in culture..... 71

3.2 p16 CpG methylation sequencing analysis of HMECs..... 72

4.1 Methylation in the p16 CpG island of HMECs..... 98

5.1 Prevalence of p15, $p14^{ARF}$, and p16 methylation in Barrett's esophagus in patients without cancer..... 124

5.2 Number of p16 Lesions in Barrett's esophagus in patients without cancer..... 125

LIST OF ABBREVIATIONS

HMEC	human mammary epithelial cell culture
HPV-16	human papillomavirus type 16
LOH	loss of heterozygosity
M0	mortality stage 0
M1	mortality stage 1
PEP	primer-extension preamplification
Rb	retinoblastoma

ACKNOWLEDGEMENTS

I wish to express my gratitude to Brian Reid for the opportunity to conduct my graduate school training and dissertation work in his laboratory. Brian is an exemplary mentor and a good friend. Our one-on-one discussions about science, medicine, and life have taught me lessons that will never be forgotten. This experience has been a privilege.

I wish to thank all of my friends in Brian's laboratory, past and present, who made work fun and contributed to this dissertation. I thank Mike Barrett for our discussions about the latest in science, for his scientific ideas and advice, for sharing a laboratory bay, and, of course, for our daily analysis of major league baseball. I thank Rissa Sanchez for always handling my laboratory requests as a high priority and for our discussions about Seattle theater and restaurants. Patty Galipeau helped me establish a novel methylation analysis method using direct sequencing. I thank her for being the best lab partner. I thank Laura Prevo for her help with database analysis and would like to acknowedge her for her work on 9p21 LOH and p16 mutation. I thank Tom Paulson for continuing the methylation project, for always reading my paper drafts, and for the golfing tips. I thank Jessica Arnaudo and Vinaya Murthy for the flow cytometric cell sorting. I thank Dave Cowan for the computer systems support. I thank Mary Kunz for the administrative support. Patty Blount and Christine Karlsen manage the care of the patients, conduct the endoscopies, and acquire the biopsies.

I thank Scott Foster and Denise Galloway for a fun and fruitful collaboration. Scott established and characterized the primary human mammary epithelial cell strains that I used to study the de novo methylation process.

I thank my excellent thesis committee, which consists of Brian, Mark Groudine, Maynard Olson, Charles Laird, and Dave Myerson, for their intellectual input into my project. I thank Brian, Mark, and Maynard for also being on my reading committee and providing helpful suggestions that has improved this written work.

I am grateful to Reinhard Stoger for his advice and Jim Herman and Steve Baylin for the control DNA, both of which helped me get started with methylation analysis.

I thank the Biotechnology Center and the Murdock Center at the Fred Hutchinson Cancer Research Center for running my sequencing gels and the Image Analysis Center for their assistance with my figures and with making slides.

I wish to thank the directors and administrators of the Medical Scientist Training Program and the Molecular and Cellular Biology Program at the University of Washington and the Fred Hutchinson Cancer Research Center.

I am grateful for my various sources of funding support, which include the Poncin Fund, the National Institute of General Medical Sciences Medical Scientist Training Program grant 5T32GM07266, the American Cancer Society grant EDT80683, and the National Cancer Institute RO1 CA61202, RO1 CA78828, and RO1 CA64795.

Chapter 1 was previously published in Cancer Research (57: 2619-22, 1997). Chapter 2 was previously published in Nature Genetics (22: 106-9, 1999). Chapter 3 was previously published in Molecular and Cellular Biology (18: 1793-801, 1998). Chapter 4 was previously published in Molecular and Cellular Biology (19: 5642-51, 1999).

I thank Ella Negrou for her patience and last-minute assistance.

Finally, I would like to thank my family for their love and support and for fostering my passion for knowledge.

DEDICATION

This dissertation is dedicated to my father,

Eugene G.C Wong.

INTRODUCTION

DNA methylation is a heritable and reversible epigenetic process that typically affects the cytosine base of CpG dinucleotides in the genome. Whereas most of the genome is free of methylation in invertebrates, almost all regions of the genome are methylated in vertebrates. The majority of the vertebrate genome (98%) is methylated at a low density because CpG dinucleotides are found at a lower than the statistically expected frequency, which is believed to be a result of the hypermutability of methylcytosines to form thymines (Bird, 1993). The remaining 2% of the vertebrate genome consists of dispersed regions of DNA typically between 200 and 1400 base pairs that are rich in CpG dinucleotides, called CpG islands. CpG islands have a G + C content greater than 50% and have the statistically expected CpG content which is more than 10 times that of the bulk DNA (Bird, 1986; Larsen et al., 1992). Approximately 45,000 CpG islands have been estimated per haploid genome in humans (Antequera and Bird, 1993). CpG islands are found associated with all housekeeping genes and about 40% of tissue-specific genes. They span at least a part of one exon, and in housekeeping genes, are biased toward the 5' end of the gene usually covering the promoter region. Unlike the rest of the genome, CpG islands are typically not methylated which is believed to contribute to the maintenance of CpG dinucleotides in these parts of the genome (Bird, 1986; Larsen et al., 1992).

De novo methylation and maintenance methylation are required for the establishment and mitotic inheritance of methylation patterns (Lei et al., 1996; Stein et al., 1982; Wigler et al., 1981). A family of DNA methytransferase enzymes is

responsible for these processes. Dnmt1, the primary maintenance methyltransferase, is specific for hemimethylated DNA, is sequestered to the DNA replication fork, and maintains methylation after each round of DNA replication by copying the methylation on the parent strands to the daughter strands (Bestor, 1992; Leonhardt et al., 1992; Li et al., 1992). On the other hand, Dnmt3a and Dnmt3b, which were recently discovered by screening EST databases for sequences containing the catalytic domain of Dnmt1, are de novo methyltransferases (Okano et al., 1998). In addition, a DNA demethylase has been recently identified that directly removes methyl groups from methylcytosines in the genome (Bhattacharya et al., 1999). The signals that recruit de novo methyltransferases or demethylases to particular regions of the genome are still unknown.

The ancestral function of DNA methylation has been hypothesized to be the neutralization of potentially damaging sequences. Over 90% of methylcytosines are found within transposons that occupy more than one third of the human genome (Yoder et al., 1997). However, the vertebrate lineage is postulated to have adapted the DNA methylation process to additionally serve as a repressor of endogenous promoters (Bird, 1993). DNA methylation of either exogenous or endogenous promoters results in stable transcriptional silencing, which is mediated by a family of methyl-CpG binding proteins that recruit histone deacetylases and the resulting change in chromatin structure (Bird and Wolffe, 1999; Knoepfler and Eisenman, 1999). Methylation of bulk DNA in the large vertebrate genomes is believed to suppress the background transcriptional noise. In addition, methylation of CpG islands can repress individual genes. Although CpG islands are typically not methylated, there are two important exceptions: imprinting, which results in expression of only alleles inherited from parents of one sex, and X-

inactivation, which is essential for dosage compensation in female mammals (Ferguson-Smith et al., 1993; Riggs and Pfeifer, 1992; Stoger et al., 1993).

DNA methylation is critical for mammalian embryonic development. Both demethylation and de novo methylation occur during gametogenesis to re-establish the parental-specific methylation tags in the CpG islands of imprinted genes, which are maintained in developing embryos and into adulthood (Chaillet et al., 1991; Stoger et al., 1993; Tremblay et al., 1995). X-inactivation is reinforced by de novo methylation of the CpG island of the Xist gene on the active X chromosome as well as the CpG islands of the genes on the inactive X chromosome during early embryonic development (Riggs and Pfeifer, 1992). In addition, a wave of global demethylation initially occurs after fertilization, followed by a wave of de novo methylation after implantation that establishes a new embryonic methylation pattern (Howlett and Reik, 1991; Kafri et al., 1992; Monk et al., 1987; Sanford et al., 1987). The significance of this reprogramming of DNA methylation in early development is unknown, but the process is essential. Mouse embryos deficient in both Dnmt3a and Dnmt3b, the de novo methyltransferases, are unable to remethylate the genome after the wave of global demethylation and die at postimplantation stages (Okano et al., 1999). Moreover, mouse embryos deficient in Dnmt1, the maintenance methyltransferase, have a reduced methylation content and die at a similar stage because of their inability to maintain the global remethylation or the parental methylation imprints (Li et al., 1992).

Aberrant DNA methylation plays a central role in a number of disease processes, including neoplasia. A decrease in the overall level of methylation in the genome, called global hypomethylation, was found to occur early in neoplastic progression (Goelz et al.,

1985). The global hypomethylation in mouse embryonic stem cells deficient in Dnmt1 results in transcription of endogenous transposons and a mutator phenotype (Chen et al., 1998; Walsh et al., 1998). However, the consequences of this epigenetic change during neoplastic progression are still poorly understood. In addition to global hypomethylation, neoplastic cells acquire hypermethylation of the normally not methylated CpG islands. The mechanism of aberrant CpG island methylation remains unclear, but may be due to dysregulation of the methylation enzymatic machinery or a loss of protective factors against de novo methylation in CpG islands. As mentioned above, CpG island hypermethylation in the promoter regions of genes directs a change in chromatin structure that results in the transcriptionally silencing of the affected gene. Through this mechanism, CpG island hypermethylation acts as an alternative to genetic abnormalities to inactivate tumor suppressor genes during neoplastic progression. The reported tumor suppressor genes that are transcriptionally silenced by aberrant CpG island hypermethylation in primary tumors continues to rise in number (Baylin et al., 1998; Jones and Laird, 1999).

$p16^{INK4a}$, a cyclin-dependent kinase inhibitor, has been found to be transcriptional silenced by aberrant CpG island methylation in a variety of primary tumors, which has provided further evidence of its role as a critical tumor suppressor gene (Gonzalez-Zulueta et al., 1995; Herman et al., 1995; Merlo et al., 1995). p16 was originally demonstrated to be a tumor suppressor gene by deletion mapping in human tumor cell lines and primary tumors which have a high frequency of deletions of the 9p21 chromosomal region. The common minimal region of 9p21 chromosomal loss included

p16, but not its related family member, $p15^{INK4b}$, that lies adjacent to p16 at the 9p21 locus (Cairns et al., 1995; Kamb et al., 1994; Nobori et al., 1994). In addition, although p16 mutations are rare in most varieties of primary tumors, somatic mutations of p16, in addition to homozygous deletions, were found at a high frequency in pancreatic adenocarcinoma and germline mutations of p16 were detected in 9p21-linked familial melanoma kindreds (Cairns et al., 1994; Caldas et al., 1994; Hussussian et al., 1994). Methylation-mediated transcriptional silencing of the p16 gene has subsequently been shown to be an important alternative mechanism during neoplastic progression in a variety of human cancers. p16 CpG island methylation correlates with loss of expression in cell lines and primary tumors, and p16 expression can be reactivated with the DNA methyltransferase inhibitor, 5-azacytidine (Gonzalez-Zulueta et al., 1995; Herman et al., 1995; Merlo et al., 1995). Thus, multiple mechanisms for p16 inactivation in primary tumors have been reported including homozygous deletion, hemizygous deletion, mutation, and methylation, although the frequency of each mechanism varies among tumor types. The incidence of p16 inactivation appears to be second only to p53 inactivation in human neoplasia (Sherr, 1996).

The tumor suppressor function of the p16 protein is dependent on its regulation of cellular progression through the G1 phase of the cell cycle. p16 was first identified as a protein associating with cyclin dependent kinase 4, CDK4, in transformed human fibroblasts and was subsequently isolated by a yeast two hybrid screen for proteins that interact with CDK4 (Serrano et al., 1993; Xiong et al., 1993). p16 binds specifically to cyclin D-dependent kinases, CDK4 and CDK6, and inhibits their association with D-type cyclins and their ability to phosphorylate the retinoblastoma protein (pRb), thereby

leading to an accumulation of hypophosphorylated pRb and arrest in G1 (Figure 0.1) (Koh et al., 1995; Lukas et al., 1995). Overexpression of p16 results in G1 arrest only in cells that have functional pRb, demonstrating that pRb mediates p16-triggered growth arrest (Koh et al., 1995; Lukas et al., 1995; Medema et al., 1995). The pRb gene is a tumor suppressor gene like the p16 gene, as evidenced by germline mutations in familial retinoblastoma and somatic deletions, mutations, and methylation in sporadic primary tumors (Wang et al., 1994). pRb negatively controls progression from G1 to S phase by forming a complex with E2F that actively represses the transcription of cell cycle genes required for this transition (Bremner et al., 1995; Weintraub et al., 1995; Zhang et al., 1999). The ability of pRb to bind to E2F and act as a transcriptional repressor is blocked by phosphorylation, enabling cells to proceed from G1 to S phase (Harbour et al., 1999; Ludlow et al., 1990; Lundberg and Weinberg, 1998; Mihara et al., 1989; Zhang et al., 2000). Thus, p16 inactivation, which occurs in neoplasia, results in higher CDK4 and CDK6 activity, functional inactivation of pRb, and an inability to control cell proliferation through the p16-pRb pathway.

At least two additional cell cycle regulators besides p16 are located at human chromosomal region 9p21: p15 and $p14^{ARF}$ (Figure 0.2). Approximately 15 to 20 kilobases centromeric of p16 lies one of its homologs, p15, which is a member of the INK4 family of cyclin-dependent kinase inhibitors that specifically bind and inhibit CDK4 and CDK6 (Figure 0.1). Through the inhibition of CDK4 and CDK6, p15 has the unique function of the INK4 cyclin-dependent kinase inhibitors of mediating transforming growth factor-β-induced arrest at G1 (Hannon and Beach, 1994;

Reynisdottir et al., 1995). p15 is commonly deleted along with p16 in tumor cell lines and primary human tumors, but p15-specific deletions or point mutations have not been reported (Jen et al., 1994; Kamb et al., 1994; Stone et al., 1995; Washimi et al., 1995). However, p15 has been shown to be inactivated by CpG island methylation in the absence of p16 methylation in gliomas and leukemias but not epithelial-derived tumors, suggesting that p15 may be a tumor suppressor gene in certain cancer types (Herman et al., 1996).

The third cell cycle gene at the 9p21 chromosomal region is $p14^{ARF}$ (known as $p19^{ARF}$ in mouse), which has its own unique promoter as well as a unique first exon (exon 1β) that is spliced to exon 2 of p16 in an alternative reading frame (Figure 0.2) (Duro et al., 1995; Mao et al., 1995; Quelle et al., 1995; Stone et al., 1995). Exon 1β is approximately 15 to 20 kilobases centromeric to the first exon of p16 (exon 1α) and thus lies directly adjacent to p15 (Figure 0.2). Thus, although their genes are overlapping, because the shared exon 2 is spliced in different reading frames, the $p14^{ARF}$ and p16 proteins share no homology. In contrast to the p16 and p15 proteins, $p14^{ARF}$ protein does not bind to or inhibit cyclin-dependent kinases but can arrest cells at both G1 and G2 (Quelle et al., 1995). $p14^{ARF}$ protein regulates p53 protein levels by binding to and sequestering MDM2 to the nucleolus, thereby inhibiting MDM2-mediated degradation of p53 and inducing p53-mediated cell cycle arrest (Figure 0.3) (Pomerantz et al., 1998; Tao and Levine, 1999; Weber et al., 1999; Zhang et al., 1998). In addition, $p14^{ARF}$ can induce a p53-independent cell cycle arrest (Carnero et al., 2000). However, neither mutations in exon 1β nor mutations in the shared exon 2 that specifically disrupts $p14^{ARF}$, have been

reported in primary human tumors. Although mutations in the shared exon 2 that affect both p16 and $p14^{ARF}$ have been found, such mutations do not appear to disrupt $p14^{ARF}$ function. Moreover, exon 1β alone has been shown to be sufficient to induce cell cycle arrest, suggesting that exon 2 may not be critical to $p14^{ARF}$ function (Quelle et al., 1997). However, $p14^{ARF}$ has its own unique promoter and CpG island that has recently been shown to be aberrantly methylated in colorectal cancer cell lines and primary colorectal carcinomas (Esteller et al., 2000; Robertson and Jones, 1998). In addition, mice with a disruption of exon 1β, similar to mice lacking the shared exon 2, are viable but develop spontaneous tumors (Kamijo et al., 1997; Serrano et al., 1996). Thus, it remains unclear whether $p14^{ARF}$ is a tumor suppressor gene. Nevertheless, p16 appears to be the only known major tumor suppressor gene at the 9p21 locus.

p16 is thought to be involved in cellular senescence because its levels are induced in senescent cells but are either low or undetectable in immortalized cells (Alcorta et al., 1996; Hara et al., 1996; Loughran et al., 1996; Noble et al., 1996; Reznikoff et al., 1996). Primary mammalian cells exhibit a finite proliferative potential in culture, and senescence is the growth arrest that terminates cellular proliferation of these cells (Hayflick, 1965). Senescent cells become larger and flattened and arrest growth with 2N DNA content in G1 or G0 but remain viable and metabolically active. Thus, senescence is a barrier to immortalization in culture (Dimri and Campisi, 1994). The following observations suggest that senescence may also occur *in vivo*. The number of population doublings that normal cells undergo in culture is inversely related to the donor's age, and the proliferative capacity of fibroblasts in culture is related to the longevity of the donor

species (Hayflick, 1976; Martin et al., 1970; Rohme, 1981; Schneider and Mitsui, 1976). In addition, the progression of cells to immortalization in culture shares many common features with the development of cancer *in vivo*, including acquiring similar genetic abnormalities (Dimri and Campisi, 1994). Thus, senescence, which limits the proliferative capacity of cells, has been hypothesized to serve as a natural barrier to neoplastic progression *in vivo*.

This dissertation describes a study to understand CpG island methylation of the p16 gene and its role in neoplastic progression. Two model systems were used in this study, one of which was primary human mammary epithelial cells in culture. Primary human mammary epithelial cells, derived from normal breast tissue, proliferate in culture until they undergo senescence at a stage called mortality stage 0 (M0) (Foster and Galloway, 1996). The second model system used in this study was Barrett's esophagus, a human premalignant condition in which a hyperproliferative metaplastic columnar epithelium has replaced the normal stratified squamous epithelium of the esophagus (Phillips and Wong, 1991). This condition develops in 10-12% of patients with chronic gastroesophageal reflux and predisposes to the development of esophageal adenocarcinoma (Hamilton et al., 1988; Phillips and Wong, 1991). Barrett's esophagus provides a unique model system for investigation of events during human neoplastic progression. Patients with Barrett's esophagus frequently present at an early stage due to symptoms of gastroesophageal reflux, such as heartburn (Phillips and Wong, 1991). In addition, because endoscopic biopsy surveillance is recommended for early detection of esophageal adenocarcinoma, events in the progression to cancer can be examined in serial biopsies. Furthermore, esophagectomy specimens from patients with

adenocarcinoma often contain surrounding premalignant epithelium from which the cancer evolved (Neshat et al., 1994). Thus, tissue samples at various stages of neoplastic progression from Barrett's esophagus to esophageal adenocarcinoma are available for analysis. Neoplastic progression of Barrett's esophagus to cancer involves cell cycle and DNA content abnormalities including increases in G1 fractions, the appearance of tetraploid (4N) populations, and the development of aneuploidy, as well as somatic genetic abnormalities, including p53 inactivation (Barrett et al., 1996; Galipeau et al., 1996; Neshat et al., 1994).

This dissertation demonstrates that de novo CpG island methylation of the p16 gene is a progressive, region-specific, and highly dynamic process. In addition, this study shows that p16 CpG island methylation and the associated escape from senescence at M0 is the earliest detected event in the progression of primary human mammary epithelial cells to an immortalized cell line. Similarly, p16 inactivation by methylation, mutation, and/or loss of heterozygosity (LOH) is the earliest detected abnormality in the progression of Barrett's esophageal epithelium to adenocarcinoma. Moreover, Barrett's epithelium is composed of a mosaic of p16 hemizygous and/or p16 nullizygous populations. Both p16 hemizygous and p16 nullizygous populations clonally expand, which lengthens the Barrett's segment in individual patients.

Figure 0.1. Cell cycle regulatory mechanism of p16 and p15. p16 and p15 are members of the INK4 family of cyclin-dependent kinase inhibitors. They bind specifically to cyclin D-dependent kinases, CDK4 and CDK6, and inhibits their association with cyclin D and their ability to phosphorylate the retinoblastoma protein ("pRb"), thereby leading to an accumulation of hypophosphorylated pRb and arrest in G1. The ability of pRb to bind to E2F and act as a transcriptional repressor is blocked by phosphorylation, enabling cells to proceed from G1 to S phase. The circle labeled "pRb" with attached circles labeled "P" represents hyperphosphorylated pRb. The circle labeled "pRb" without attached circles represents hypophosphorylated pRb. "CDK4/6" is an abbreviation for cyclin-dependent kinases 4 or 6.

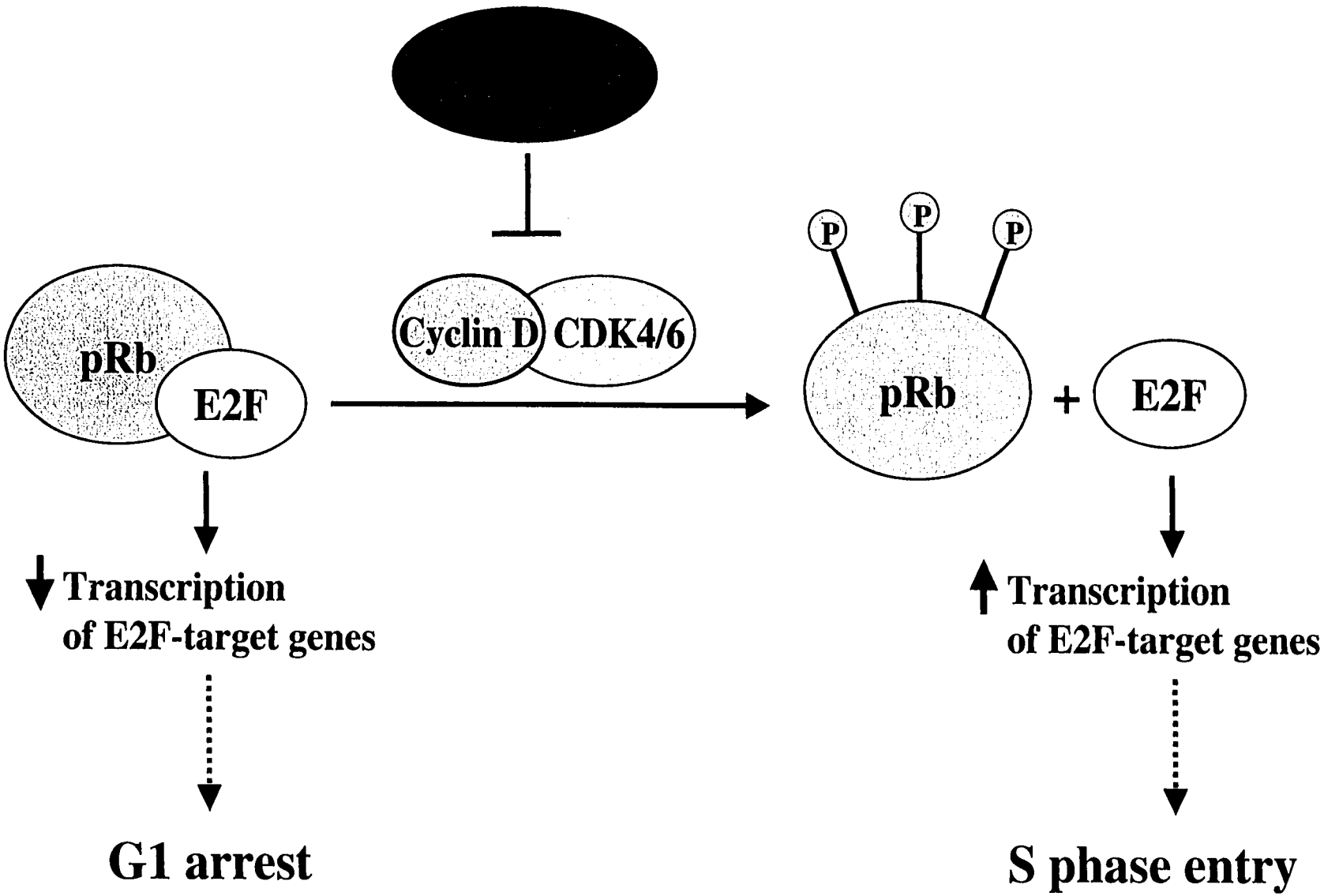
pRb
E2F
Cyclin D
CDK4/6
P
P
P
pRb
+
E2F
Transcription
of E2F-target genes
Transcription
of E2F-target genes
G1 arrest
S phase entry

Figure 0.2. Genomic structure and RNA processing of the $p15^{INK4b}$, $p14^{ARF}$, and $p16^{INK4a}$ genes at human chromosomal region 9p21. p16 and $p14^{ARF}$ share exons 2 and 3 but are coded in different reading frames. Exons 1 and 2 of p15 and exon 1 of $p14^{ARF}$ are located approximately 20 kilobases (Kb) centromeric of exon 1 of p16 and exons 2 and 3 of both p16 and $p14^{ARF}$. The exons are represented by boxes. "CpG" is an abbreviation for a CpG island located at the 5' region of each of the three genes.

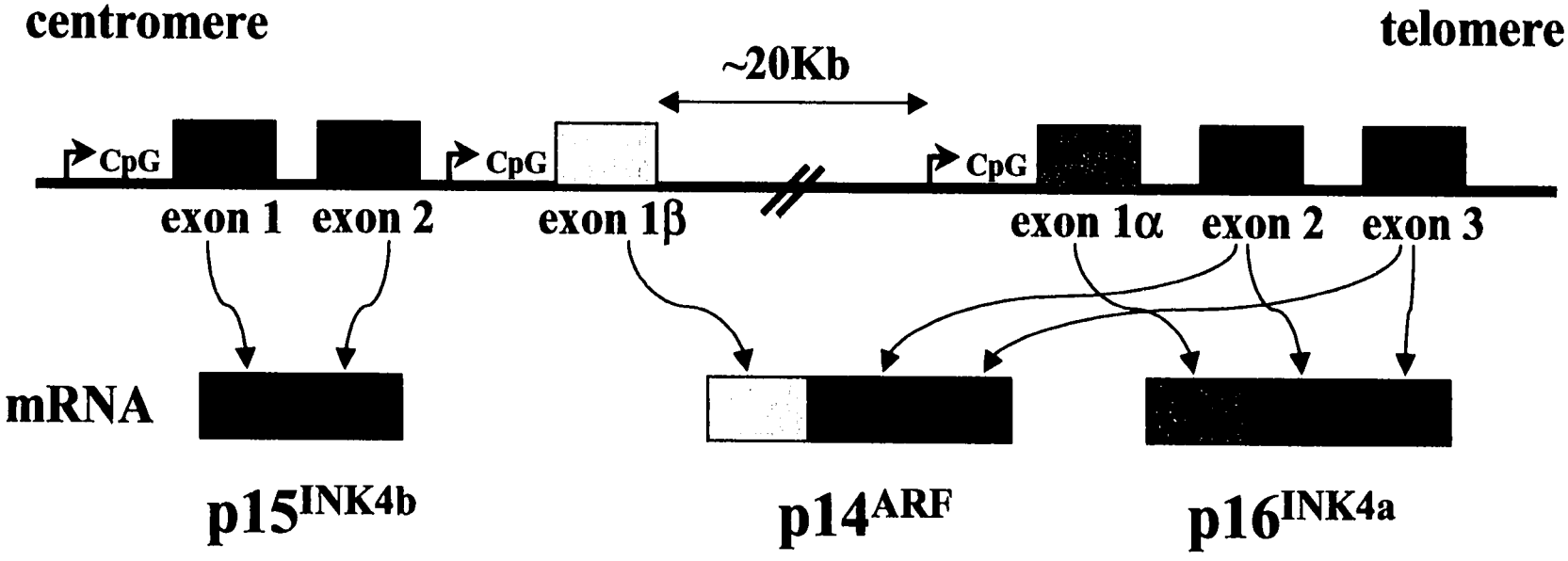
centromere
telomere
~20Kb
CpG
CpG
CpG
exon 1
exon 2
exon 1β
exon 1α
exon 2
exon 3
mRNA
p15INK4b
p14ARF
p16INK4a

Figure 0.3. Cell cycle regulatory mechanism of $p14^{ARF}$. $p14^{ARF}$ regulates p53 protein levels by binding to and sequestering MDM2 to the nucleolus, thereby inhibiting MDM2-mediated degradation of p53 and inducing p53-mediated cell cycle arrest or apoptosis.

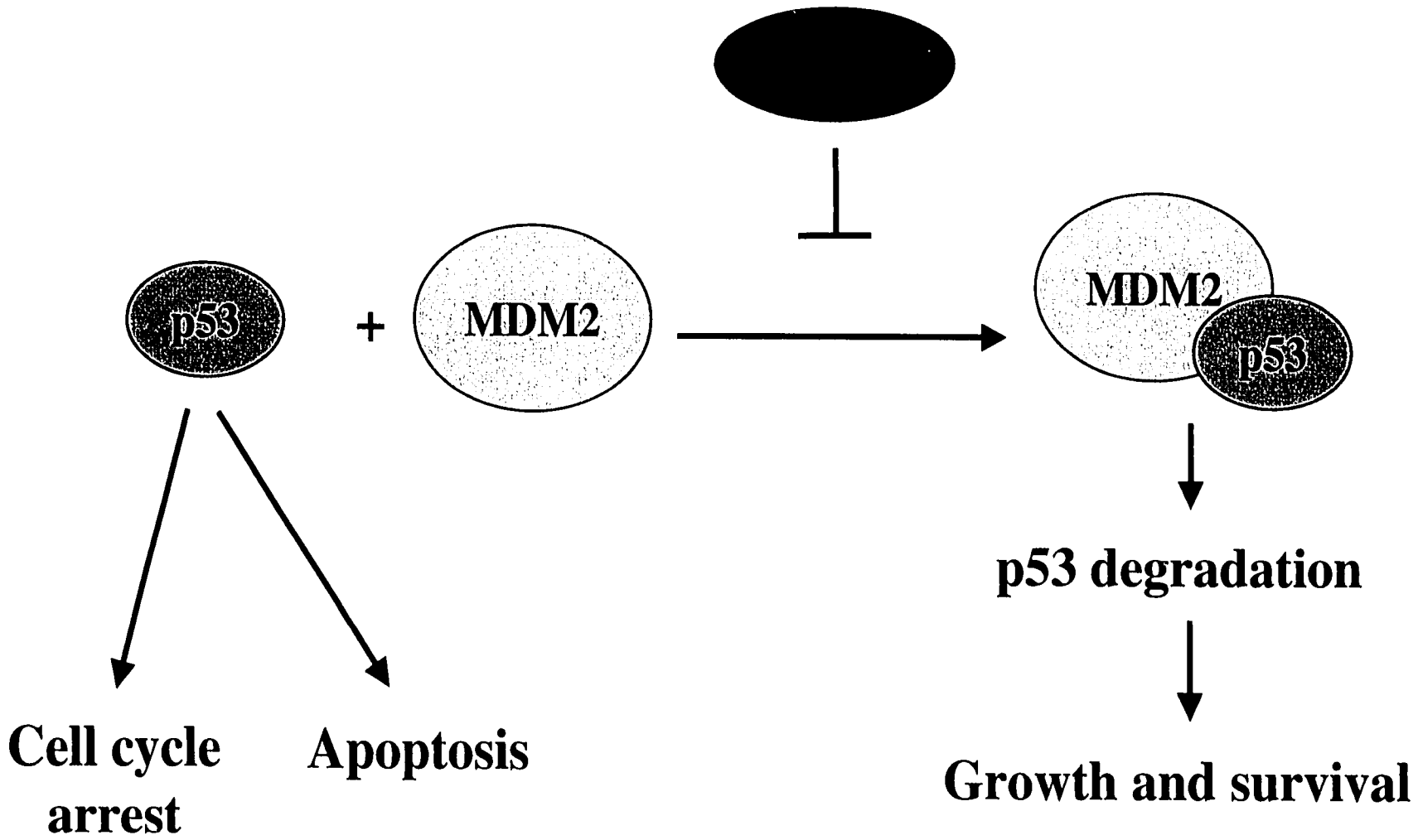
p53
+
MDM2
MDM2
p53
p53 degradation
Cell cycle arrest
Apoptosis
Growth and survival

CHAPTER 1: $p16^{INK4a}$ CpG ISLAND IS HYPERMETHYLATED AT A HIGH FREQUENCY IN ESOPHAGEAL ADENOCARCINOMAS

ABSTRACT

Loss of heterozygosity (LOH) of 9p21, which contains the $p16^{INK4a}$ tumor suppressor gene locus, is one of the most frequent genetic abnormalities in human neoplasia, including esophageal adenocarcinomas. Only a minority of Barrett's adenocarcinomas with 9p21 LOH have a somatic mutation in the remaining p16 allele, and none have been found to have homozygous deletions. To determine whether p16 promoter region hypermethylation may be an alternative mechanism for p16 inactivation in esophageal adenocarcinomas, we examined the methylation status of the p16 CpG island in flow-sorted aneuploid cell populations from 21 patients with premalignant Barrett's epithelium or esophageal adenocarcinoma. Using bisulfite modification, primer-extension preamplification and methylation-specific PCR, we demonstrate that the methylation assay can be performed on 2 ng of DNA (~275 cells). Eight of 21 patients (38%) had p16 promoter region hypermethylation and 9p21 LOH, including three patients who had only premalignant Barrett's epithelium. Our data suggest that promoter region hypermethylation with LOH is a common mechanism for inactivation of p16 in the pathogenesis of esophageal adenocarcinomas.

INTRODUCTION

9p21 LOH is a highly selected abnormality in Barrett's esophagus, previously reported in 24 of 32 patients (75%) with premalignant Barrett's epithelium or esophageal adenocarcinoma (Barrett et al., 1996). Furthermore, 9p21 LOH is an early lesion in the progression from Barrett's esophagus to adenocarcinoma, occurring before the evolution of aneuploid cell populations and cancer (Barrett et al., 1996). However, mutations in the remaining p16 allele were detected in only five of 22 patients (23%) (Barrett et al., 1996). Homozygous deletions of p16 have been reported in several types of primary tumors but were not detected in esophageal adenocarcinomas (Barrett et al., 1996; Cairns et al., 1995; Caldas et al., 1994). These results suggested that either a second tumor suppressor exists at this locus or p16 is inactivated by an alternative mechanism in esophageal adenocarcinomas. p15 mutations are rare in a variety of human tumor cell lines and primary tumors, including esophageal adenocarcinomas (Barrett et al., 1996; Jen et al., 1994; Stone et al., 1995). Thus, we tested the hypothesis that the promoter region of the remaining wild-type p16 allele is hypermethylated.

Highly purified aneuploid cell populations from Barrett's premalignant epithelium and adenocarcinomas were isolated with DNA content flow cytometric cell sorting (Reid et al., 1987). Small quantities of DNA are a major limitation for assaying highly purified flow-sorted cells from human biopsy specimens. Previous approaches for assessing methylation status, using methylation-sensitive restriction enzymes with Southern hybridization or PCR, required large amounts of DNA and were prone to false-positive results due to incomplete digestion. Bisulfite treatment of DNA, which converts all

unmethylated, but not methylated, cytosines to uracil, has provided an effective alternative to restriction enzymes, but genomic sequencing of bisulfite-modified DNA is relatively labor-intensive and time-consuming (Frommer et al., 1992). Recently, Herman *et al.* developed an efficient PCR-based assay, methylation-specific PCR, that takes advantage of DNA sequence differences between methylated and unmethylated alleles after bisulfite modification by using primers that distinguish between the two types of alleles (Herman et al., 1996).

However, the amount of DNA required for methylation-specific PCR still precludes routine analysis of flow-sorted endoscopic biopsy samples from patients with Barrett's esophagus. We now report the ability to reduce the amount of DNA necessary for the assay at least 60-fold with primer-extension preamplification (PEP), a PCR-based method for whole genome amplification using a mixture of degenerate 15-base oligonucleotide primers (Barrett et al., 1995; Zhang et al., 1992). DNA extracted from flow-sorted biopsy samples was modified with bisulfite, amplified by PEP and then amplified with the methylation-specific primers, and finally, visualized on an agarose gel.

We assessed the p16 methylation status of flow-sorted aneuploid populations from 21 patients who had Barrett's esophagus with premalignant epithelium or adenocarcinoma. Fourteen of the 21 patients had 9p21 LOH without p16 mutation, five patients had both 9p21 LOH and p16 mutation, and two patients retained both alleles at 9p21. Our results demonstrate that hypermethylation of the p16 promoter is a frequent abnormality in esophageal adenocarcinomas and that 9p21 LOH with *de novo* p16

promoter region hypermethylation is a common mechanism for the two-hit inactivation of p16.

MATERIALS AND METHODS

Patient Tissue Samples, Flow Cytometic Sorting, and DNA Extraction. The Barrett's esophagus study was approved by the Human Subjects Division of the University of Washington in 1982 and renewed annually thereafter. Endoscopic and/or surgical tissue from 21 patients who had Barrett's esophagus with premalignant epithelium or adenocarcinoma was collected using mapping protocols that have been described previously (Reid et al., 1987). Aneuploid populations were isolated by DNA content flow cytometric cell sorting using a Coulter Elite Flow Sorter as described previously (Reid et al., 1987). Gastric tissue was obtained from each patient and used as a constitutive control. DNA from the flow-sorted aneuploid samples and the gastric samples was extracted by standard SDS-proteinase K treatment. All aneuploid populations were previously screened for 9p21 LOH and p16 mutation (Barrett et al., 1996; Barrett et al., 1999).

Bisulfite Modification. Bisulfite modification protocols (Frommer et al., 1992; Herman et al., 1996) were adapted for use with small quantities of DNA (Stoger et al., 1997). Briefly, 6 ng (~800 cells) of each DNA sample were denatured, in a final volume of 20 µl, in freshly prepared NaOH at a final concentration of 0.3 M for 20 min at 42°C.

Freshly prepared 3.8 M sodium bisulfite (Sigma)/1.0 mM hydroquinone (Sigma) mixture (pH 5.0) was added to each denatured DNA sample to a final volume of 100 μl and incubated under mineral oil at 55°C for 6 to 8 h. DNA samples were then purified with the Wizard PCR Preps DNA purification resin (Promega), as specified by the manufacturer, and eluted in 50 μl of water, followed by treatment with NaOH at a final concentration of 0.3 M for 20 min at 37°C. Each DNA sample was purified by ethanol precipitation and resuspended in 20 μl of water.

PEP. Each PEP reaction contained the 20-μl bisulfite-modified DNA sample in a final volume of 60 μl. Reaction conditions used were described previously (Zhang et al., 1992). All PCR reactions were performed using a MJ DNA Engine Tetrad Thermal Cycler (MJ Research, Inc.).

Methylation-specific PCR. Primer pairs for p16 (p16-W, p16-M, p16-U) and for p15 (p15-W, p15-M, p15-U) were used for methylation-specific PCR, as described previously (Herman et al., 1996). The PCR mixture included GeneAmp PCR buffer (Perkin Elmer Corp.), $MgCl_2$ (1.5 mM), dNTPs (200 μM), primer pair (10 pmol each/reaction), 10 μl of the PEP sample, and 1.25 units of AmpliTaq Gold (Perkin Elmer Corp.) in a final volume of 25 μl. PCR reaction conditions used were as described previously (Herman et al., 1996), except for use of touchdown PCR for primer pairs p16-W and p15-W. Ten-μl aliquots of each allele-specific PCR sample were loaded onto a 2.5% agarose gel, stained

with ethidium bromide, and visualized with the Gel Documentation System 1000 (BioRad).

Statistical Analysis. The prevalence of hypermethylation in different groups was compared using Fisher's exact test.

RESULTS

We investigated whether PEP of bisulfite-modified DNA would be an accurate and efficient method by which we could reduce the starting amounts of DNA required for detection by methylation-specific PCR. To test the accuracy of methylation status results with the introduction of PEP into the protocol, we used the lung cancer cell lines H249, which is unmethylated at the p16 and p15 promoters, and H1618, which is methylated at both promoters (Herman et al., 1996). The methylation status results were identical with and without the use of PEP on the same bisulfite-treated samples of H249 and H1618 (data not shown). Without PEP, the methylation-specific PCR assay required bisulfite treatment of 120 ng of DNA (~16,000 cells) to investigate the methylation status of a single promoter region. We found that with PEP, 6 ng (~800 cells) of each DNA sample provided sufficient DNA to investigate the methylation status of three different loci. Thus, PEP enabled us to use 60-fold less DNA, without the need to design methylation-specific nested primers for each promoter region (McDonald and Kay, 1997).

We examined the methylation status of the p16 promoter in aneuploid populations from 21 patients with Barrett's esophagus that had been screened for 9p21 LOH. Nineteen of 21 patients had 9p21 LOH, and five of the 19 had p16 mutations in the remaining allele (Table 1.1). The H249 and H1618 cell lines were used as positive controls for unmethylated and methylated alleles, respectively (Figure 1.1 A and B). To test whether promoter region hypermethylation may be an alternative mechanism for inactivation of the remaining p16 allele, we initially investigated the prevalence of p16 promoter region hypermethylation in the 14 patients who had 9p21 LOH without p16 mutation (Table 1.1, patients 1-14). p16 CpG island methylation of the remaining allele was found in eight of the 14 patients (57%) (Table 1.1, patients 1-8; Figure 1.1 C and D). Three patients had p16 promoter region hypermethylation in premalignant Barrett's epithelium without cancer (Table 1.1, patients 1-3). The remaining six of the 14 patients who had 9p21 LOH without p16 mutation, were not hypermethylated at the p16 CpG island (Table 1.1, patients 9-14; Figure 1.1 E). None of the corresponding gastric samples had p16 promoter hypermethylation (Figure 1.1 C-F). The difference in prevalence of hypermethylation between Barrett's aneuploid cell populations and normal gastric tissues for these 14 patients is highly significant ($p = 0.002$). Thus, our data suggest that p16 promoter region hypermethylation is a *de novo* event that occurs at a high frequency in the pathogenesis of esophageal adenocarcinomas.

The five patients who had both 9p21 LOH and p16 mutation were found to be unmethylated at the promoter of the remaining mutant p16 allele (Table 1.1, patients 15-19; Figure 1.1 F), resulting in a significant difference in the prevalence of

hypermethylation in cases with and without p16 mutation ($p = 0.04$). Neither of the two patients without 9p21 LOH was hypermethylated at the p16 promoter (Table 1.1, patients 20 and 21). Thus, our results support the hypothesis that p16 promoter region hypermethylation is an alternative mechanism to p16 mutation for inactivation of the remaining p16 allele in cases with 9p21 LOH.

We also investigated whether p15, in addition to p16, may be a target for *de novo* hypermethylation in esophageal adenocarcinomas. In contrast to the p16 promoter, the p15 promoter was not hypermethylated in any of the 21 patients (data not shown). In the patients who had 9p21 LOH without p16 mutation, the difference between the prevalence of p16 hypermethylation (8 of 14) and p15 hypermethylation (0 of 14) is highly significant ($p = 0.002$), suggesting that p15 is not a selected target of 9p21 LOH in esophageal adenocarcinomas.

DISCUSSION

Our study has provided evidence that p16 may be inactivated in esophageal adenocarcinomas with 9p21 LOH by at least two different mechanisms: mutation or promoter region hypermethylation. Nineteen of the 21 patients with Barrett's esophagus (90%) had 9p21 LOH, and only five of these 19 patients (26%) had p16 mutations in the remaining allele (Table 1.1). However, hypermethylation of the p16 CpG island, which previously has been correlated with transcriptional silencing and decreased promoter accessibility (Costello et al., 1996; Gonzalez-Zulueta et al., 1995; Herman et al., 1995;

Merlo et al., 1995), was found in eight of the 14 patients who had 9p21 LOH without p16 mutation (57%) (Table 1.1, patients 1-8). Overall, eight of 21 (38%) patients had p16 promoter region hypermethylation, suggesting that p16 promoter region hypermethylation and 9p21 LOH is a common mechanism for inactivation of the p16 gene in esophageal adenocarcinomas. Six patients had 9p21 LOH without p16 mutation or promoter region hypermethylation of the remaining allele (Table 1.1, patients 9-14), which may indicate a second tumor suppressor gene on 9p21 or an undetected p16 mutation or deletion (Wiest et al., 1997). Nevertheless, p16 was selectively mutated or hypermethylated in 13 of 19 patients with 9p21 LOH (68%), suggesting that it is a primary target for inactivation during neoplastic progression in Barrett's esophagus.

Because the p15 gene is linked to the p16 gene at 9p21, the absence of p15 promoter region hypermethylation suggests that *de novo* hypermethylation is a selective abnormality at the p16 CpG island in Barrett's adenocarcinomas. p15 previously has been shown to be selectively inactivated in gliomas and leukemias (Herman et al., 1996; Jen et al., 1994). However, consistent with our previous mutational analysis of p15 (Barrett et al., 1996) and data from other primary tumors (Herman et al., 1996; Kamb et al., 1994; Stone et al., 1995), the lack of p15 CpG island hypermethylation in esophageal adenocarcinomas suggests that, unlike p16, p15 does not act as a tumor suppressor in Barrett's esophagus.

We have previously shown that both 9p21 LOH and p16 mutation are early genetic abnormalities in the pathogenesis of esophageal adenocarcinomas, occurring in premalignant tissue before the evolution of aneuploidy and cancer (Barrett et al., 1996;

Reid et al., 1996). The present study included 10 patients who had premalignant Barrett's epithelium without cancer. Nine of the 10 premalignant aneuploid samples had 9p21 LOH, and three of these nine had p16 promoter region hypermethylation (Table 1.1). The presence of p16 hypermethylation and 9p21 LOH in premalignant aneuploid cell populations suggests that p16 inactivation is an early event in the progression from Barrett's esophagus to adenocarcinoma. However, additional studies need to be performed to determine whether p16 hypermethylation occurs in premalignant diploid populations similar to 9p21 LOH and p16 mutation.

Human neoplastic tissue samples are characterized by cellular heterogeneity, which often limits the ability to assay for somatic genetic lesions. Therefore, we use flow cytometric cell sorting, which permits the enrichment of highly purified cell populations. We have previously shown that DNA content flow cytometry purifies aneuploid cell populations to 99% or greater homogeneity, which allows unambiguous detection of LOH and mutations (Barrett et al., 1996; Reid et al., 1987). The absence of residual normal unmethylated alleles in aneuploid cell populations with promoter region hypermethylation is consistent with the homogeneity of our flow-sorted biopsies (Figure 1.1 C and D).

PEP of bisulfite-modified DNA is an accurate and efficient method to reduce the starting amounts of DNA required for methylation-specific PCR. Only 2 ng of DNA (~275 cells) are needed to determine the methylation status at one locus with primer pairs specific for the unmethylated and methylated alleles. The combination of PEP and methylation-specific PCR will be valuable in a variety of applications in which quantities

of DNA are limited, such as in premalignant biopsies or in embryonic tissue. In addition, the use of PEP avoids the necessity of designing a set of nested primers for each locus in the genome, which will increase the efficiency of assessing methylation status at multiple loci.

In summary, we have demonstrated that p16 promoter region hypermethylation occurs at a high frequency in esophageal adenocarcinomas and that hypermethylation and LOH is a common mechanism for the inactivation of p16 in this cancer. We have also shown that p16 promoter region hypermethylation can occur in premalignant epithelium, analogous to 9p21 LOH and p16 mutation. An important question will be to determine the stage of progression to Barrett's adenocarcinomas at which p16 promoter region hypermethylation occurs.

Figure 1.1. Methylation-specific PCR analysis of the p16 CpG island in patients with Barrett's esophagus. H249 and H1618 are control cell lines that are unmethylated and methylated, respectively, at the p16 CpG island. Normal gastric tissue and Barrett's aneuploid cell populations were analyzed for each patient. Patient numbers refer to those in Table 1.1. The lane designated "mw" is the 50 bp DNA ladder (Life Technologies) with the 200 bp and 150bp bands labeled. Primer pairs used for amplification are designated as unmethylated, "U", or methylated, "M".

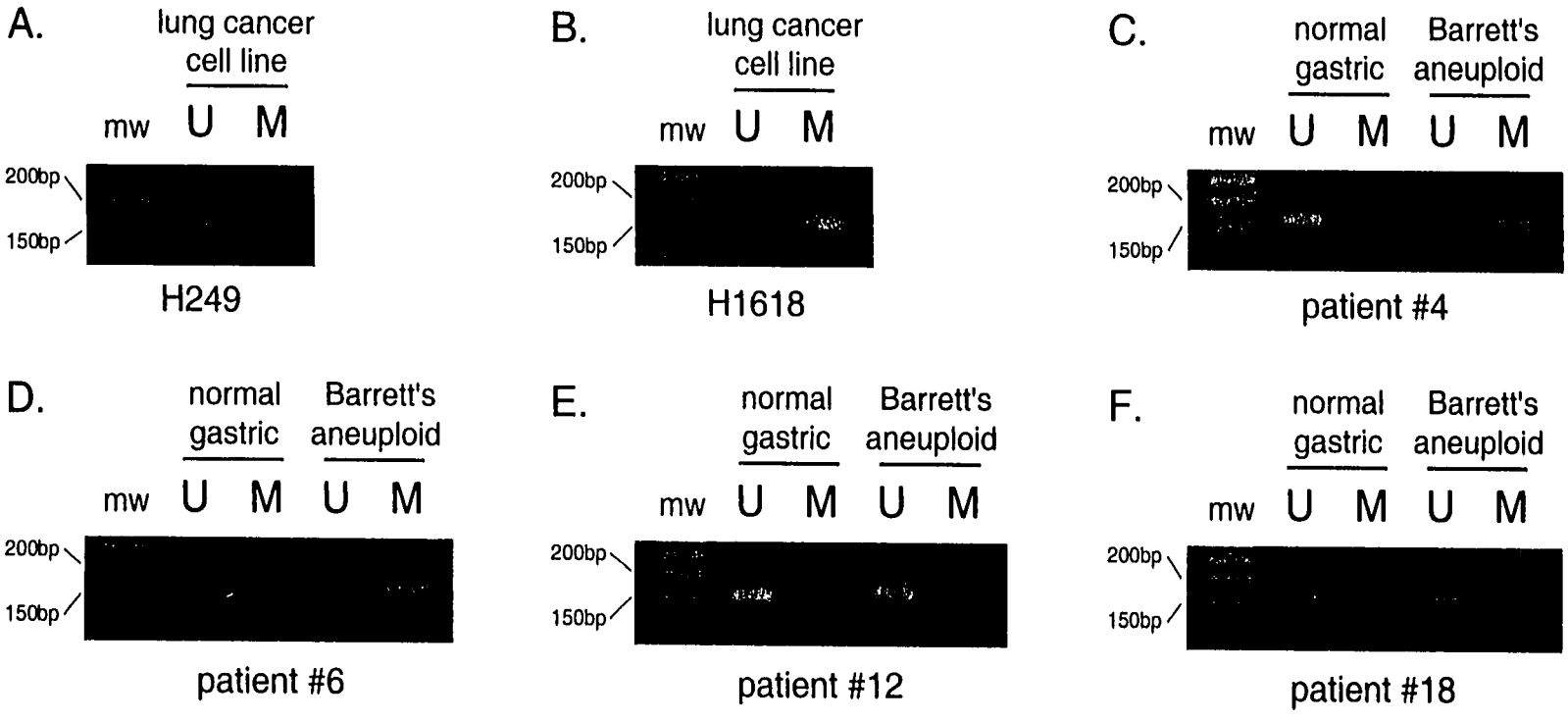
A.
lung cancer cell line
mw U M
200bp
150bp
H249
B.
lung cancer cell line
mw U M
200bp
150bp
H1618
C.
normal gastric
Barrett's aneuploid
mw U M U M
200bp
150bp
patient #4
D.
normal gastric
Barrett's aneuploid
mw U M U M
200bp
150bp
patient #6
E.
normal gastric
Barrett's aneuploid
mw U M U M
200bp
150bp
patient #12
F.
normal gastric
Barrett's aneuploid
mw U M U M
200bp
150bp
patient #18

Table 1.1. p16 promoter region methylation in aneuploid cell populations from premalignant Barrett's epithelium and adenocarcinoma

Patient		DNA content	Neoplastic stage	p16 hypermethylation
9p21 LOH/p16 wt[a]				
1.[b]	17421[c]	3.1N[d]	pre[e]	+
2.	95931	3.2N	pre	+
3.	21631	4.3N	pre	+
4.	17031	3.5N	ca[f]	+
5.	13010	2.8N	ca	+
6.	00010	3.7N	ca	+
7.	92041	3.7N	ca	+
8.	73010	3.3N	ca	+
9.	43251	3.1N	pre	-
10.	50051	3.2N	pre	-
11.	02010	2.7N	ca	-
12.	02911	3.0N	ca	-
13.	87711	3.1N	ca	-
14.	71010	3.2N	ca	-
9p21 LOH/*p16* mut[g]				
15.	18431[h]	2.9N	pre	-
16.	69421[i]	3.0N	pre	-
17.	99041[i]	3.5N	pre	-
18.	92461[j]	3.3N	pre	-
19.	10010[j]	3.9N	ca	-
9p21 het[k]				
20.	51061	3.2N	pre	-
21.	46421	3.7N	ca	-

[a] wt, wild-type
[b] patient number
[c] patient code
[d] N, ploidy
[e] pre, premalignant
[f] ca, cancer
[g] mut, mutation
[h] Codon 102, del 1
[i] Codon 58, R->stop
[j] Codon 80, R->stop
[k] het, retention of both alleles

CHAPTER 2: EVOLUTION OF NEOPLASTIC CELL LINEAGES IN BARRETT'S ESOPHAGUS

ABSTRACT

It has been hypothesized that neoplastic progression develops as a consequence of an acquired genetic instability and the subsequent evolution of clonal populations with accumulated genetic errors (Nowell, 1976). The evolution of neoplastic cell lineages has been difficult to study in individual patients because most premalignant lesions are removed when detected, precluding prospective evaluation. Barrett's esophagus is a premalignant condition which predisposes to esophageal adenocarcinoma, that can be biopsied prospectively over time because endoscopic surveillance is recommended for early detection of cancer (Levine et al., 1993; Spechler, 1987). In addition, esophagectomy specimens frequently contain the premalignant epithelium from which the cancer arose (Rabinovitch et al., 1989). Here, we determine the evolutionary relationships of non-random losses of heterozygosity (LOH), *TP53* (also known as p53) and *CDKN2A* (also known as $p16^{INK4a}$) mutations, *CDKN2A* CpG island methylation and ploidy during neoplastic progression. Diploid cell progenitors with somatic genetic or epigenetic abnormalities involving *TP53* and *CDKN2A* were capable of clonal expansion, spreading to large regions of esophageal mucosa. The subsequent evolution of neoplastic progeny frequently involved bifurcations and LOH at 5q, 13q, and 18q that occurred in no

obligate order relative to each other, DNA content aneuploidy or cancer. Our results indicate that clonal evolution is more complex than predicted by linear models.

INTRODUCTION

Human cancers and some premalignant lesions contain multiple genetic abnormalities not present in the normal tissues from which the neoplasms arose, consistent with the predictions of Nowell's model (Boland et al., 1995; Fearon and Vogelstein, 1990; Nowell, 1976). In Barrett's esophagus, neoplastic progression is associated with alterations in *TP53* (17p13 LOH and mutation) and *CDKN2A* (9p21 LOH and mutation or CpG island methylation), and non-random LOH involving chromosomes 5q, 13q, and 18q (Barrett et al., 1996; Barrett et al., 1996; Galipeau et al., 1996; Neshat et al., 1994; Wong et al., 1997). Aneuploid and/or increased 4N populations occur in greater than 90-95% of esophageal adenocarcinomas, arise in premalignant epithelium and predict progression (Galipeau et al., 1996; Reid et al., 1992; Reid et al., 1987). We have shown previously in small numbers of patients that disruption of *TP53* and *CDKN2A* typically occurs before aneuploidy and cancer (Barrett et al., 1996; Blount et al., 1994; Blount et al., 1993; Galipeau et al., 1996). In this study, we comprehensively evaluate the evolution of cell lineages with diverse abnormalities during neoplastic progression.

MATERIALS AND METHODS

Patients and tissues. We evaluated flow-sorted samples (n=266) from multiple premalignant and/or cancer biopsies (n=189) from 49 patients who had specialized columnar epithelium in esophageal biopsies, aneuploidy and a maximum diagnosis of high-grade dysplasia or cancer. None received radiation or chemotherapy prior to tissue acquisition. The Barrett's Esophagus Study was approved by the Human Subjects Review Boards at the University of Washington and the Fred Hutchinson Cancer Research Center. Patients were counseled concerning risks and benefits of endoscopic surveillance for Barrett's esophagus and informed of potential alternatives, including surgery for high-grade dysplasia. Premalignant biopsies were available from 31 patients, 25 of whom had progressed to cancer. Cancer biopsies were available from 32 patients, including 14 patients who had both premalignant and cancer biopsies available. Normal gastric tissue served as a constitutive control for each patient. This study included 10, 15 and 3 patients for whom the orders of 17p, 9p, and 18q LOH, respectively, with cancer or aneuploidy were previously reported (Barrett et al., 1996; Barrett et al., 1996; Blount et al., 1994; Blount et al., 1993).

Flow cytometric sorting. DNA content and multiparameter Ki67/DNA content flow sorting were performed as described previously (Galipeau et al., 1996; Reid et al., 1992). DNA content flow cytometry for 2N, 4N and aneuploid sorting was performed as follows. Biopsies were minced with scalpel blades in a petri dish (35x100 mm) in NST buffer (146 mM NaCl, 10 mM Tris-HCl, pH 7.5, 1 mM $CaCl_2$, 0.5 mM $MgSO_4$, 21 mM $MgCl_2$,

0.05% bovine serum albumin, 0.2% Nonidet P40 (Sigma, St. Louis, MO)) with 4,6-diamindino-2-phenylindole (DAPI; 10 ug/ml ;Boehringer Mannheim, Indianapolis, IN). To disaggregate and enucleate the cells, the suspension was forced through a 1-cc syringe with a 25-gauge needle typically 7-10 times. After mincing, samples were always kept on ice. Ki67/DNA content multiparameter flow-cytometric cell sorting was used to purify populations of proliferating diploid epithelial cells. Ki67-R-phycoerythrin is a directly conjugated proliferation-associated monoclonal antibody that identifies cells in late G_1, S, G_2 and mitosis, but not G_0. Biopsies were minced and sheared in NST buffer. Nuclei for Ki67/DNA content sorting were centrifuged at 2,000 r.p.m for 10 min at 4°C, resuspended in NST buffer with 10% normal goat serum (Caltag, Burlingame, CA), divided and incubated with Ki67-RPE (3.75 μg/ml) and IgG1-RPE isotype antibodies (DAKO, Carpinteria, CA), respectively. After incubation, samples were centrifuged as above and resuspended in NST buffer with 10% NGS and DAPI (10 μg/ml). To disaggregate the nuclei immediately before analysis, the suspension was forced through a 1-cc syringe with 25-gauge needle 7 times and then filtered through a 40-μm mesh filter. All samples were sorted using a Coulter Elite ESP cell sorter.

Microsatellite analysis. LOH was assessed with the following polymorphic markers: *D5S107, D5S299, D5S346, D9S942, D9S43, BRCA2, D13S314, TP53, D17S786, D17S261, D18S474, D18S34, D18S46, D18S53.* Retention of heterozygosity was assessed with *D9S55, D9S162, IFNA,* and *D9S156* in patients heterozygous for 9p21. Data were reviewed in a coded fashion.

DNA sequence analysis. Aneuploid populations from 21 of 48 patients with 17p LOH and from all patients with 9p LOH were screened for *TP53* and *CDKN2A* mutations, respectively, by dye terminator fluorescent sequencing (Barrett et al., 1996; Galipeau et al., 1996; Neshat et al., 1994).

Methylation analysis. DNA samples were treated with bisulfite as described previously (Wong et al., 1997). Briefly, 6 ng (~800 cells) of each DNA sample were denatured in freshly prepared 0.3M NaOH (20 min at 42^0C), treated with 3.8M sodium bisulfite/1.0mM hydroquinone (pH 5.0) (6-8 hrs at 55^0C) and desulfonated with 0.3M NaOH (20 min at 37^0C). Bisulfite-treated samples were subsequently whole-genome amplified by primer extension preamplification (PEP) as described previously (Barrett et al., 1996; Wong et al., 1997). Aliquots of PEP reactions were used for methylation-specific PCR (MSP) analysis using primer pairs p16-M and p16-U as described previously (Wong et al., 1997).

RESULTS

LOH at 5q, 9p, 13q, 17p and 18q was detected in 54%, 91%, 48%, 100%, and 41%, respectively, of patients with aneuploid populations in premalignant epithelium, and 66%, 75%, 66%, 100% and 57%, respectively, of patients with cancer. Mutations in exons 5-9 of *TP53* were detected in 20 of 21 patients (95%) with 17p LOH, and *CDKN2A* mutations were present in 11 of 43 patients (26%) with 9p LOH. Twenty-four patients

with 9p LOH were evaluated for both *CDKN2A* mutations by direct sequencing and for *CDKN2A* CpG island methylation by methylation-specific PCR. Seventeen of the 24 patients (71%) had either a mutation (5/24; 21%) or CpG island methylation (12/24; 50%). CpG island methylation was not detected in patients (5/5) who retained heterozygosity at 9p21. In addition, we found no evidence for homozygous *CDKN2A* deletions in our highly purified flow-sorted samples by microsatellite or sequencing analysis.

Premalignant diploid clones with somatic genetic abnormalities involving *TP53*, or both *TP53* and *CDKN2A*, were frequently found in multiple biopsies extending over large areas (2-11 cm) of Barrett's epithelium as early as six years before detection of cancer (Figure 2.1). Identical *TP53* and *CDKN2A* mutations were present at many levels of the Barrett's segment, indicating early clonal expansion (Figure 2.1 A and B). The progenitor in patient 391 was a 2N (*TP53* R306X, *CDKN2A* R58X) clone whose evolution included bifurcations, multiple aneuploidies and a neoplastic cell lineage that accumulated 13q and 18q LOH before culminating in cancer after six years (Figure 2.1 B). The 2.0N (*TP53* R306X, *CDKN2A* R58X, 13q-), 3.0N (*TP53* R306X, *CDKN2A* R58X, 13q-), and 3.6N (*TP53* R306X, *CDKN2A* R58X, 13q-, 18q-) clones were all potential precursors of the cancer. The 3.0N clone, however, had no evidence of 18q LOH, was not detected prior to cancer and arose in a region spatially separated from the cancer, suggesting that it was not the precursor. We investigated all premalignant 2.0N clones detected from 1990 to 1996, and none showed 18q LOH. The 3.6N premalignant and 2.0N cancer clones, however, shared the same interstitial deletion of proximal 18q

with retention of 18p and distal 18q, based on evaluation by 14 chromosome 18 STRs (data not shown). Thus, the 3.6N clone was the precursor to the cancer. The progenitor in patient 772 was a 2N (*TP53* R248E) clone whose evolution was characterized by bifurcations, loss of alternate 5q alleles, multiple aneuploid populations, and a neoplastic cell lineage that accumulated 9p and 5q LOH before developing 4N and aneuploid populations (Figure 2.1 C). An intermediate in the neoplastic lineages leading to the 3.6N and 3.4N clones was not detected due to failure of the intermediate to persist or sampling limitations. This case also had a non-progressing 2N clone with loss of an alternate 9p allele not detected after 1991. In patient 779, the progenitor was a 2N (*TP53* R306X, *CDKN2A* E88X) clone present in an endoscopic biopsy taken three years before detection of a cancer containing three aneuploid populations and a 13q LOH that evolved after cancer (Figure 2.1 D).

We used clonal ordering to further investigate relationships among genetic events in these neoplastic cell lineages (Table 2.1). LOH at 17p and 9p typically preceded aneuploidy ($p<0.0001$ and $p<0.001$, respectively) and cancer ($p<0.0001$ and $p<0.001$, respectively). However, there was no obligate order of 17p and 9p LOH during neoplastic progression ($p=1.000$). Mutations in *TP53* and *CDKN2A* were also detected before aneuploidy (7/7 and 7/7 patients, respectively) and cancer (4/4 and 3/3 patients, respectively). Furthermore, patients (7/7) had *CDKN2A* CpG island methylation in premalignant diploid as well as aneuploid populations. LOH at 17p was typically detected before and not after 5q ($p<0.0001$), 13q ($p=0.002$), and 18q LOH ($p=0.004$). Although 9p LOH was also typically detected before 5q ($p=0.006$) and 13q ($p=0.004$), it

showed no obligate order relative to 18q LOH. LOH at 5q, 13q and 18q showed no obligate order relative to each other, although the number of cases in which these were evaluated was small.

DISCUSSION

Our observations of the evolution of neoplastic cell lineages *in vivo* confirm a pattern of events probably shared by most human neoplasms (Bedi et al., 1996; Califano et al., 1996; Franklin et al., 1997; Gazdar et al., 1994; Kuukasjarvi et al., 1997; Sidransky et al., 1992). A progenitor clone undergoes expansion and, with the development of genetic instability, enters a phase of clonal evolution that begins in premalignant cells, proceeds over a period of years and continues after the emergence of cancer (Figure 2.2). There have been reports that some cancers do not contain genetic abnormalities detectable in the premalignant epithelium from which the cancer arose (Wu et al., 1998). Although some such cases may result from inadequate purification of neoplastic cells, others probably represent bifurcations leading to mosaics that include clonal populations not represented on the lineage that progesses to cancer. In addition, most human premalignant tissues do not appear to progress to cancer, even when highly prevalent somatic lesions are present (Correa et al., 1990; Mao et al., 1997; Rozen et al., 1995; van der Burgh et al., 1996). For example, it is estimated that only 2.5 adenomatous polyps per 1,000 per year progress to colon cancer (Eide, 1986). Flow cytometry has detected clonal heterogeneity in many neoplasias, and flow purification may be required to detect

minority subclones with different LOHs developing before and after cancer (Figure 2.1 C) (Petersen et al., 1980). Our approach of flow sorting and clonal ordering to relate objective abnormalities (for example aneuploidy, LOH, *TP53* and *CDKN2A* mutations) to each other, rather than histologic abnormalities, can be used to study the evolution of cell lineages in other human neoplasms.

Figure 2.1a. Clonal evolution in patients with Barrett's esophagus *in vivo*. In patient 391 (21 samples, six years), *TP53* (CGA→TGA; R306X) and *CDKN2A* (CGA→TGA; R58X) mutations were found at all levels of an 8-cm Barrett's segment. Endoscopic and surgical biopsies from patient 391 are from 1990-1996. For each cell population, ploidy, LOH ($5q^-$, $9p^-$, $13q^-$, $17p^-$, $18q^-$) and mutations are given below. Cancer clones are red. Epithelial populations were purified by flow sorting. Ploidies were scored as different if DNA contents differed by 0.2N or more, as previously described (Levine et al., 1991). The distribution of clones with somatic genetic abnormalities in premalignant epithelium at the baseline endoscopy and the evolution of neoplastic cell lineages are shown. Other somatic events may precede p53 and p16 abnormalities or lead linearly to cancer, but we found no evidence for them among the non-random LOHs detected in our allelotype of esophageal adenocarcinoma (Barrett et al., 1996).

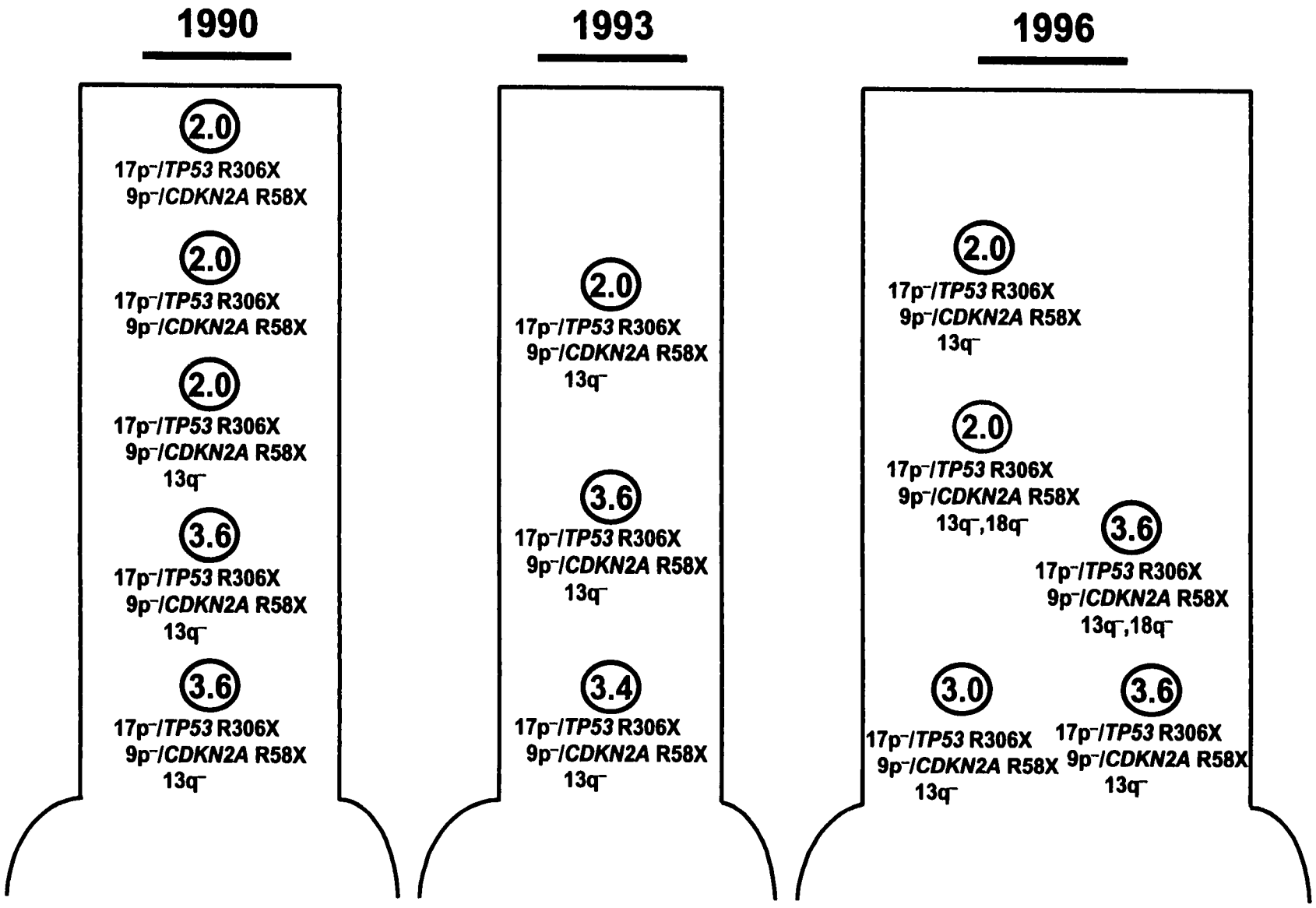
1990
2.0
17p⁻/TP53 R306X
9p⁻/CDKN2A R58X
2.0
17p⁻/TP53 R306X
9p⁻/CDKN2A R58X
2.0
17p⁻/TP53 R306X
9p⁻/CDKN2A R58X
13q⁻
3.6
17p⁻/TP53 R306X
9p⁻/CDKN2A R58X
13q⁻
3.6
17p⁻/TP53 R306X
9p⁻/CDKN2A R58X
13q⁻
1993
2.0
17p⁻/TP53 R306X
9p⁻/CDKN2A R58X
13q⁻
3.6
17p⁻/TP53 R306X
9p⁻/CDKN2A R58X
13q⁻
3.4
17p⁻/TP53 R306X
9p⁻/CDKN2A R58X
13q⁻
1996
2.0
17p⁻/TP53 R306X
9p⁻/CDKN2A R58X
13q⁻
2.0
17p⁻/TP53 R306X
9p⁻/CDKN2A R58X
13q⁻,18q⁻
3.6
17p⁻/TP53 R306X
9p⁻/CDKN2A R58X
13q⁻,18q⁻
3.0
17p⁻/TP53 R306X
9p⁻/CDKN2A R58X
13q⁻
3.6
17p⁻/TP53 R306X
9p⁻/CDKN2A R58X
13q⁻

Figure 2.1b. Clonal evolution in patients with Barrett's esophagus *in vivo*. Summary of cell lineages in patient 391. In patient 391 (21 samples, six years), *TP53* (CGA→TGA; R306X) and *CDKN2A* (CGA→TGA; R58X) mutations were found at all levels of an 8-cm Barrett's segment. Endoscopic and surgical biopsies from patient 391 are from 1990-1996. For each cell population, ploidy, LOH ($5q^-$, $9p^-$, $13q^-$, $17p^-$, $18q^-$) and mutations are given below. Cancer clones are red. Epithelial populations were purified by flow sorting. Ploidies were scored as different if DNA contents differed by 0.2N or more, as previously described (Levine et al., 1991). The distribution of clones with somatic genetic abnormalities in premalignant epithelium at the baseline endoscopy and the evolution of neoplastic cell lineages are shown. Other somatic events may precede p53 and p16 abnormalities or lead linearly to cancer, but we found no evidence for them among the non-random LOHs detected in our allelotype of esophageal adenocarcinoma (Barrett et al., 1996).

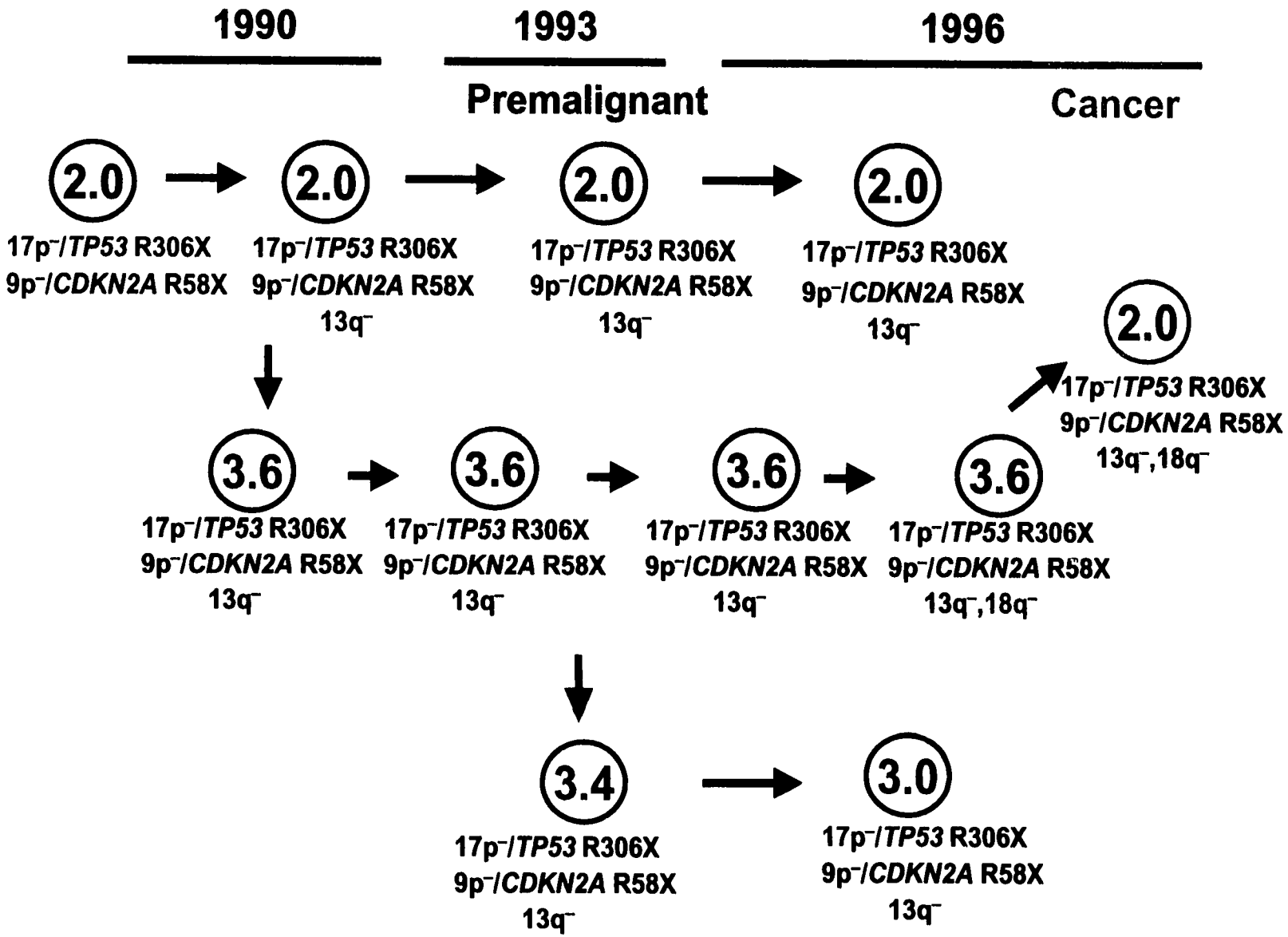
1990
1993
1996
Premalignant
Cancer
2.0
17p⁻/TP53 R306X
9p⁻/CDKN2A R58X
2.0
17p⁻/TP53 R306X
9p⁻/CDKN2A R58X
13q⁻
2.0
17p⁻/TP53 R306X
9p⁻/CDKN2A R58X
13q⁻
2.0
17p⁻/TP53 R306X
9p⁻/CDKN2A R58X
13q⁻
2.0
17p⁻/TP53 R306X
9p⁻/CDKN2A R58X
13q⁻,18q⁻
3.6
17p⁻/TP53 R306X
9p⁻/CDKN2A R58X
13q⁻
3.6
17p⁻/TP53 R306X
9p⁻/CDKN2A R58X
13q⁻
3.6
17p⁻/TP53 R306X
9p⁻/CDKN2A R58X
13q⁻
3.6
17p⁻/TP53 R306X
9p⁻/CDKN2A R58X
13q⁻,18q⁻
3.4
17p⁻/TP53 R306X
9p⁻/CDKN2A R58X
13q⁻
3.0
17p⁻/TP53 R306X
9p⁻/CDKN2A R58X
13q⁻

Figure 2.1c. Clonal evolution in patients with Barrett's esophagus *in vivo*. Summary of cell lineages in patient 772. In patient 772 (13 samples, three years), *TP53* (CGG→CAG; R248E) mutation was found at all levels of an 11-cm Barrett's segment. For each cell population, ploidy, LOH ($5q^-$, $9p^-$, $13q^-$, $17p^-$, $18q^-$) and mutations are given below. LOH of alternate alleles is denoted by ($^{-1}$, $^{-2}$). Cancer clones are red. Epithelial populations were purified by flow sorting. Ploidies were scored as different if DNA contents differed by 0.2N or more, as previously described (Levine et al., 1991). The distribution of clones with somatic genetic abnormalities in premalignant epithelium at the baseline endoscopy and the evolution of neoplastic cell lineages are shown. Other somatic events may precede p53 and p16 abnormalities or lead linearly to cancer, but we found no evidence for them among the non-random LOHs detected in our allelotype of esophageal adenocarcinoma (Barrett et al., 1996).

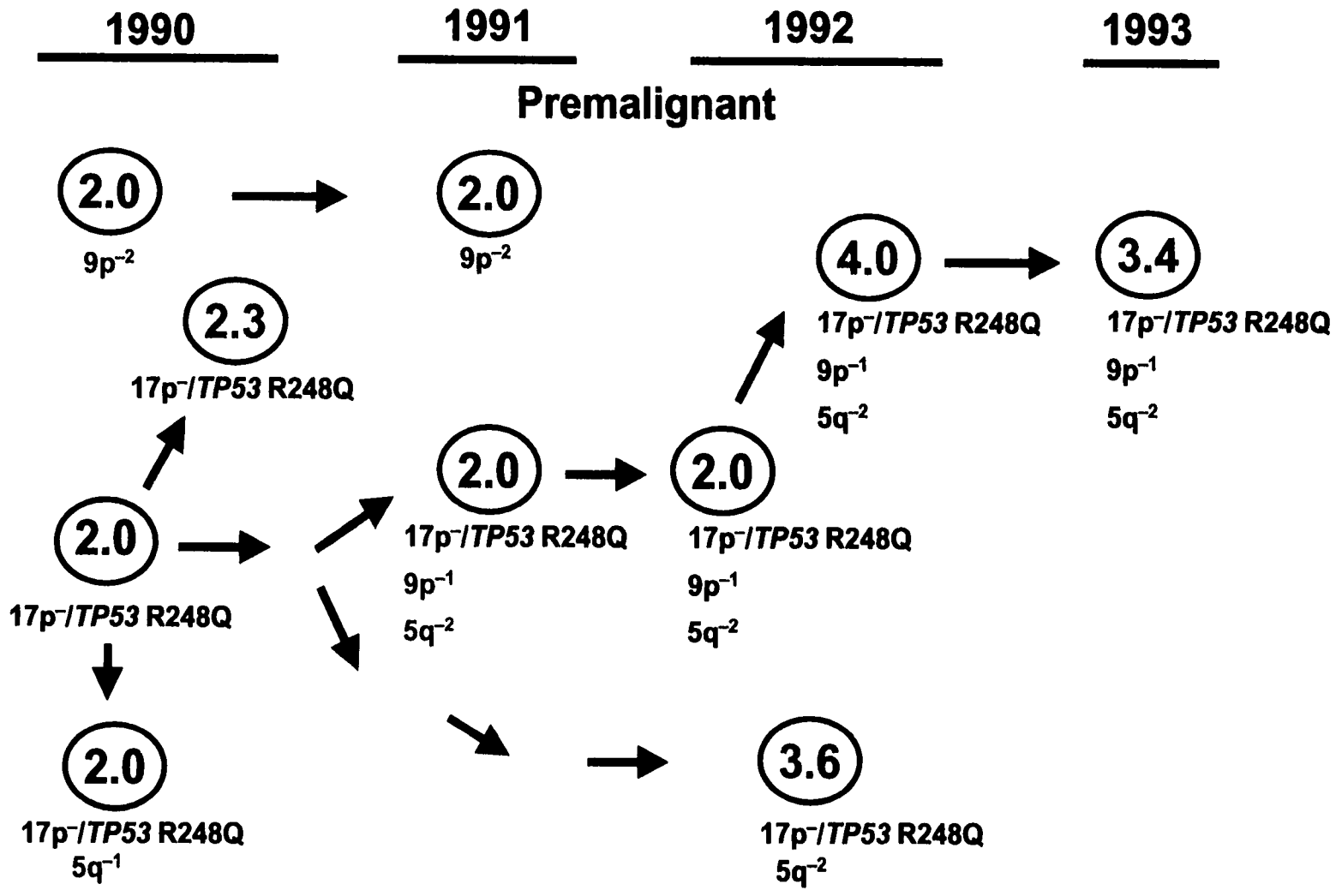
1990
1991
1992
1993
Premalignant
2.0
9p-2
2.0
9p-2
2.3
17p-/TP53 R248Q
4.0
17p-/TP53 R248Q
9p-1
5q-2
3.4
17p-/TP53 R248Q
9p-1
5q-2
2.0
17p-/TP53 R248Q
2.0
17p-/TP53 R248Q
9p-1
5q-2
2.0
17p-/TP53 R248Q
9p-1
5q-2
2.0
17p-/TP53 R248Q
5q-1
3.6
17p-/TP53 R248Q
5q-2

Figure 2.1d. Clonal evolution in patients with Barrett's esophagus *in vivo*. Summary of cell lineages in patient 779. In patient 779 (17 samples, three years), *TP53* (CGA→TGA; R306X) and *CDKN2A* (GAG→TAG; E88X) mutations were found in endoscopic and surgical biopsies from 1989 and 1992. For each cell population, ploidy, LOH ($5q^-$, $9p^-$, $13q^-$, $17p^-$, $18q^-$) and mutations are given below. Cancer clones are red. Epithelial populations were purified by flow sorting. Ploidies were scored as different if DNA contents differed by 0.2N or more, as previously described (Levine et al., 1991). The distribution of clones with somatic genetic abnormalities in premalignant epithelium at the baseline endoscopy and the evolution of neoplastic cell lineages are shown. Other somatic events may precede p53 and p16 abnormalities or lead linearly to cancer, but we found no evidence for them among the non-random LOHs detected in our allelotype of esophageal adenocarcinoma (Barrett et al., 1996).

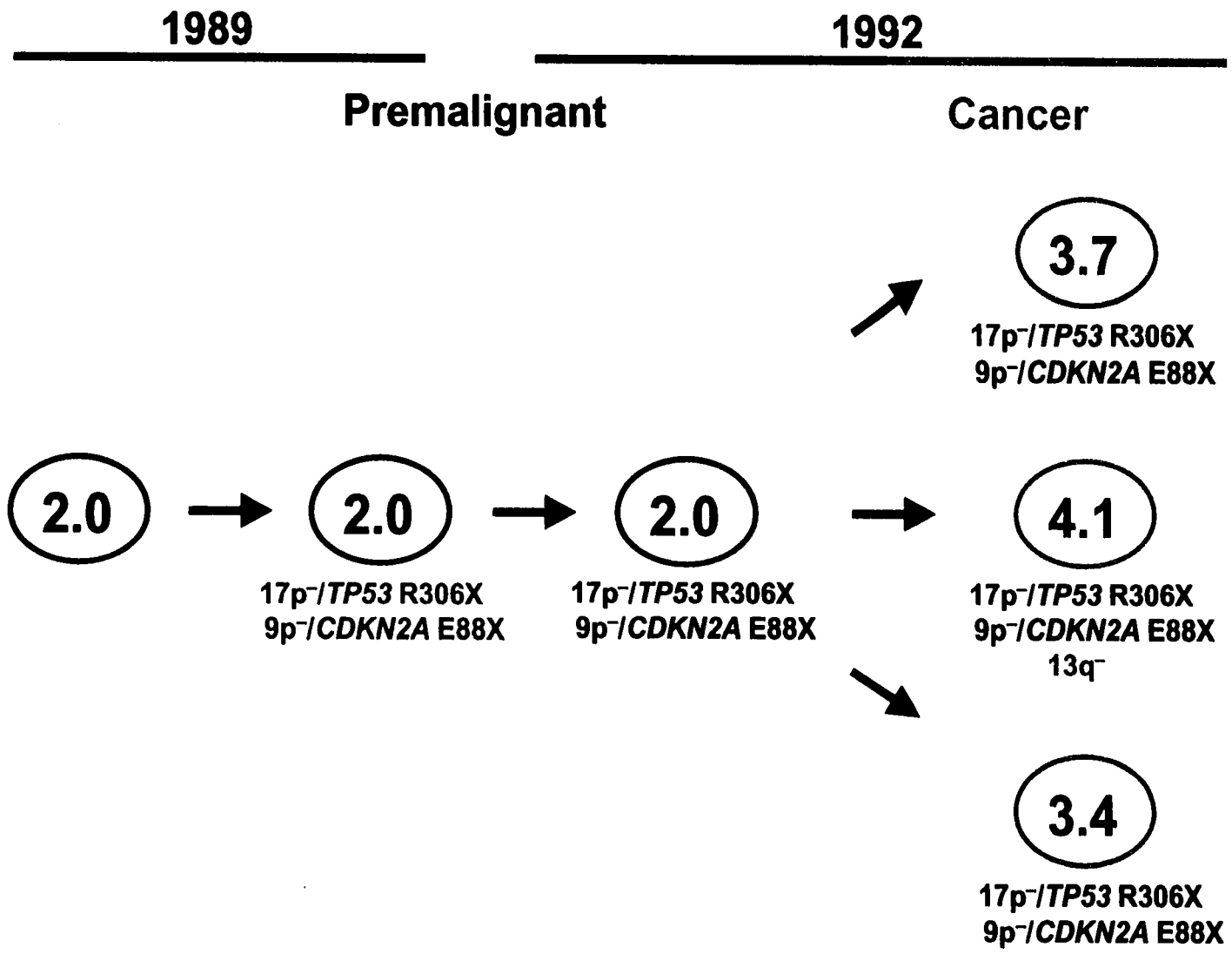
1989
1992
Premalignant
Cancer
2.0
2.0
17p⁻/TP53 R306X
9p⁻/CDKN2A E88X
2.0
17p⁻/TP53 R306X
9p⁻/CDKN2A E88X
3.7
17p⁻/TP53 R306X
9p⁻/CDKN2A E88X
4.1
17p⁻/TP53 R306X
9p⁻/CDKN2A E88X
13q⁻
3.4
17p⁻/TP53 R306X
9p⁻/CDKN2A E88X

Figure 2.2. Multiple genetic routes to cancer in Barrett's esophagus. Each clone represents a cell population detected in this study, but the figure is not intended to be comprehensive because the lack of obligate orders creates multiple genetic pathways to cancer, only some of which are represented. Although there are multiple pathways to cancer, some general patterns appear to be consistent among many patients. LOH events arise in diploid Ki67-positive populations (2N) within Barrett's metaplasia (M). We detected 2N populations that developed LOH without lesions involving either *TP53* or *CDKN2A* in 4 patients but these clones failed to progress. LOH at either 17p ($17p^-$) or 9p ($9p^-$) can occur in diploid populations and can precede mutations in *TP53* and *CDKN2A*. Although both 17p and 9p LOH develop as early events, they occur in no obligate order. 2N clones with somatic genetic abnormalities involving *TP53* ($17p^-$/*TP53*$^-$) and *CDKN2A* ($9p^-$/*CDKN2A*$^-$; $9p^-$) frequently give rise to populations with elevated 4N fractions (4N) that can evolve aneuploid cell populations (An). Methylation of the *CDKN2A* CpG island was also detected in diploid cells before the development of aneuploidy. The 4N abnormality was not always detected, possibly from sampling limitations or failure of a genetically unstable intermediate to persist. In some cases, such as patient 391 (Figure 2.1), changes in ploidy may result in a clone with a 2N or near-2N DNA content, yet with multiple genetic abnormalities. 5q, 13q, and 18q LOH have no obligate order relative to aneuploidy, cancer or each other. During evolution, neoplastic cell lineages may bifurcate, giving rise to mosaics with the same *TP53* and *CDKN2A* abnormalities but different ploidies and additional LOHs. Some clones in these mosaics develop into cancer (Ca), whereas others are either delayed in their progression or represent dead ends. Subsequently, multiple malignant clones (Ca) with different ploidies and additional LOHs evolve as the cancer progresses.

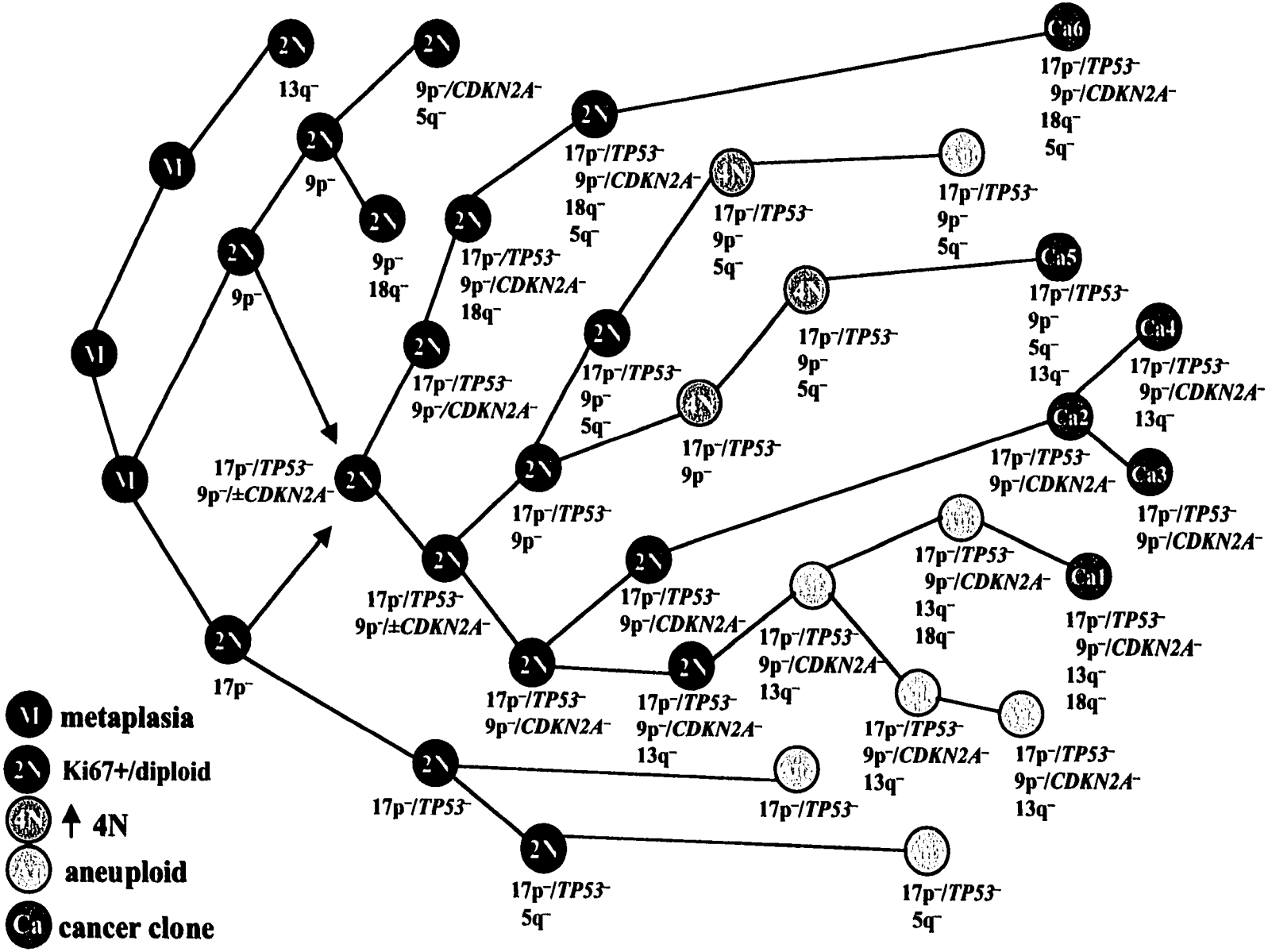
MI
2N
4N
AN
Ca
metaplasia
Ki67+/diploid
4N
aneuploid
cancer clone
13q⁻
9p⁻/CDKN2A⁻
5q⁻
9p⁻
9p⁻
18q⁻
17p⁻/TP53⁻
9p⁻/CDKN2A⁻
18q⁻
17p⁻/TP53⁻
9p⁻/CDKN2A⁻
5q⁻
17p⁻/TP53⁻
9p⁻
5q⁻
17p⁻/TP53⁻
9p⁻/CDKN2A⁻
18q⁻
5q⁻
17p⁻/TP53⁻
9p⁻
5q⁻
17p⁻/TP53⁻
9p⁻/±CDKN2A⁻
17p⁻/TP53⁻
9p⁻
17p⁻/TP53⁻
9p⁻
17p⁻/TP53⁻
9p⁻/±CDKN2A⁻
17p⁻/TP53⁻
9p⁻/CDKN2A⁻
17p⁻/TP53⁻
9p⁻/CDKN2A⁻
13q⁻
17p⁻/TP53⁻
9p⁻/CDKN2A⁻
13q⁻
17p⁻/TP53⁻
9p⁻/CDKN2A⁻
13q⁻
18q⁻
17p⁻/TP53⁻
9p⁻/CDKN2A⁻
13q⁻
18q⁻
17p⁻
17p⁻/TP53⁻
17p⁻/TP53⁻
17p⁻/TP53⁻
9p⁻/CDKN2A⁻
13q⁻
17p⁻/TP53⁻
9p⁻/CDKN2A⁻
13q⁻
17p⁻/TP53⁻
5q⁻
17p⁻/TP53⁻
5q⁻
Ca6
17p⁻/TP53⁻
9p⁻/CDKN2A⁻
18q⁻
5q⁻
Ca5
17p⁻/TP53⁻
9p⁻
5q⁻
13q⁻
Ca4
17p⁻/TP53⁻
9p⁻/CDKN2A⁻
13q⁻
Ca2
17p⁻/TP53⁻
9p⁻/CDKN2A⁻
Ca3
17p⁻/TP53⁻
9p⁻/CDKN2A⁻
Ca1
17p⁻/TP53⁻
9p⁻/CDKN2A⁻
13q⁻
18q⁻

Table 2.1. Clonal orders in Barrett's esophagus. Patients with Ki67-positive-2N, 4N, or aneuploid flow-sorted samples (range 2-24 per patient; total 266) from multiple biopsies (range 2-13 per patient; total 189) were evaluated. In each case, two events, A and B, were compared to each other to determine whether A preceded B, A and B were detected together, or A was detected after B. For each non-random LOH (17p, 9p, 18q, 5q, 13q), three types of orders were determined: i) LOH and aneuploidy; ii) LOH and LOH; iii) LOH and cancer. In all tests, the null hypothesis is the probability that A precedes B 50% of the time among cases in which order could be determined. The level of significance (p) versus the null hypothesis for each test was determined as previously described but without adjustment for multiple comparisons (Barrett et al., 1996). The observation of a statistically significant order does not necessarily indicate causality.

Events		A before B	A,B together	A after B	p
A	B	patients (%)	patients (%)	patients (%)	
17p LOH	Aneuploidy	19 (79)	5 (21)	0 (0)	<0.0001
	9p	7 (24)	16 (55)	6 (21)	1.000
	5q	19 (86)	3 (14)	0 (0)	<0.0001
	13q	10 (63)	6 (37)	0 (0)	0.002
	18q	9 (56)	7 (44)	0 (0)	0.004
	Cancer	23 (96)	1 (4)	0 (0)	<0.0001
9p LOH	Aneuploidy	20 (80)	3 (12)	2 (8)	<0.001
	5q	11 (73)	3 (20)	1 (7)	0.006
	13q	9 (60)	6 (40)	0 (0)	0.004
	18q	7 (50)	3 (21)	4 (29)	0.549
	Cancer	20 (87)	0 (0)	3 (13)	<0.001
18q LOH	Aneuploidy	7 (64)	0 (0)	4 (36)	0.549
	5q	7 (78)	1 (11)	1 (11)	0.070
	13q	4 (44)	3 (33)	2 (23)	0.688
	Cancer	9 (82)	0 (0)	2 (18)	0.065
5q LOH	Aneuploidy	4 (20)	5 (25)	11 (55)	0.118
	13q	2 (25)	3 (37.5)	3 (37.5)	1.000
	Cancer	10 (53)	3 (15)	6 (32)	0.454
13q LOH	Aneuploidy	5 (36)	3 (21)	6 (43)	1.000
	Cancer	8 (57)	1 (7)	5 (36)	0.581

CHAPTER 3: INACTIVATION OF $p16^{INK4a}$ IN HUMAN MAMMARY EPITHELIAL CELLS BY CpG ISLAND METHYLATION

ABSTRACT

Proliferation of human mammary epithelial cells (HMEC) is limited to a few passages in culture due to an arrest in G1 termed selection or mortality stage 0, M0. A small number of cells spontaneously escape M0, continue to proliferate in culture, and then enter a second mortality stage, M1, at which they senesce. Evidence that M0 involves the Rb pathway comes from the observation that expression of human papillomavirus type 16 E7 alleviates the M0 proliferation block, and we further show that the Rb-binding region of E7 is required to allow cells to bypass M0. In contrast, E6 does not prevent HMEC from entering M0 but, rather, is involved in M1 bypass. Here we show that inactivation of the D-type cyclin-dependent kinase inhibitor $p16^{INK4a}$ is associated with escape from the M0 proliferation block. Early-passage HMEC express readily detectable amounts of p16 protein, whereas normal or E6-expressing HMEC that escaped M0 expressed markedly reduced amounts of p16 mRNA and protein. This initial reduction of p16 expression was associated with limited methylation of the p16 promoter region CpG island. At later passages a further reduction in p16 expression occurred, accompanied by increased CpG island methylation. In contrast, reduction of p16 expression did not occur in E7-expressing HMEC that bypassed M0 due to inactivation of Rb. These observations in the E6-expressing HMEC correlate well with the finding that

CpG island methylation is a mechanism of p16 inactivation in the development of human tumors, including breast cancer.

INTRODUCTION

The progression of cells in culture to an immortalized state, although not identical, has many features in common with the development of cancer *in vivo*. For example, high-risk human papillomaviruses (HPVs) that are associated with anogenital cancer readily immortalize human cells in culture while low-risk HPVs that are associated with benign lesions do not (Halbert et al., 1991; Hawley-Nelson et al., 1989; Munger et al., 1989). The E6 and E7 genes of the high-risk HPVs inactivate p53 and Rb, respectively, two of the most commonly inactivated tumor suppressors in human cancer (Dyson et al., 1989; Scheffner et al., 1990; Werness et al., 1990). HPV-immortalized cells can progress to tumorigenicity by continued passaging or by treatment with carcinogens (Garrett et al., 1993; Hurlin et al., 1991). These tumorigenic derivatives have additional alterations, such as deletions on 18q, in common with cancers (Klingelhutz et al., 1993).

For human mammary epithelial cells (HMEC) to become immortalized, they must overcome several distinct proliferation blocks (Foster and Galloway, 1996; Shay et al., 1993). Initially, the proliferation of HMEC is limited to a few passages in culture due to a proliferation block termed selection or M0 (mortality stage 0), a period when cells become larger and flattened and accumulate in G1 or G0 (Foster and Galloway, 1996;

Stampfer, 1985). Expression of E7 in early-passage HMEC allows the cells to bypass M0 (Foster and Galloway, 1996), suggesting that Rb-related proteins play an important role in the M0 arrest (Foster and Galloway, 1996). Although E7 is efficient at allowing cells to bypass M0, most of the cells arrest at a later stage and do not become immortalized (Foster and Galloway, 1996; Wazer et al., 1995). A subpopulation of normal cells (not expressing HPV oncogenes) can occasionally escape M0 and continue to proliferate until they senesce at M1 (mortality stage 1) (Shay et al., 1993; Stampfer, 1985). Expression of E6 allows these cells to bypass M1 and exhibit an extended life span. The E6-expressing cells eventually enter a crisis period (M2, mortality stage 2) from which immortalized cells emerge (Band et al., 1991; Shay et al., 1993). Thus, E7 allows HMEC to bypass M0, E6 allows them to bypass M1, and additional changes are thought to allow escape from M2 and to yield immortalized cells (Band et al., 1991; Foster and Galloway, 1996; Shay et al., 1993). In this study, we examined the expression patterns of various cell cycle regulatory proteins to begin to elucidate the mechanisms involved in the M0 arrest. The results suggest a role for the p16 cyclin-dependent kinase inhibitor protein in the arrest of cells at M0, and indicate that escape from M0 is associated with methylation of the p16 promoter region CpG island and inactivation of p16 expression.

MATERIALS AND METHODS

Cell Culture. Human mammary epithelial cells were isolated from tissue specimens from reduction mammoplasties as described by Stampfer (Stampfer, 1985). HMEC1 and

HMEC3 were grown in MEGM (Clonetics) and were described previously (Foster and Galloway, 1996) while HMEC4, HMEC6, and HMEC9 were grown in DFCI-1 (Band and Sager, 1989). HMEC8 cells were isolated from normal breast tissue from a patient undergoing a mastectomy and grown in DFCI-1. LXSN-based retroviruses expressing HPV oncogenes were used to infect HMEC as soon as possible after establishment of the cultures (Demers et al., 1996; Halbert et al., 1991; Miller and Rosman, 1989), followed by selection with 100 μg/ml of G418 to eliminate uninfected cells. The cultures were maintained by feeding fresh medium every other day and passaging at a ratio of 1:5 before the cultures were confluent. Population doublings were estimated based on 2.25 doublings per 1:5 split. For the purposes of this study, cells were deemed to be immortalized if they achieved 50 passages (>100 population doublings). Cells that were not expressing HPV oncogenes achieved fewer than 25 passages. Cell lines H249 and H1618 (both donated by J. Herman and S. Baylin) were used as negative and positive controls, respectively, for p15 and p16 promoter region methylation analysis.

Immunoprecipitation of E7. Cells were labeled with [^{35}S]cysteine and [^{35}S]methionine and equivalent counts per minute (cpm) were immunoprecipitated with rabbit antisera to HPV-16 E7 or HPV-6 E7 (Halbert et al., 1991).

Western blots. Whole-cell extracts were prepared in WE buffer and protein concentrations were determined by the BioRad DC protein assay (Foster and Galloway, 1996). Protein samples (20 μg)were separated by sodium dodecyl sulfate-polyacrylamide

gel electrophoresis (SDS-PAGE), and blots were prepared on nitrocellulose or Immobilon-P membranes (Millipore). The following antibodies were used as probes: p53 and p21 (Oncogene Science, clones DO-1 and EA10); Rb, cyclin A, cyclin E, cyclin D1, and p16 (PharMingen, clones G3-245, BF683, HE12, G124-326, and G175-405); and CDK2, CDK4, and p27 (Transduction Laboratories, no. C18520, C18720, and K25020). The original films were scanned on a Sharp JX-325 scanner with Adobe Photoshop software and, where noted, quantitation was done on the scanned image with ImageQuant software (Molecular Dynamics).

Northern analysis. Total RNA was isolated by pelleting through CsCl cushions (Glisin et al., 1974). Poly(A)$^+$ RNA was isolated from total RNA by using oligo(dT) cellulose (New England Biolabs). RNA samples were separated on formaldehyde-agarose gels and blotted to Hybond N membranes (Amersham) in 20X SSC (1X SSC is 0.15 M NaCl plus 0.015 M sodium citrate). After UV cross-linking, the membranes were hybridized in 0.5 M sodium phosphate (pH 7.2) and 5% SDS at 68°C and washed in 50 mM sodium phosphate and 0.1% SDS at 68°C (Glisin et al., 1974). PE1 probe, containing p16 exon 1, was generated by PCR as described previously (Merlo et al., 1995) and labeled with [^{32}P]dCTP by the random-primer method (Boerhinger Mannheim). No cross-hybridization between the PE1 probe and p15 RNA was detected when using *in vitro*-transcribed p16 and p15 test RNAs. The blots were stripped and reprobed with 36B4 as a loading control (Laborda, 1991). Quantitation was done on a Molecular Dynamics PhosporImager with ImageQuant software.

Southern analysis. Genomic DNA was prepared, digested with *Eco*RI or *Bam*HI and separated on 0.8% agarose gels. After transferring to Hybond N^+ (Amersham), the blots were probed for HPV-16 E6 under the conditions described above.

p16 deletion analysis. To screen the p16 locus (9p21) for possible homozygous deletions or allelic loss, DNA from clonal cell populations was amplified by the primer-extension preamplification (PEP) (Barrett et al., 1995; Zhang et al., 1992). Aliquots from each sample were evaluated for STS marker c5.1, located within the p16 gene (Kamb et al., 1994), or polymorphic markers D9S942 or D9S161 in locus-specific PCR reactions as described previously (Barrett et al., 1996).

p16 promoter region methylation analysis. The PCR-based assay for CpG island methylation of the p16 and p15 promoter regions was carried out as described previously (Herman et al., 1996; Wong et al., 1997). Briefly, this assay consists of sodium bisulfite modification, followed by a PEP reaction and methylation-specific PCR. For some samples, DNA sequencing of the sodium bisulfite-modified genomic DNA was used to screen for methylation not detected by the PCR assay. Briefly, after sodium bisulfite treatment and PEP, the p16 promoter region from -159 to +135 (according to the numbering system of Hara *et al.* (Hara et al., 1996)) was amplified using primers 5'-TTT TTA GAG GAT TTG AGG GAT AGG-3' and 5'-CTA CCT AAT TCC AAT TCC CCT ACA-3' under the conditions described by Herman *et al.* (Herman et al., 1996). The resulting PCR products were gel purified and cloned (Invitrogen TA cloning kit) and

individual clones were sequenced on an ABI sequencer with dye terminators. Based upon non-CpG cytosines, which are expected to be rarely methylated, the bisulfite conversion efficiency was estimated to be at least 99.7%.

RESULTS

Growth characteristics of HMEC in culture — effects of E6 and E7 expression. LXSN-based retroviruses expressing HPV-16 E6, E7, or E6/E7 were used to infect early-passage HMEC, and the resulting cells were serially passaged. Uninfected, vector-infected, and E6-infected cells all entered M0, as evidenced by reduced proliferation and the appearance of large, flat cells. This usually occurred by passage 7, but the timing was variable depending on the particular HMEC strain. In one uninfected cell strain, HMEC4, a subpopulation of cells spontaneously escaped M0 and then senesced at M1 (approximately passage 20). In all E6-expressing strains, a subpopulation of HMEC escaped from M0 and readily became immortalized. Cells infected with E7 or E6/E7 consistently bypassed M0, failing to show large, flat cells or reduced proliferation. However, HMEC expressing E7 alone did not readily become immortalized; they eventually grew in tight clumps and failed to proliferate beyond passage 25. The E6/E7-expressing HMEC continued to proliferate after bypassing M0 and were immortalized, with little evidence of crisis. Table 3.1 summarizes these results for six HMEC strains.

By using the retrovirus integration site(s) as tags to monitor the fate of individual infected cells, it was possible to estimate the frequency of M0 escape in the E6-

expressing HMEC. Genomic DNA was prepared at various stages of culture and Southern blots were probed for E6 (data not shown). In E6-expressing HMEC6, only two virus integration sites (representing two initially infected cells) were evident after M0 escape (data not shown). Therefore, based on an estimate of between 5,000 and 10,000 cells initially transduced, fewer than 0.1% of the E6-expressing cells proliferated beyond M0. Only one of the two clones was detected in the immortalized culture. In E6-expressing HMEC8, three or four integration sites were detected after M0 escape, again less than 0.1% of the initial population. The pattern of integration sites changed over time and two sites were detected in the immortalized population, representing either two clones or one clone containing two viral integrations. We also monitored the fate of E6-expressing HMEC6 cells individually cloned after M0 escape. Of 23 clones selected at passage 18, only 4 proliferated to passage 25. These results argue that 99.9% of E6-expressing cells fail to proliferate beyond M0 and that continued selection of clones (and subclones) occurs even among the few cells that do escape M0.

The Rb-binding region of HPV-16 E7 is required to allow HMEC to bypass M0. The best-characterized activity of HPV-16 E7 is its ability to bind to Rb and related proteins, releasing transcription factor E2F. To determine whether the Rb-binding region of E7 is important for its ability to allow cells to bypass M0, several mutated forms of E7 were tested. HPV-16 E7Δ21-24 has a deletion of 4 amino acids within the LXCXE motif (amino acids 22 to 26 of HPV-16 E7) which have previously been shown to be required for binding of Rb and related proteins (Munger et al., 1989). HPV-16 E7C24G carries a

point mutation within this region and similarly disrupts binding of Rb and related proteins (Banks et al., 1990; Davies et al., 1993). The HPV-16 E7E26G mutation disrupts Rb-binding but leaves intact the ability of E7 to interact with the Rb-related protein p107 (Banks et al., 1990; Davies et al., 1993). HPV-16 E7D21S contains a mutation just outside the LXCXE motif and leaves intact Rb and p107 binding as well as the ability to release E2F from Rb in a gel shift assay (4,11,14). HPV-16 E7H2P retains the ability to bind to Rb but is at least partially defective in its ability to dissociate E2F in a gel shift assay (Davies et al., 1993) (unpublished data) and is transformation defective (Banks et al., 1990). HPV-16 E7Δ6-10 and HPV-16 E7C58G/C91G are able to bind Rb but are transformation defective. In addition, HPV-6 E7 was tested; HPV-6 E7 does bind to Rb but with a greatly reduced efficiency compared to HPV-16 E7 (Munger et al., 1989).

To compare the abilities of the HPV E7 proteins to allow M0 bypass, early-passage HMEC6 cells were infected with the retroviruses and selected with G418 to eliminate uninfected cells. Initial observation of the cultures indicated that wild-type HPV-16 E7 was active; i.e., few large, flat cells emerged, and the population remained proliferative. HPV-16 E7D21S was only partially active; i.e., the cells did not proliferate as well as those expressing HPV-16 E7, and some large cells emerged. Cells infected with other E7 proteins were similar to vector-infected control cells (Figure 3.1 A and data not shown).

Cyclin A expression is greatly reduced concomitant with a reduction in the S-phase fraction as early-passage HMEC accumulate in M0 (Foster and Galloway, 1996) (see below). Therefore, cyclin A expression was used as a marker for M0, independent of

cell morphology, to evaluate the mutated E7 proteins. As expected, the uninfected control cells and the LXSN vector-infected cells showed very low cyclin A expression whereas cells expressing 16 E7 continued to express abundant cyclin A (Figure 3.1 B). Cells expressing HPV-16 E7D21S expressed cyclin A at a higher level than that of the control cells, although only about one-fourth as high as the level observed in the wild-type HPV-16 E7-expressing cells. Cells expressing the other E7 proteins expressed cyclin A at low levels, similar to the vector-infected control cells. These results indicate that the Rb-binding region of HPV-16 E7 is required to allow HMEC to bypass M0 but do not exclude the possibility that other regions of E7 are also required.

To confirm the expression of the various E7 proteins, extracts of HMEC4 cells expressing the E7 proteins were immunoprecipitated with polyclonal E7 antibody. HMEC4 cells that had escaped from M0 were chosen for this analysis because they had a sufficiently long life span to be infected, selected with G418, and have their proteins labeled. All of the E7 proteins were detected at comparable levels (Figure 3.1 C and D). Two proteins, HPV-16 E7Δ6-10 and HPV-16 E7C58G/C91G, were detected at lower levels and were not included in the above analysis (data not shown).

Cell cycle-related proteins in early-passage HMEC. To begin to dissect possible mechanisms involved in arrest of HMEC at M0, protein extracts were prepared sequentially from passage 3 (early-proliferating cells) to passage 7 (cells mostly arrested at M0). Figure 3.2 shows the results for HMEC9 cells. Early-passage cells (passage 3) expressed abundant Rb which was predominantly in the hyperphosphorylated form. As

the cells accumulated in M0, the hypophosphorylated form predominated and the overall level of Rb was greatly reduced. Among the cyclins and CDKs involved in Rb phosphorylation, cyclin A expression was dramatically reduced while the levels of cyclins E and D1 remained unchanged. CDK2 and CDK4 were reduced but only at the later passages. Consistent with our previous report (Foster and Galloway, 1996), neither p53 nor p21 was induced at M0. Similarly, p27 was not induced. In contrast, the level of p16 increased by about 60% during this period. Similar trends were observed for HMEC6 and HMEC8. Although the increase in the p16 level was not dramatic, it was consistent with a possible role in the M0 arrest given its known ability to inhibit CDK4 and CDK6, two cyclin-dependent kinases that play a central role in Rb phosphorylation.

p16 levels in early passage and post-M0 HMEC. Given the above results implicating the Rb pathway in the arrest of cells at M0 and the fact that p16 is commonly deleted in human cancers and cancer cell lines, we compared the levels of p16 in the early-passage HMEC to the levels in post-M0 HMEC. Early-passage, uninfected HMEC1 and HMEC3 expressed p16 that was detectable by Western blotting; however, major differences in p16 expression were detected among the post-M0 cells (Figure 3.3). Cells that expressed E7 or E6/E7 and had bypassed M0 showed levels of p16 as high as or higher than the early-passage cells. However, cells that expressed E6 and had escaped from M0 showed very low levels of p16. A similar pattern of p16 expression was seen in HMEC6 and HMEC9 (see below). The low level of p16 expression in the post-M0 E6-expressing cells was not a direct result of E6 expression because the E6/E7 expressing cells had abundant p16.

Furthermore, expression of E6 in the early-passage HMEC8 cells did not reduce p16 expression (Figure 3.4 A). HMEC4 spontaneously escaped M0, and this was associated with a five-fold reduction in p16 protein levels (Figure 3.4 A). p16 levels further decreased 2.5-fold with continued passage in culture. As HMEC4 aged and approached M1, the level of p16 remained low. In contrast, the levels of p53, p21, and p27 were increased after M0 and remained high at late passage (Figure 3.4 A and data not shown). Overall, these results are consistent with a model in which the Rb pathway limits proliferation at M0. In cells that express E7, inactivation of Rb would allow continued proliferation of cells with high levels of p16. In contrast, cells with intact Rb function would arrest at M0, followed by selection for cells having low levels of p16 during M0 escape.

The patterns of p16 expression in HMEC6, HMEC8 and HMEC9 expressing E6 were examined at various passages after M0 escape. In E6-expressing HMEC6, the p16 level was reduced after M0 escape (passage 12), in contrast to uninfected cells prior to M0 (passage 3) (Figure 3.4 A). This low level of p16 was maintained through passage 18, was further reduced by passage 25, and reached an undetectable level by passage 59 (a trace of p16 was detected in the passage 29 cells on a longer exposure (data not shown)). E6-expressing HMEC9 showed a pattern of p16 expression very similar to that of the E6-expressing HMEC6 (data not shown). E6-expressing HMEC8 at passage 8 had not escaped M0 and expressed abundant p16 (Figure 3.4 A). At passage 14, these cells had escaped M0 and showed a reduced level of p16 compared to the passage 8 cells. Surprisingly, the level of p16 was increased again at passages 21 to 32 and then was

dramatically reduced to undetectable levels by passage 41. In culture, a mild crisis with noticeable cell death was noted in the E6-expressing HMEC8 at passages 29 through 32; thereafter, the cells formed a more stable population. In contrast, p16 was expressed at high levels in all the late passage cells expressing E6/E7 (Figure 3.4 A, HMEC6-E6/E7 passage 66, and data not shown). Note that p27 expression was not decreased during the course of these experiments (Figure 3.4 A). These results are consistent with the idea that selection against the Rb/p16 pathway beginning around M0 results in the emergence of cells with low levels of p16. In the E6-expressing HMEC8, the emergence of cells with low levels of p16 was delayed. It is interesting that HMEC8 cells were derived from normal breast tissue from a patient undergoing a mastectomy while all other cells in this study were derived from breast reduction tissue.

p16 gene inactivation occurs at the mRNA level. To begin to address the mechanism underlying the loss of p16 expression, p16 mRNA levels were analyzed by Northern blotting. In early-passage HMEC4 (passage 5), p16 mRNA was detected as a major band of about 0.8 kb and a minor band at about 1.1 kb (Figure 3.4 B). The low levels of p16 protein detected in the population that escaped M0 (passages 12 and 18) correlated with reduced levels of p16 mRNA expression.

In HMEC6, p16 mRNA was detected at early passage (passage 3), but it was not detected in the E6-expressing cells at passage 59 (Figure 3.4 B). E6/E7-expressing HMEC6 expressed an elevated level of p16 mRNA at passage 66 (Figure 3.4 B). This result was somewhat surprising since the E6/E7-expressing HMEC6 expressed no more

p16 protein than the early-passage HMEC6 did. The results with HMEC9 were very similar to those with HMEC6 (data not shown). In E6-expressing HMEC8, p16 mRNA was detected at passage 29, when abundant p16 protein was detected, but was not detected at passage 41, when p16 protein became undetectable (Figure 3.4 B). These results suggest that the reduction in p16 protein after M0 escape can be explained, at least in part, by alterations at the RNA level.

Deletions in p16 do not explain the loss of p16 expression. Since p16 gene deletion is known to occur readily in cell lines, various HMEC were cloned and DNA was extracted to check for possible deletions affecting the 9p21 region. Three markers were used for this analysis. The c5.1 STS marker is located within the p16 gene (Kamb et al., 1994). The D9S942 and D9S161 STR markers are located within 9p21 and allow identification of loss of heterozygosity (LOH). Analysis of the early passage cells showed that all were informative for LOH analysis (data not shown). In HMEC4 that had escaped from M0, 3 of 10 clones contained apparent homozygous deletions affecting the p16 gene at 9p21 while the remaining 7 clones had no deletions (data not shown). In E6-expressing HMEC1 that had escaped M0, no deletions were detected in 10 clones (data not shown). As expected, no deletions were observed among 10 clones of E6/E7-expressing HMEC1 which retained p16 expression (data not shown). To determine whether frequent p16 deletions occurred at later passages, we also tested 10 clones each of HMEC6 and HMEC8 immortalized by E6 (> 100 population doublings). Again, no homozygous deletions or LOH were detected (data not shown). Based on these results, deletion of p16

did not appear to play a major role in the emergence of cells expressing low levels of p16 during M0 escape.

The p16 gene is methylated in E6-expressing HMEC. Methylation of the CpG island within the promoter region of p16 has been reported as a mechanism of p16 gene inactivation in tumors and cancer cell lines (Herman et al., 1995; Merlo et al., 1995; Wong et al., 1997). Therefore, a methylation-sensitive PCR assay was used to compare the methylation status of this region between cells which expressed high levels of p16 and those which expressed low levels of p16.

HMEC4 that escaped from M0 exhibited dramatically less p16 than did the early-passage cells. However, no p16 gene methylation was detected by the PCR assay in these cells up to passage 18, which is near the end of their proliferative lifespan (Figure 3.4 C). Similarly, no p16 gene methylation was detected in the E6-expressing cells that escaped M0 (HMEC3, HMEC6, and HMEC9), even though these cells expressed dramatically less p16 than did the corresponding early-passage cells (Figure 3.4 and data not shown). At later stages of culture, however, cells with p16 CpG island methylation were detected. In E6-expressing HMEC6, methylation was first readily detected by the PCR assay at passage 25, and by passage 59, the p16 gene was predominantly methylated, although a low level (≈10% based on mixing experiments) of unmethylated p16 gene was still detected (Figure 3.4 C). E6-expressing HMEC9 exhibited a similar pattern; after M0 escape (passage 16), no methylation was detected, but subsequently (passage 44) the cells displayed a mixture of methylated and unmethylated p16 alleles (data not shown). E6-

expressing HMEC8 exhibited no evidence of p16 gene methylation up to passage 32, but only methylated alleles were detected by passage 41 (Figure 3.4 C). Therefore, the change in methylation status coincided with the elimination of p16 protein expression between passages 32 and 41. No p16 gene methylation was detected by the PCR assay in any of the cells expressing E7 alone (Figure 3.5 A), the three clones of late passage E6/E7-expressing HMEC8 (Figure 3.5 B), or the late-passage E6/E7-expressing HMEC9 (data not shown).

Because the PCR-based methylation assay is inherently limited to the detection of methylation within the short regions recognized by the methylation-specific primers, a sequencing approach was used to determine whether methylation was present in regions missed by the PCR assay. After sodium bisulfite modification, individual PCR products of the region from -159 to +135 (according to the numbering system of Hara et al. (Hara et al., 1996)), which contains 35 potential CpG methylation sites, were cloned, and four clones of each sample were sequenced. The results are summarized in Table 3.2. In HMEC6, methylation was detected on 0 or 1 CpG site at passage 3, 6 to 14 sites after M0 escape (passage 12), and 19 to 25 sites by passage 25. In E6-expressing HMEC9, 7 to 10 sites were methylated after M0 escape (passage 16) and 9 to 28 of the sites were methylated later (passage 42). In contrast, E6/E7-expressing HMEC9 (passage 32) contained no methylation in the four clones examined. The immortalized cell line H1618, which was used as a positive control for p16 methylation, contained methylation at all 35 CpG sites of all four clones (data not shown).

Surprisingly, a low level of p16 gene methylation was detected by the PCR assay in immortalized E6/E7-expressing HMEC6 (Figure 3.5 C). To further investigate this methylation, late-passage E6/E7-expressing HMEC6 were cloned and assayed individually for their p16 methylation status. Of 10 clones, six (C3, C6, C7, C8, C9 and C10) contained predominantly unmethylated p16, two (C1 and C2) contained predominantly methylated p16, and the other two (C4 and C5) contained mixtures of methylated and unmethylated alleles (Figure 3.5 C). Analysis of the viral integration sites of these clones by Southern blotting revealed that clones containing methylated or mixed p16 alleles (C1, C2, C4, and C5) originated from a single parent containing one viral integration. Clones containing unmethylated alleles originated from a single parent containing three viral integrations (C3, C6, C7, C8, and C10) or as many as five or six viral integrations (C9) (data not shown).

To assess whether the methylation was specific for p16, the methylation status of $p15^{INK4b}$ was determined. p15, like p16, is a member of the INK4 family of cyclin-dependent kinase inhibitors and is very similar to p16 both in terms of amino acid sequence and ability to specifically inhibit CDK4 and CDK6. It is located next to the p16 gene at chromosomal position 9p21. None of the cells tested showed evidence for p15 methylation, including all of those in which p16 methylation was detected (data not shown). Therefore, the methylation was specifically selected for in the p16 CpG island.

DISCUSSION

The results presented here show that the Rb-binding region of E7 is required to allow cells to bypass M0, consistent with a role for Rb or related proteins in mediating the M0 proliferation block. Three distinct mutations within the LXCXE Rb-binding motif of HPV-16 E7 (Δ21-24, C24G, and E26G) each resulted in failure to allow M0 bypass. One mutation, HPV-16 E7H2P, which does not disrupt Rb-binding, also failed to allow M0 bypass. However, HPV-16 E7H2P is defective in its ability to dissociate E2F from Rb *in vitro* (unpublished data). The reason why HPV-16 E7D21S was less effective than wild-type HPV-16 E7 in allowing M0 bypass, despite its having the ability to bind Rb and p107 and dissociate Rb/E2F complexes, could be subtle defects in its interaction with Rb-related proteins that are not apparent in the *in vitro* assays. Alternatively, D21S may be defective in some other activity that is needed for full wild-type HPV-16 E7 function. It is worth noting that the ability of E7 to bind Rb is not sufficient for its ability to transform rodent cells (Banks et al., 1990) or abrogate growth arrest signals induced by DNA damage, transforming growth factor-β, or suprabasal quiescence (Demers et al., 1996). Conversely, the ability of HPV-16 E7 to bind Rb is not essential for its ability to immortalize human keratinocytes in the context of the full HPV-16 genome (Jewers et al., 1992). Recently, HPV-16 E7 has been shown to inactivate the ability of p27 and p21 to inhibit cyclin-dependent kinases (Funk et al., 1997; Zerfass-Thome et al., 1996). Therefore, activities other than binding to Rb are likely to contribute to full wild-type HPV-16 E7 function.

What mechanisms are involved in arrest at M0? Analysis of cell cycle-related proteins revealed that Rb accumulated in the hypophosphorylated form and its level of expression decreased as the early-passage HMEC aged in culture, consistent with its playing a role in blocking proliferation at M0. The level of cyclin A was dramatically reduced as cells arrested at M0, presumably as a consequence of arrest in G1 (Foster and Galloway, 1996). The levels of CDK2 and CDK4 also decreased, but only as a late event. Expression of CDK inhibitors p21 and p27 declined, while the level of p16 increased. An increase in the level of p16 in aging cells is consistent with the results of other studies with human keratinocytes, uroepithelial cells, and fibroblasts, which show increases in p16 levels as the cells enter senescence (Alcorta et al., 1996; Hara et al., 1996; Loughran et al., 1996; Reznikoff et al., 1996). Whether the observed increase in the p16 level would be sufficient to arrest the cells or whether additional factors, such as the decrease in the CDK4 level, are important is not clear. Nevertheless, this increase in the p16 level, the emergence of cells having low levels of p16 expression, and the observation that the Rb-binding region of E7 was important to allow cells to bypass M0, point to p16 as being a proliferation-limiting factor at M0.

Other studies have reported loss of p16 expression in cultured cells. Reznikoff *et al.* (Reznikoff et al., 1996) reported loss of p16 expression in human uroepithelial cells immortalized by E6 but not those immortalized by E7. In that study, hemizygous p16 deletions appeared to be involved in p16 inactivation. Noble *et al.* (Noble et al., 1996) also reported loss of p16 expression at or prior to immortalization in fibroblasts derived from a patient with Li-Fraumeni syndrome and human mesothelial cells that had been

transfected with HPV-16 E6/E7, although not all cells that lost p16 expression became immortalized. Where examined, homozygous p16 deletion appeared to account for the lack of p16 expression (Noble et al., 1996). Loughran *et al.* (Loughran et al., 1996), reported the loss of p16 expression in immortalized cancer-derived keratinocytes, although two cultures lost p16 expression but did not become immortalized. p16 expression was reactivated by 5-azacytidine treatment, suggesting inactivation by methylation (Loughran et al., 1996). Brenner and Aldaz (Brenner and Aldaz, 1995) reported homozygous deletion of p16 in two immortalized human mammary epithelial cell lines and LOH at the p16 locus (9p21) coupled with a nonsense mutation in the remaining allele in another line.

Our study is consistent with the above reports, but is unique in several respects. Loss of p16 expression was observed in normal, non-cancer-derived HMEC that had not been immortalized or exposed to viral oncogenes, i.e., HMEC4. Loss of p16 expression was correlated with escape from M0 and was evident at the p16 mRNA level. As in the above studies, loss of p16 expression was not sufficient for immortalization, and these cells underwent senescence. Importantly, senescence of the HMEC4 culture was not associated with re-expression of p16; instead, high levels of p53, p21, and p27 were present. Therefore, two different mechanisms appear to limit the life span of HMEC in culture, the first involving the Rb/p16 pathway and the second involving p53, p21, and possibly p27. This would be consistent with the observation that E7 alleviates M0 by inactivating Rb but does not readily immortalize HMEC, whereas E6, by inactivating

p53, readily immortalizes HMEC that have previously escaped M0 (Band et al., 1991; Shay et al., 1993).

In contrast to published reports of experiments with other cell culture systems, we found that methylation, rather than deletion, was associated with p16 inactivation in the HMEC that escaped M0. We had expected to find deletions, especially in the E6-expressing cells, because of the dramatic shutoff of p16 expression and the fact that E6 effectively renders the cells negative for p53, thus creating an environment in which genetic changes would be tolerated. However, no 9p21 LOH was detected among 30 clones of E6-expressing cells, 20 of which had been in culture for over 100 population doublings. Studies of primary breast tumors indicate that homozygous deletions in p16 are not common (0 of 37 and 0 of 5) (Herman et al., 1995; Xu et al., 1994). In one study, 14 of 24 primary breast tumors revealed LOH or allelic imbalance at the p16 locus (Brenner and Aldaz, 1995). However, mutations were not detected in the remaining alleles (Brenner and Aldaz, 1995), suggesting that p16 is not the target of these deletions or that another mechanism exists to inactivate the remaining p16 allele. Importantly, Herman *et al.* (Herman et al., 1995) found p16 CpG island methylation in 5 of 16 primary breast cancers, suggesting that methylation is a common mechanism of p16 inactivation *in vivo*. This finding may well explain why 9p21 LOH is not always coupled to mutation of the remaining p16 allele and why some tumors show no apparent alterations in p16 (Wong et al., 1997). Our finding that E6-expressing HMEC contained p16 CpG island methylation is consistent with the observations of p16 methylation in primary breast tumors (Herman et al., 1995). The finding that the p15 CpG island was not methylated in

any HMEC suggests that p15 methylation was not selected for during culture, similar to results from many primary tumors (Herman et al., 1996; Wong et al., 1997).

The cell culture system allowed a more detailed examination of p16 expression and methylation over time than would be possible in studies of human tumors. Upon escape from M0, p16 expression was reduced at the protein and mRNA levels in E6-expressing HMEC6 and HMEC9 but no p16 deletions were detected. Analysis of the p16 promoter region CpG island for methylation by the PCR-based assay revealed methylation only in the later-passage cells and thus did not explain the initial downregulation of p16. However, a more detailed methylation analysis based on DNA sequencing of all 35 CpG sites in the p16 promoter region from -159 to +135 revealed partial methylation among the cells that escaped M0. At later stages, the E6-expressing cells showed a further decrease in p16 levels and increased CpG island methylation. Sequencing confirmed that at later passages, methylation had extended to sequences recognized by the methylation-specific primers. Evidence that CpG methylation can spread from an initial methylated seed patch comes from studies of methylation spreading within the adenovirus E2A promoter (Toth et al., 1989). Thus, the increased methylation observed over time could be explained by a spreading mechanism.

It was apparent from the expression data that the majority of the p16 inactivation occurred early after M0 escape when relatively few CpG sites were methylated, suggesting the possibility that initially, specific methylation sites are more important than the total number of methylated sites in p16 inactivation. Only at later passages was methylation readily detected in the PCR assay. How does the initial methylation event(s)

occur? The leading hypothesis is that initial methylation occurs by chance followed by clonal selection of cells with progressively inactivated growth-inhibitory genes (Jones, 1996). The initial methylation event(s) could have occurred *in vivo*, during culture, or both. Our results that E6-expressing cells are more likely to escape M0 than are uninfected cells raises the question of whether E6 expression increases the frequency of unrepaired random methylation events. Currently, there is insufficient data to make an argument either way. However, a recently published report suggests that proliferating cell nuclear antigen (PCNA) interacts with and possibly regulates the activity of DNA (cytosine-5)-methyltransferase (Chuang et al., 1997). p21 regulates the PCNA/DNA (cytosine-5)-methyltransferase interaction by competing for binding to PCNA (Chuang et al., 1997). Thus, it is possible that E6, by disrupting the ability of p53 to transactivate p21 expression, causes disregulated methylation. E7 has been shown recently to disrupt the interaction between p21 and PCNA (Funk et al., 1997) and thus could also potentially cause disregulated methylation. Clearly, further work is needed to sort out these possibilities.

The finding that p16 continued to be expressed after M0 in cells that express E7 or E6/E7 suggests that E7 can obviate the selection pressure against p16. No p16 methylation was detected in any of the E7-expressing cells or in the majority of E6/E7-expressing cells by the PCR assay. Strikingly, E6/E7-expressing HMEC9 did not contain a single methylated site in our sequencing analysis. However, some clones of E6/E7-expressing HMEC6 did contain methylation. These clones contained a single copy of

E6/E7 (whereas others contained multiple copies), suggesting that lower levels of E7 may be insufficient to completely inactivate Rb.

Thus, we suggest the following model to explain inactivation of the Rb/p16 pathway in HMEC. Expression of E7 inactivates Rb directly, allowing cells to bypass M0. In cells not expressing E7, a selection pressure against the Rb/p16 pathway results in the selection of cells expressing low levels of p16 during M0 escape. p16 gene inactivation is associated with limited methylation within the p16 CpG island. This region of methylation may spread over time to result in more complete gene inactivation. A more extensive analysis would be needed to determine whether methylation of specific regions of the CpG island is associated with the initial downregulation of p16 and to conclusively document the spreading of methylation.

The finding of p16 methylation in the E6-expressing cells correlates well with the finding that CpG island methylation is a mechanism of p16 inactivation in the development of human tumors, including breast cancer (Herman et al., 1995; Merlo et al., 1995). Thus, the *in vitro* culture system recapitulates this aspect of breast tumor biology and provides a useful model for further understanding events in neoplastic progression.

Figure 3.1. Analysis of different E7 proteins for their abilities to allow M0 bypass in HMEC. (A) Abilities of HMEC expressing different E7 proteins to bypass M0. -, the cells behaved very similarly to uninfected or LXSN-infected controls; +, some activity, but less than that of HPV-16 E7; +++, wild-type HPV-16 E7 activity. Results are shown for uninfected HMEC6 (UN), HMEC6 infected with LXSN retroviral vector (LXSN), or LXSN containing HPV-16 E7, HPV-6 E7, HPV-16 E7D21S, HPV-16 E7Δ21-24, HPV-16 E7C24G, HPV-16 E7E26G, or HPV-16 E7H2P. (B) Western blot for cyclin A in HMEC6 expressing different E7 proteins. (C) Immunoprecipitation with HPV-16 E7 polyclonal antibody of ^{35}S-labeled HMEC4 expressing the indicated E7 proteins to demonstrate expression. PRE denotes use of nonimmunized rabbit serum. (D) Immunoprecipitation as in panel C but with HPV-6 E7 polyclonal antibody.

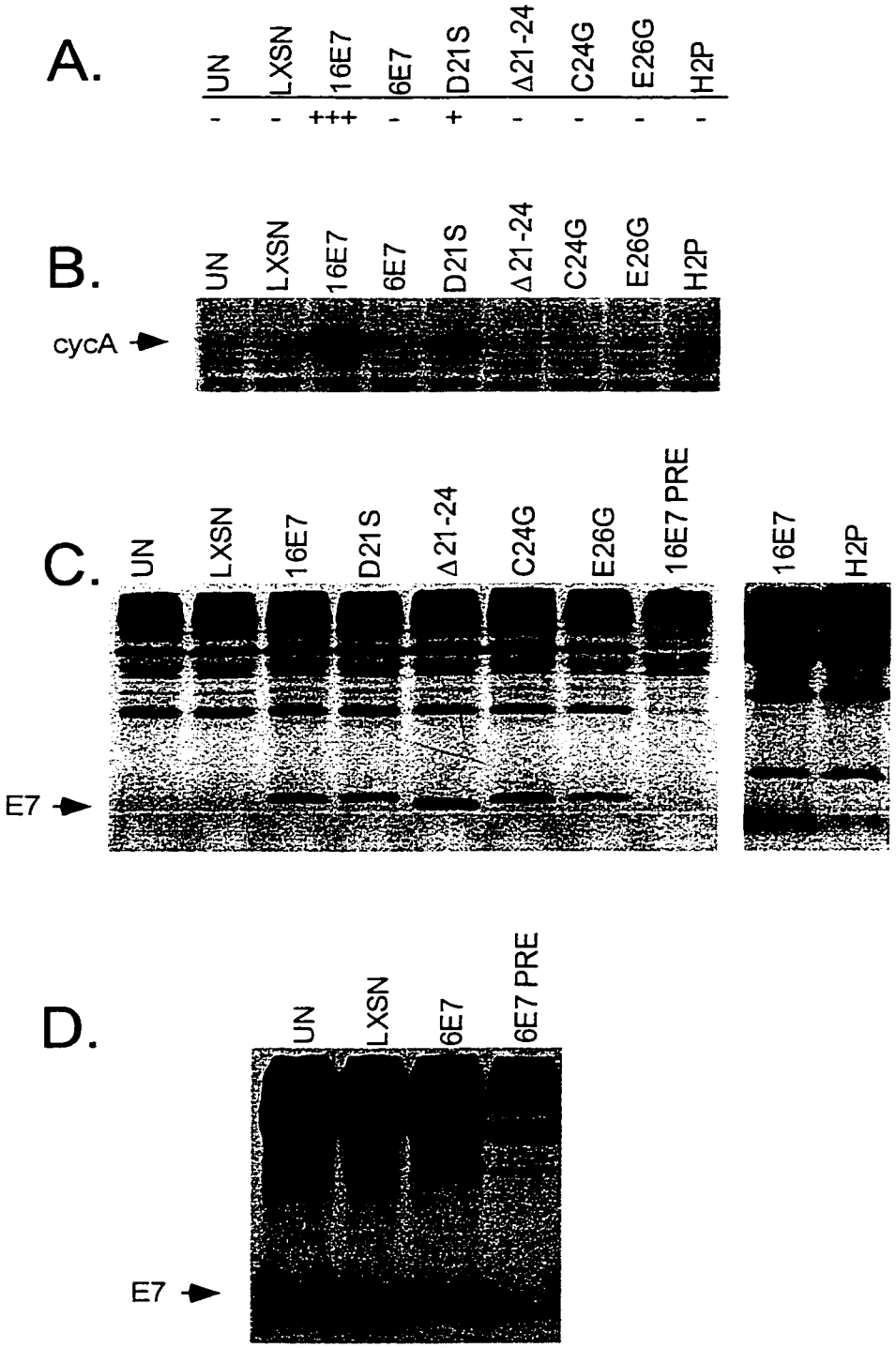
A.
UN
LXSN
16E7
6E7
D21S
Δ21-24
C24G
E26G
H2P
-
-
++
-
+
-
-
-
-
B.
UN
LXSN
16E7
6E7
D21S
Δ21-24
C24G
E26G
H2P
cycA
C.
UN
LXSN
16E7
D21S
Δ21-24
C24G
E26G
16E7 PRE
16E7
H2P
E7
D.
UN
LXSN
6E7
6E7 PRE
E7

Figure 3.2. Western blots for cell cycle-related proteins in HMEC9. Cells were harvested early after establishment of the culture (passage 3) and at subsequent passages through passage 7, when the cells were predominantly in M0. The blots were probed with the indicated antibodies.

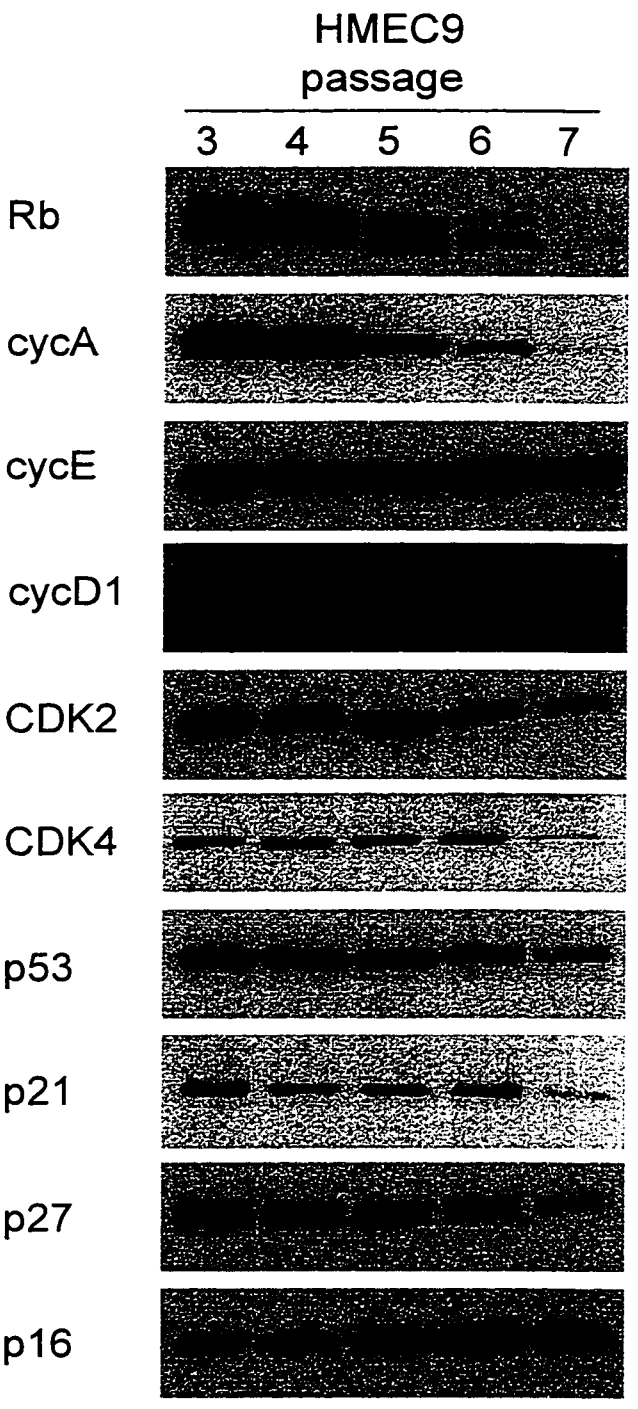
HMEC9
passage
3
4
5
6
7
Rb
cycA
cycE
cycD1
CDK2
CDK4
p53
p21
p27
p16

Figure 3.3. Expression of p16 in HMEC1 and HMEC3 before and after M0. Western blots for p16 in uninfected early passage cells before M0 (E.P.), cells expressing E6 after escaping from M0 (E6), or cells expressing E7 or E6/E7 after bypassing M0 (E7, E6/E7).

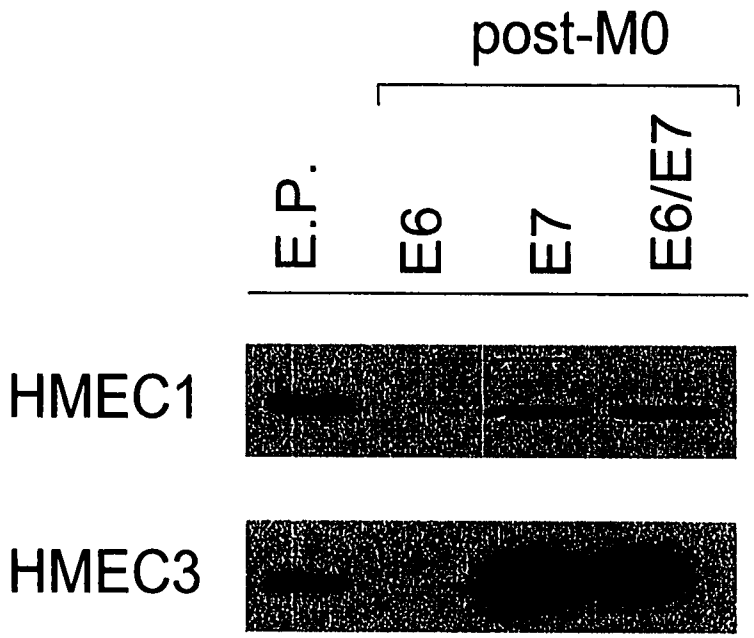
post-M0
E.P.
E6
E7
E6/E7
HMEC1
HMEC3

Figure 3.4. Expression and methylation-specific PCR analyses of p16 in HMECs. Passage numbers are indicated above the lanes. M0 usually occurred around passage 7 to 10, as indicated; M1 for uninfected cells usually occurred around passage 20. UN, uninfected HMEC. E6 or E6/E7, HMEC infected with E6- or E6/E7-expressing retrovirus. (A) Western blots for p16 and p27. Numbers in brackets below the lanes indicate the relative amounts of p16. (B) Northern blots for p16 exon 1 with 36B4 loading control. Numbers in brackets below the lanes indicate the relative amounts of p16 mRNA normalized for 36B4. (C) p16 promoter CpG island methylation assay. U and M indicate the primer pairs specific for unmethylated and methylated p16 CpG islands, respectively. Molecular size markers (in base pairs) are indicated in the far left lane. H249 and H1618 are lung cancer cell lines used as controls for unmethylated and methylated p16 alleles, respectively.

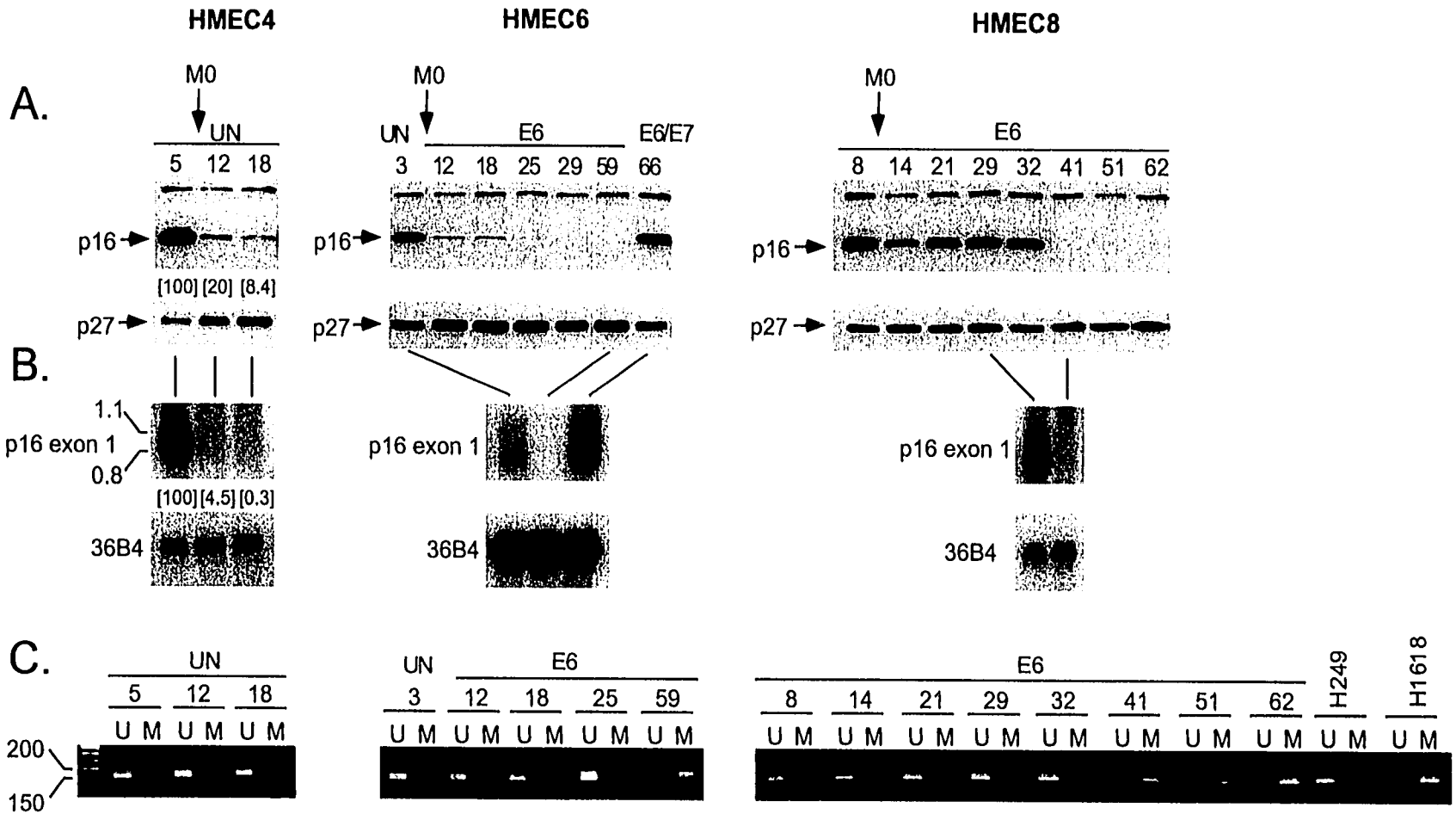
HMEC4
HMEC6
HMEC8
A.
M0
UN
E6
E6/E7
5 12 18
3 12 18 25 29 59 66
8 14 21 29 32 41 51 62
p16
[100] [20] [8.4]
p27
B.
1.1
p16 exon 1
0.8
[100] [4.5] [0.3]
36B4
C.
UN
E6
5 12 18
3 12 18 25 59
8 14 21 29 32 41 51 62
U M
200
150
H249
H1618

Figure 3.5. Methylation-specific PCR analysis of p16 in E7 and E6/E7-expressing HMECs. (A) E7-expressing cells (HMEC1, passage 15; HMEC3, passage 23; HMEC6, passage 16; and HMEC8, passage 24). (B) Clones of E6/E7-expressing HMEC8 (passage 50). (C) E6/E7-expressing HMEC6, pooled population (passage 66), and clones thereof. Primers specific for unmethylated (U) or methylated (M) p16 promoter regions are indicated. H249 and H1618 are described in the legend to Figure 3.4.

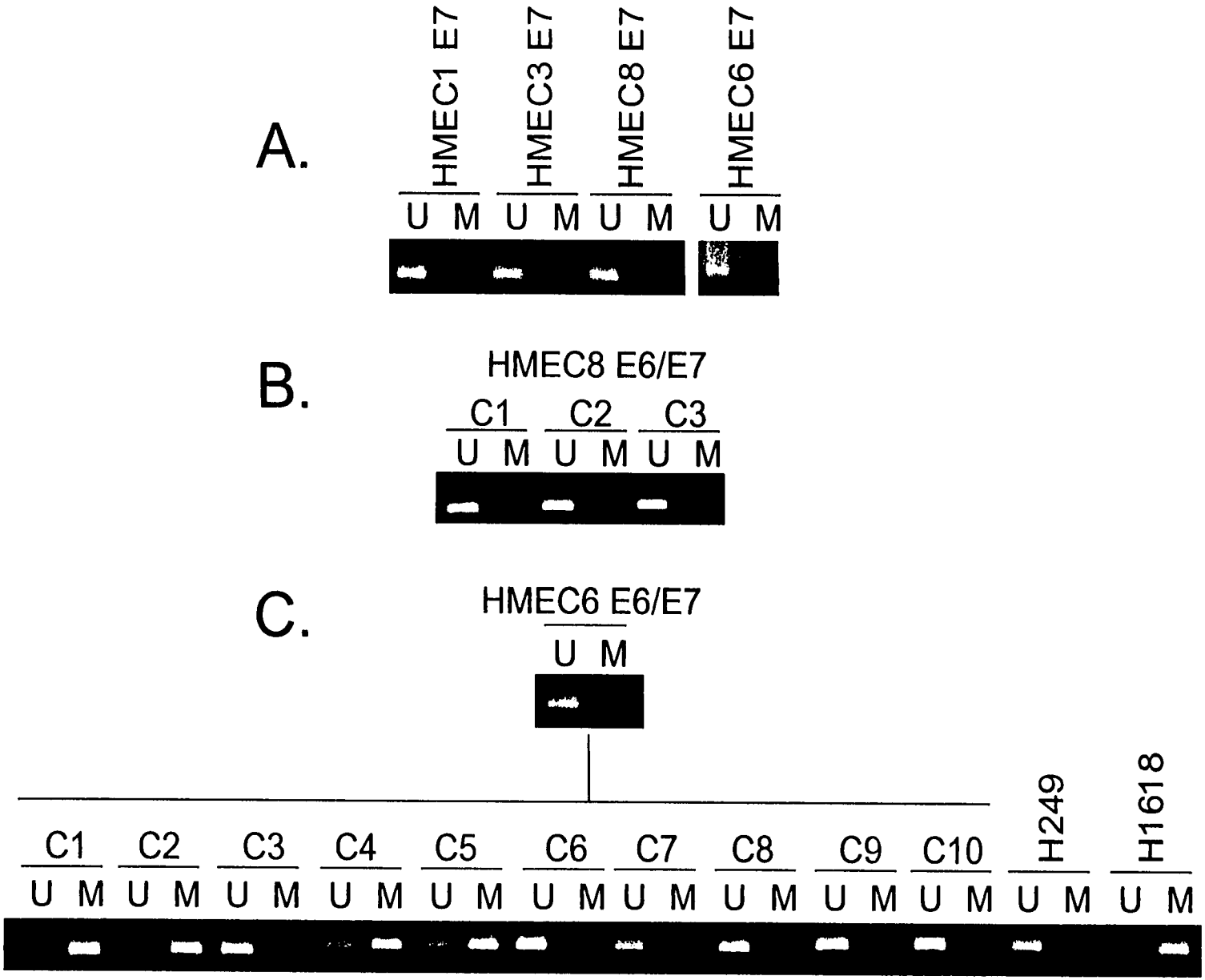
A.
HMEC1 E7
HMEC3 E7
HMEC8 E7
HMEC6 E7
U M U M U M U M
B.
HMEC8 E6/E7
C1 C2 C3
U M U M U M
C.
HMEC6 E6/E7
U M
C1 C2 C3 C4 C5 C6 C7 C8 C9 C10 H249 H1618
U M U M U M U M U M U M U M U M U M U M U M U M

Table 3.1. Effects of E6 and E7 on proliferation of HMEC in culture.

Cell strain[a]	Vector[a]	M0[b]	Immortalization[b]
HMEC1[c]	UN/LXSN	-	-
	E6	+ (escape)	ND
	E7	+ (bypass)	ND
	E6/E7	+ (bypass)	+
HMEC3[c]	UN/LXSN	-	-
	E6	+ (escape)	ND
	E7	+ (bypass)	ND
	E6/E7	+ (bypass)	+
HMEC4	UN	+ (escape)	-
HMEC6	UN/LXSN	-	-
	E6	+ (escape)	+
	E7	+ (bypass)	-
	E6/E7	+ (bypass)	+
HMEC8	UN/LXSN	-	-
	E6	+ (escape)	+
	E7	+ (bypass)	-
	E6/E7	+ (bypass)	+
HMEC9	UN/LXSN	-	-
	E6	+ (escape)	+
	E6/E7	+ (bypass)	+

[a] HMEC strains were infected with the indicated retroviruses or not infected (UN).

[b] The ability of the cells to escape (or bypass) M0 and to yield immortalized cells is indicated. ND, not done. See reference (Foster and Galloway, 1996) for a description of M0 escape versus M0 bypass.

[c] Results for HMEC1 and HMEC3 are from ref. (Foster and Galloway, 1996).

Table 3.2. p16 CpG methylation sequencing analysis of HMECs[a].

	HMEC6		HMEC9	
	Clone[b]	Methylation[c]	Clone[b]	Methylation[c]
Early passage	Passage 3		ND[d]	
Without E6	Clone A	0		
	Clone B	1		
	Clone C	1		
	Clone D	0		
After M0 escape	Passage 12		Passage 16	
With E6	Clone A	6	Clone A	8
	Clone B	6	Clone B	9
	Clone C	14	Clone C	10
	Clone D	10	Clone D	7
Later passage	Passage 25		Passage 42	
With E6	Clone A	19	Clone A	17
	Clone B	20	Clone B	28
	Clone C	25	Clone C	9
	Clone D	19	Clone D	18
Later passage	ND		Passage 32	
With E6/E7			Clone A	0
			Clone B	0
			Clone C	0
			Clone D	0

[a] Methylation in the p16 CpG island region from -159 to +135 (according to the numbering system of Hara *et al.* (Hara et al., 1996)), with +1 being the translational start site) which contains 35 CpG dinucleotides.

[b] Each clone represents an individual PCR product.

[c] Each value is the number of methylated sites out of the 35 CpG sites.

[d] ND, not done.

CHAPTER 4: PROGRESSIVE REGION-SPECIFIC DE NOVO METHYLATION OF THE $p16^{INK4a}$ CpG ISLAND IN PRIMARY HUMAN MAMMARY EPITHELIAL CELLS

ABSTRACT

CpG island methylation plays an important role in normal cellular processes, such as genomic imprinting and X-inactivation, as well as in abnormal processes, such as neoplasia. However, the dynamics of de novo CpG island methylation, during which a CpG island is converted from an unmethylated, active state to a densely methylated, inactive state, are largely unknown. It is unclear whether the development of de novo CpG island methylation is a progressive process, in which a subset of CpG sites are initially methylated with a subsequent increase in methylation density, or a single event, in which the initial methylation event encompasses the entire CpG island. The tumor suppressor gene, $p16^{INK4a}$, is inactivated by CpG island methylation during neoplastic progression in a variety of human cancers. We investigated the development of methylation in the p16 CpG island in primary human mammary epithelial cell strains during escape from mortality stage 0 (M0) growth arrest. The methylation status of 47 CpG sites in the p16 CpG island on individual DNA molecules was determined by sequencing PCR clones of bisulfite-treated genomic DNA. The p16 CpG island was initially methylated at a subset of sites in three discrete regions in association with p16 transcriptional repression and escape from M0 growth arrest. With continued passage,

methylation gradually increased in density and expanded to sites in adjacent regions. Thus, de novo methylation in the p16 CpG island is a progressive process that is neither site-specific nor completely random but instead is region-specific. Our results suggest that early detection of methylation in the CpG island of the p16 gene will require methylation analysis of the three regions and that the identification of region-specific methylation patterns in other genes may be essential for an accurate assessment of methylation-mediated transcriptional silencing.

INTRODUCTION

The methylation of CpG islands plays a critical role in heritable states of gene expression. De novo CpG island methylation is established during gametogenesis at imprinted loci as well as during early development in X inactivation, resulting in the stable maintenance of monoallelic expression in somatic cells (Riggs and Pfeifer, 1992; Surani, 1998). In addition, de novo methylation occurs aberrantly during neoplastic progression as well as in fragile X syndrome, resulting in stable transcriptional silencing of the methylated genes (Baylin et al., 1998; Oberle et al., 1991). The differential methylation patterns of the active and inactive states have been extensively studied by comparing the alleles on active and inactive X chromosomes, maternal and paternal alleles of imprinted genes, genes in normal and cancer tissue, and the FMR1 gene in males with normal X chromosomes and males with fragile X syndrome (Hornstra and Yang, 1994; Pfeifer et al., 1990; Stirzaker et al., 1997; Stoger et al., 1997; Tremblay et

al., 1997). Typically, the CpG island of a transcriptionally active allele is completely unmethylated, whereas the CpG island of a transcriptionally inactive allele is densely methylated. Although differential CpG island methylation has been extensively studied, the dynamics of de novo methylation in endogenous CpG islands that mediate the transition from the unmethylated, active state to the densely methylated, inactive state remain largely unknown. However, based on the differential CpG island methylation states, two models have been proposed for the de novo methylation process (Stirzaker et al., 1997). The first model proposes that de novo CpG island methylation is a progressive process in which a subset of sites are initially methylated, followed by an increase in methylation density. The alternative model proposes that de novo CpG island methylation is a single event that encompasses the entire CpG island and is stably maintained. In addition, it remains unclear whether the addition of methyl groups to specific sites or regions in the CpG island plays an important role in the de novo methylation process (Iguchi-Ariga and Schaffner, 1989; Riggs et al., 1998; Watt and Molloy, 1988).

In this study, we investigated the temporal development of methylation in the CpG island of the p16 gene, one of the most commonly inactivated tumor suppressor genes in human cancer (Sherr, 1996). The 5' CpG island of the p16 gene spans the putative transcription start sites and exon 1α, and has been found to be methylated at a high frequency in a variety of human cancers (Reed et al., 1996; Schutte et al., 1997; Wong et al., 1997). Thus, methylation-mediated silencing of the p16 gene is an important epigenetic event during neoplastic progression.

To investigate the temporal development of methylation in the p16 CpG island, we used primary human mammary epithelial cell strains (HMECs), which have previously been shown to undergo spontaneous selection for p16 transcriptional silencing by p16 CpG island methylation (Brenner et al., 1998; Foster et al., 1998; Huschtscha et al., 1998). HMECs, derived from normal breast tissue, undergo a proliferative block termed mortality stage 0 (M0), which is the first mortality stage of this cell type (Foster and Galloway, 1996; Foster et al., 1998). At M0, the cells enlarge and flatten, accumulate in G1 or G0, express senescence-associated β-galactosidase, and have increased p16 expression (Brenner et al., 1998; Foster and Galloway, 1996; Huschtscha et al., 1998; Stampfer, 1985). A small subpopulation of cells that can escape M0 is characterized by the methylation of the p16 CpG island and a marked decrease in p16 mRNA and protein levels. Human papillomavirus 16 (HPV16) E7, through its ability to disrupt Rb function, allows HMECs to bypass M0 arrest in the presence of abundant p16 (Foster and Galloway, 1996; Foster et al., 1998). In contrast, HMECs expressing HPV16 E6 arrest at M0 in the presence of abundant p16 and undergo a selection for p16 methylation similar that of normal cells, but unlike normal cells, the subpopulation that escapes M0 has an extended life span (Foster et al., 1998; Kiyono et al., 1998). Thus, inactivation of the Rb/p16 pathway by either p16 methylation or E7 expression allows the continued proliferation of HMECs past M0.

Using bisulfite genomic sequencing, we investigated the changes in methylation profiles of the p16 CpG island over time as normal and E6-expressing HMECs escaped M0 arrest and lost p16 expression. In contrast to methylation-sensitive restriction

enzymes that are limited to a subset of CpG cytosines, bisulfite genomic sequencing allows the analysis of the methylation status at each cytosine in a CpG island (Frommer et al., 1992). In addition, sequencing individual PCR clones of bisulfite-treated DNA allows the determination of the methylation profiles of individual DNA molecules (epigenotypes). In this study, we demonstrated that the subpopulation of HMECs escaping M0 arrest underwent methylation preferentially in three distinct regions of the p16 CpG island with associated loss of p16 mRNA and protein expression. With continued passage, this methylation in the HMECs expressing E6 increased in density and expanded to sites in adjacent regions of the p16 CpG island, demonstrating that de novo CpG island methylation is progressive and region-specific.

MATERIALS AND METHODS

Cell culture. HMEC cultures were derived from reduction mammoplasty specimens, as described previously (Foster et al., 1998). HMEC strains 4, 6, and 9 (HMEC4, HMEC6, and HMEC9, respectively) were derived from tissues of three patients. Cells were cultured in DFCI-1 medium (Band and Sager, 1989). LXSN-based retroviruses expressing HPV16 oncogenes (E6 and/or E7) (Halbert et al., 1991) were used to infect HMECs after the establishment of the cultures, followed by selection with 100 μg of G418 per ml. E6-expressing HMEC6, E6-expressing HMEC9, and E6/E7-expressing HMEC9 were used in this study, and each achieved greater than 50 passages. HMEC4 was not infected with E6 or E7 and achieved 20 passages. H249 and H1618, lung cancer

cell lines provided by J. Herman and S. Baylin, were used as controls for unmethylated and methylated p16 CpG islands, respectively (Herman et al., 1996).

Western analysis. Whole-cell protein extracts were used to prepare Western blots as described previously (Foster et al., 1998). Antibodies against p16 (PharMingen clone G175-405) and p27 (Transduction Laboratories no. K25020) were used as probes. Proteins were visualized with horseradish peroxidase-conjugated anti-mouse immunoglobulin G (Jackson Immunoresearch Labs) and chemiluminescence (kit from Dupont NEN). Quantification was done on a scanned image with ImageQuant software (Molecular Dynamics).

Northern analysis. Poly(A)$^+$ RNA was isolated from 100 μg of total RNA and used to prepare Northern blots as described previously (Foster et al., 1998). Blots were probed with a p16 exon 1 probe generated by PCR as described previously (Merlo et al., 1995) and labeled with [^{32}P]dCTP by using the random-primed DNA labeling kit (Boehringer Mannheim). The Northern blots were stripped and reprobed with 36B4 as an RNA-loading control (Laborda, 1991). Quantification was done on a phosphorimager with ImageQuant software (Molecular Dynamics).

Bisulfite conversion reactions. Bisulfite converts unmethylated cytosines to uracils whereas methylated cytosines are resistant to conversion. Bisulfite sequence analysis of the 200 CpG cytosines from the H249 cell line (unmethylated control) and the >14,000

non-CpG cytosines from all the samples in the study indicated that bisulfite conversion of unmethylated cytosines was at least 99.8% efficient. Analysis of the 185 CpG cytosines from the H1618 cell line (methylated control) indicated that methylation conferred at least 99.5% resistance to bisulfite conversion.

Total genomic DNA was extracted either with the QIAamp Blood Kit (Qiagen) or as described previously (Erlich, 1992). Bisulfite reactions were performed as described previously (Wong et al., 1997). Each DNA sample (75 to 150 ng) was denatured in freshly prepared NaOH at a final concentration of 0.3 M for 20 min at 42°C. A freshly prepared 3.8 M sodium bisulfite (Sigma) and 1.0 mM hydroquinone (Sigma) mixture (pH 5.0) was added to each sample, which was then incubated at 55°C for 6 to 8 h. The DNA samples were purified using QIAquick columns (Qiagen), desulfonated with NaOH at a final concentration of 0.3 M for 20 min at 37°C, and ethanol precipitated.

PCR amplification of bisulfite-treated DNA. Each bisulfite-treated DNA sample was whole genome-amplified using a degenerate 15-mer and the primer-extension preamplification (PEP) protocol in a final volume of 60 µl, as described previously (Zhang et al., 1992). p16-specific PCR amplifications were performed in a mixture containing 2 to 5 µl of PEP DNA, 200 µM dNTPs, 1.5 to 1.75 mM $MgCl_2$, 20 pmol of each primer, GeneAmp PCR buffer (Perkin-Elmer Corp.), and 1.25 units of AmpliTaq Gold (Perkin Elmer Corp.) in a final volume of 25 µl. Primer set A was described previously: 5' GTA GGT GGG GAG GAG TTT AGT T 3' (-355 to -334) and 5' TCT AAT AAC CAA CCA ACC CCT CC 3' (-95 to -73) (Gonzalgo and Jones, 1997). The

nucleotide positions are numbered relative to the translation start site (+1). Reaction conditions were as described previously, except with a 64°C annealing temperature. PCR product A starts just upstream of the transcription start sites and extends into the untranslated 5' sequence, and it contained 15 CpG and 61 non-CpG cytosines internal to the primers. Primer set B was described previously: 5' TTT TTA GAG GAT TTG AGG GAT AGG 3' (-159 to -136) and 5' CTA CCT AAT TCC AAT TCC CCT ACA 3' (+209 to +233) (Herman et al., 1996). PCR product B overlapped with the 3' end of PCR product A and extended to within a few bases of the 3' end of exon 1, and it contained 35 CpG and 48 non-CpG cytosines internal to the primers. Reaction conditions were as described previously, except with a 59°C annealing temperature. The overlapping regions share three CpG and five non-CpG cytosines. Both primer sets A and B allow determination of methylation on the coding strand of the p16 gene. All PCR reactions were performed using an MJ DNA Engine Tetrad Thermal Cycler (MJ Research, Inc.).

Cloning and sequencing PCR fragments amplified from bisulfite-treated DNA. PCR products A and B were purified from a 2% agarose gel using the QIAquick gel extraction kit (Qiagen). The gel purified PCR fragments were TA cloned with the pCR2.1 plasmid vector and INVαF'-competent cells (Invitrogen). Individual clones were sequenced with M13 forward and/or reverse primers on a PRISM 377 DNA Sequencer (Applied Biosystems), using PRISM dye primer or dye terminator cycle sequencing kit with AmpliTaq DNA polymerase (Applied Biosystems).

RESULTS

We used bisulfite sequencing to investigate the development of CpG island methylation in three independent HMEC strains: HMEC4, HMEC6, and HMEC9. Genomic DNA was treated with bisulfite and then the core region of the p16 CpG island, spanning the putative transcription start sites and exon 1α, was amplified with primer sets A and B (Figure 4.1). Cloned PCR products were sequenced, each clone representing an individual epigenotype of the cell population (Table 4.1). The H249 and H1618 cell lines, which were previously shown to have unmethylated and methylated p16 CpG islands, respectively, were used as controls for the bisulfite conversion reaction (Herman et al., 1996). Analysis of the H249 and H1618 cell lines and non-CpG cytosines, showed that the bisulfite conversion was at least 99.8% efficient and at least 99.5% specific. (Table 4.1; also see Materials and Methods).

Preferential methylation in three discrete regions of the p16 CpG island. We investigated the development of methylation in the p16 CpG island as HMECs were selected for p16 transcriptional silencing and escape from proliferation arrest at M0. The p16 CpG island in HMEC9 was almost completely unmethylated at passages 3 and 8 (Table 4.1 and Figure 4.2 A). At passage 16, the subpopulation of E6-expressing HMEC9 that escaped M0 arrest underwent methylation (Figure 4.2 B). The p16 CpG island was partially methylated with a mean of 11.8 methylated sites out of 47 CpGs (~25%) per DNA strand (Table 4.1). Strikingly, methyl groups were not distributed uniformly across the 47 CpG sites but instead were clustered in three different regions of

the p16 CpG island: CpGs 8 to 12 (-206 to -164) (region I), CpGs 23-29 (-18 to +35) (region II), and CpGs 37-45 (+101 to +186) (region III) (Figure 4.2 B). This region-specific methylation correlated with 80 and 90% decreases in mRNA and protein expression, respectively (Figure 4.3). In contrast, HMEC9 expressing E6 and E7, which bypassed M0 arrest with abundant p16 mRNA and protein expression, remained unmethylated, similar to HMEC9 before M0 escape (Table 4.1 and Figure 4.3). Therefore, the subpopulation of E6-expressing HMEC9 cells that escaped M0 arrest acquired a region-specific methylation pattern in the p16 CpG island with associated p16 transcriptional repression.

In HMEC6, a similar progression was observed. The p16 CpG island of pre-M0 HMEC6 was almost completely unmethylated at passage 3 (Figure 4.4 A), while post-M0 E6-expressing HMEC6 underwent p16 CpG island methylation at passage 12 (Figure 4.4 B), correlating with the loss of p16 expression (Foster et al., 1998). The p16 CpG island was again methylated in the region-specific pattern, with methyl groups clustered in three regions similar to those of HMEC9 (Figures 4.2 B and 4.4 B).

We also examined the development of p16 CpG island methylation in HMEC4, which, unlike the other two cell strains, did not express E6. Similar to those in HMEC6 and HMEC9, the p16 CpG island of pre-M0 HMEC4 was primarily unmethylated at passage 5 (Figure 4.4 D). Post-M0 uninfected HMEC4 acquired p16 CpG island methyl groups at passage 12 that also clustered in three regions similar to those of HMEC6 and HMEC9 (Figure 4.4 E) and correlated with the loss of p16 expression (Foster et al., 1998). Therefore, the region-specific pattern of p16 CpG island methylation and

associated transcriptional silencing were similar among all three cell strains and independent of E6 expression.

Progressive increase in methylation density in the p16 CpG island with continued passages. With increasing passage after M0 escape, the density of methylation in the p16 CpG island progressively increased. In HMEC9, the methylation density increased from a mean of 11.8 methylated sites (~25%) at passage 16 to means of 16.2 (~34%) at passage 29 and 23.0 (~49%) at passage 42 (Figure 4.2 C and D and Table 4.1). The frequency of methylation increased at CpG sites across the p16 CpG island, but the region-specific pattern was maintained. p16 protein levels continued to decrease between passages 16 and 42, but p16 mRNA levels were barely detectable by passage 16, probably, in part, due to the limited sensitivity of the Northern blot (Figure 4.3). A similar progression was observed in HMEC6. The methylation density increased across the p16 CpG island from a mean of 10.9 sites (~23%) at passage 12 to 20.6 (~44%) at passage 25 (Table 4.1 and Figure 4.4B and C). Thus, with continued passages, the methylation in the p16 CpG island increased in density. A statistically significant change in methylation density was not observed with continued passages of HMEC4, this was probably because of the short lifespan of this culture and the small sample of PCR clones (Table 4.1).

Despite an increase in methylation density, some CpG sites remained infrequently methylated in all three HMECs. CpG sites 1 to 5, which are upstream of region I and encompass the putative transcription start sites of the p16 gene, were rarely methylated in all three cell strains (Figures 4.2 B to D, 4.4 B to C, and 4.4 E). In addition, CpG site 20

(between regions I and II), as well as CpG sites 33 and 34 (between regions II and III), were methylated infrequently. Interestingly, although CpG site 44, within region III, was often methylated, this occurred at a notably lower frequency than methylation at the surrounding CpG sites in region III at each passage examined in all three HMECs. Thus, the region-specific methylation pattern in the p16 CpG island of the post-M0 HMECs was characterized not only by the three preferentially methylated regions but also by the sites at which methylation seldom occurred even at later passages.

Methylation in the p16 CpG island is region specific, but not site specific. Each individual p16 CpG island epigenotype in post-M0 HMEC6 and HMEC9 had methyl groups clustered in three regions (Figure 4.5 B and data not shown). In contrast, post-M0 HMEC4 had two distinct populations of p16 CpG island epigenotypes, one that underwent methylation (Figure 4.5 A, clones B1 to B9) and one that was almost completely unmethylated (Figure 4.5 A, clones B10 to B12). Each methylated epigenotype from post-M0 HMEC4 had a methylation pattern and density similar to those of the epigenotypes from post-M0 HMEC6 and HMEC9 (Figure 4.5 A and B and data not shown). Therefore, the methylated p16 CpG island epigenotypes had a consistent region-specific methylation pattern and density within a single HMEC strain as well as among all three cell strains.

Although methyl groups in each epigenotype were clustered in three regions, the p16 CpG island epigenotypes were rarely identical, having a variable subset of methylated sites in each of the regions (Figure 4.5). The specific CpG sites that were

methylated within each region, as well as the number of methylated sites in the p16 CpG island, varied among the individual epigenotypes in each of the three post-M0 HMECs. Each HMEC strain had a few particular CpG sites that were methylated in almost every clone, but these sites differed among the three cell strains. For example, for HMEC6 at passage 12, CpG site 46 was methylated in 11 of 12 clones, whereas for HMEC9 at passage 16, the same site was methylated in only one of 11 clones (Figures 4.2 B and 4.4 B). Thus, each post-M0 cell strain consisted of a heterogenous population of p16 CpG island epigenotypes, suggesting that although methylation in the p16 CpG island is region specific, it is not site specific.

Progressive expansion of methylation in the p16 CpG island. Analysis of individual p16 epigenotypes over time demonstrated that methylation expanded to encompass CpG sites outside of regions I, II, and III upon continued passage of both HMEC6 and HMEC9. For example, in E6-expressing HMEC9, all epigenotypes were methylated within CpG sites 26 to 28 in region II at passages 16 and 42 (Figures 4.2 B and D and 4.5 B and C). However, by passage 42, the majority of clones underwent methylation at adjacent sites, such as CpG sites 16 to 22, located 5' of region II. Our data suggest that methylation in the p16 CpG island progressively expanded to sites outside the three regions during continued passages.

Non-CpG methylation in the p16 CpG island. Although methylation is found primarily at CpG cytosines, a previous study using plasmid DNA transfected into mouse

cell lines demonstrated that methylation at CpNpG cytosines can be heritable (Clark et al., 1995). We found that CpNpG methylation was rare in the p16 CpG island (only 19 of the >5,000 sites, not including CGG sites), consistent with previous studies of other CpG islands (Stirzaker et al., 1997; Stoger et al., 1997). However, these CpNpG cytosines comprised the majority of non-converted non-CpG cytosines, specifically 19 of 25, 12 of which were CCG cytosines. Methylation of the outer cytosine in a CCG trinucleotide located in region II (CpG site 26) was detected in all three post-M0 passages of HMEC9 (one clone at passage 16, three clones at passage 29, and three clones at passage 42), suggesting that methylation at a CpNpG site in an endogenous gene can be maintained.

DISCUSSION

Our results clearly distinguish between existing models of de novo methylation of CpG islands. We have demonstrated that de novo methylation of the p16 CpG island developed initially at a small subset of sites and gradually increased in density, rather than occurring at once throughout the entire CpG island. This initial methylation at a subset of sites was associated with transcriptional silencing of the p16 gene and escape from growth arrest at M0. Moreover, the de novo methylation was neither site specific nor completely random but instead developed preferentially in three discrete regions of the p16 CpG island and progressively expanded to sites in the adjacent regions.

In this study, we performed a detailed investigation of the evolution of CpG island methylation at the resolution of individual DNA molecules in three independent primary HMECs as the p16 CpG island was converted from an unmethylated active state to a

densely methylated, inactive state during escape from proliferative arrest at M0 over a time course of 40 passages. Previous studies have extensively investigated end stages of the de novo methylation process by comparing alleles on active and inactive X chromosomes, maternal and paternal alleles of imprinted genes, genes in normal and cancer tissue, and the FMR1 gene in males with normal X chromosomes and males with fragile X syndrome (Hornstra and Yang, 1994; Pfeifer et al., 1990; Stirzaker et al., 1997; Stoger et al., 1997; Tremblay et al., 1997). Demonstrations of the unmethylated, active and the densely methylated, inactive states by these studies have suggested two models for the development of CpG island methylation: initial methylation at a subset of sites followed by an increase in methylation density (progressive model) or a single methylation event encompassing the entire CpG island (single-event model) (Stirzaker et al., 1997). We have demonstrated that the development of methylation in the CpG island of the p16 gene was initiated at a small subset of CpG sites clustered in three distinct regions, followed by an increase in methylation density and the expansion of methylation to neighboring regions. Thus, we have shown that de novo CpG island methylation is a progressive process, not a single event.

Previous studies using exogenously methylated genes, including p16, have shown that the methylation of only a subset of sites is sufficient for transcriptional repression of the transfected genes (Boyes and Bird, 1992; Gonzalgo et al., 1998; Hsieh, 1994; Kass et al., 1993). Consistent with these in vitro experiments, we have demonstrated in an endogenous system that the initial methylation of a subset of sites is associated with transcriptional downregulation and escape from proliferation arrest. Thus, our results

suggest a progressive model for p16 CpG island methylation in which a cell undergoes methylation at a subset of sites in a region-specific pattern and consequently gains a selective proliferative advantage because of decreased p16 gene activity.

p16 CpG island methylation was preferentially clustered in three discrete regions in each of the individual epigenotypes. Previous studies demonstrated that the methylation of specific sites can directly disrupt transcription factor binding and that the resulting transcriptional repression is highly site-specific, suggesting that site-specific methylation may be important in the regulation of gene expression (Iguchi-Ariga and Schaffner, 1989; Watt and Molloy, 1988). However, the specific CpG sites that were methylated within the three regions varied among the epigenotypes in the three HMEC strains, suggesting that methylation in the p16 CpG island was region specific rather than site specific. Previous studies of the CpG islands of the O^6-methylguanine-DNA methyltransferase gene in human tumor cell lines and the inactive-X-chromosome hypoxanthine phosphoribosyltransferase gene in mouse tumor cell lines similarly found regions of preferential methylation, suggesting that region-specific patterns may be a common feature of methylation in CpG island-containing genes (Park and Chapman, 1994; Qian and Brent, 1997; Watts et al., 1997). The basis for the regional differences in methylation that we have discovered is unclear and will require further investigation. They may be a result of regions having differential susceptibilities to the DNA methylase(s) or DNA demethylase(s) due to differences in primary DNA sequence, secondary structures, local chromatin structure, and DNA-binding proteins (Bestor, 1987; Bolden et al., 1986; Carotti et al., 1989; Yoder et al., 1997). For example, the three

preferentially methylated regions in the p16 CpG island may be more favorable substrates for the DNA methylase(s) or less favorable substrates for the DNA demethylase(s). Alternatively, the extent of transcriptional repression may differ depending on the regional location of methylation within the p16 CpG island. For example, methylation at CpG sites within the three regions may result in a greater degree of transcriptional downregulation than methylation at sites outside those regions. Clonal selection of cells with lower p16 expression and higher proliferation rates would result in a population with preferentially methylated regions. Thus, region-specific p16 CpG island methylation suggests that the de novo methylation process is influenced by differences in the susceptibilities to DNA methylase(s) or DNA demethylase(s) and/or in the degree of methylation-mediated silencing.

Although methyl groups were preferentially clustered in the three regions, the methylation patterns of p16 CpG island epigenotypes were highly variable throughout the de novo methylation process. Molecule-to-molecule variation in methylation patterns have been similarly observed for densely methylated CpG islands in other tissue culture systems, in tumor tissue, and in leukocytes from males with fragile X syndrome, suggesting that the variability of methylation patterns is characteristic of methylated alleles (Pfeifer et al., 1990; Silva et al., 1993; Stoger et al., 1997). This complex heterogeneity of the p16 CpG island epigenotypes is consistent with a dynamic, stochastic methylation model proposed by Pfeifer et al., which predicts that the de novo methylation process is an interplay of methyl group gain by a de novo methylase and a maintenance methylase and of methyl group loss by a demethylase and errors of the maintenance

methylase (Pfeifer et al., 1990; Riggs et al., 1998). According to this model, the different frequencies of methylation at each CpG site in a cell population are the result of differential probabilities of methylation gain and loss at each site.

The HMECs expressing E6 (HMEC6 and HMEC9) had a longer life span after M0 escape, enabling investigation of methylation at later passages. As the E6-expressing cells continued to divide after M0 escape, the methylation density in the p16 CpG island increased, expanding from sites in the three preferentially methylated regions to sites in adjacent regions. The progressive increase in the methylation density in the p16 CpG island correlated with further reduction in p16 protein levels and with p16 mRNA levels, which were barely detectable due to the limited sensitivity of the Northern blot analysis (Figure 4.3) (Foster et al., 1998). Expansion of methylation may be important for the further reduction in gene expression or for increasing the stability of methylation-mediated transcriptional repression (Boyes and Bird, 1992; Gonzalgo et al., 1998; Hsieh, 1994).

The basis for the progressive nature of the de novo methylation process that we have discovered remains unknown. This progressive process may be a result of increases in the levels of a DNA methylase or decreases in the levels of a DNA demethylase, both of which may increase the de novo methylation rate (Vertino et al., 1996). Previous studies have demonstrated that *cis*-acting Sp1 elements protect CpG islands from de novo methylation, suggesting that the progressive methylation may be due to decreases in the levels of the *trans*-acting factors that interact with these Sp1 elements (Brandeis et al., 1994; Macleod et al., 1994). Alternatively, the methylation could be purely a result of a

progressive accumulation of stochastic errors by a DNA methylase or a DNA demethylase combined with clonal selection (Jones, 1996). In addition, the progressive methylation process may be due to an initial methylation rendering other sites in the CpG island more susceptible to methylation (Carotti et al., 1998; Toth et al., 1989).

We and others have demonstrated that p16 expression is generally silenced by biallelic methylation in HMEC subpopulations that escape M0 (Foster et al., 1998; Huschtscha et al., 1998). Each p16 CpG island epigenotype in post-M0 HMEC6 and HMEC9 underwent methylation in the region-specific pattern, and these post-M0 populations remained heterozygous at the 9p21 locus (data not shown) (Foster et al., 1998). In contrast, post-M0 HMEC4 had two subpopulations of epigenotypes: a major one with a methylation pattern and density similar to those of post-M0 HMEC6 and HMEC9 and a minor one that was essentially unmethylated. The subpopulation of the HMEC4 cells with unmethylated epigenotypes may have been inactivated by an alternative mechanism. We previously reported that three of 10 clones of post-M0 HMEC4 had homozygous deletions at the c5.1 STS marker located just 3' of p16 exon 2 which have also been frequently observed in cell lines and primary tumors (An et al., 1996; Cairns et al., 1995; Caldas et al., 1994; Foster et al., 1998). Thus, p16 expression in HMECs is usually transcriptionally silenced by biallelic methylation and possibly inactivated at a lower frequency by homozygous deletion.

An important implication of our results lies in screening for p16 inactivation in cancer. Our data suggest that CpG sites within the three preferentially methylated regions may serve as better markers for methylation-mediated transcriptional silencing of the p16

gene. p16 CpG island methylation is currently screened for by methylation-specific PCR or methylation-sensitive restriction enzymes. We previously demonstrated that the original p16 methylation-specific PCR primers did not detect p16 methylation in the HMECs until many passages after p16 transcriptional repression (Foster et al., 1998). These methylation-specific PCR primers assay CpG sites 16 to 18 and 30 to 33 (Herman et al., 1996), which we show here are outside of the three preferentially methylated regions in the p16 CpG island. Similarly, almost all methylation-sensitive restriction enzymes, which have been used in other studies to screen for p16 methylation, are specific for sites outside of the three regions (Gonzalez-Zulueta et al., 1995; Herman et al., 1995; Merlo et al., 1995). Thus, our results suggest that screening by these methods may be subject to false negatives that would underestimate the frequency of p16 methylation in cancerous or precancerous conditions. Further investigation of primary tumor tissue will be necessary to determine if the region-specific methylation pattern and the subsequent expansion of methylation are characteristic of neoplastic progression *in vivo*. Characterization of the methylation patterns in tumor suppressor genes may be essential for the early detection of epigenetic lesions during premalignant stages of cancer.

In summary, our results demonstrate that de novo methylation of the p16 CpG island initially develops at a subset of sites within discrete regions and then gradually increases in density and expands to sites in adjacent regions. Thus, de novo methylation is a progressive process rather than a single event and is neither site specific nor completely random but instead is region specific.

Figure 4.1. Genomic map of the 5' CpG island of the p16 gene. This CpG map is based on published genomic DNA sequences (GenBank accession no. AF022809, U12818, and AC000048). CpG sites and their genomic positions within 1.2 kb of the p16 CpG island (-621 to +521) are represented by vertical lines at the top. Nucleotide positions are numbered relative to the translation start site (+1). The genomic positions of the putative transcription start sites for the p16 gene are represented by arrows. The coding region of exon 1α is shown. The gray bar at the bottom represents a magnification of the region from -355 to +233 that was analyzed for methylation in this study. The 47 CpG sites (black boxes within the gray bar) in this region are numbered according to their 5'-to-3' order in the p16 genomic sequence and positioned based on their location within the genomic sequence. PCR products A (-355 to –73) and B (-159 to +233), amplified from bisulfite-treated DNA for sequencing, are shown.

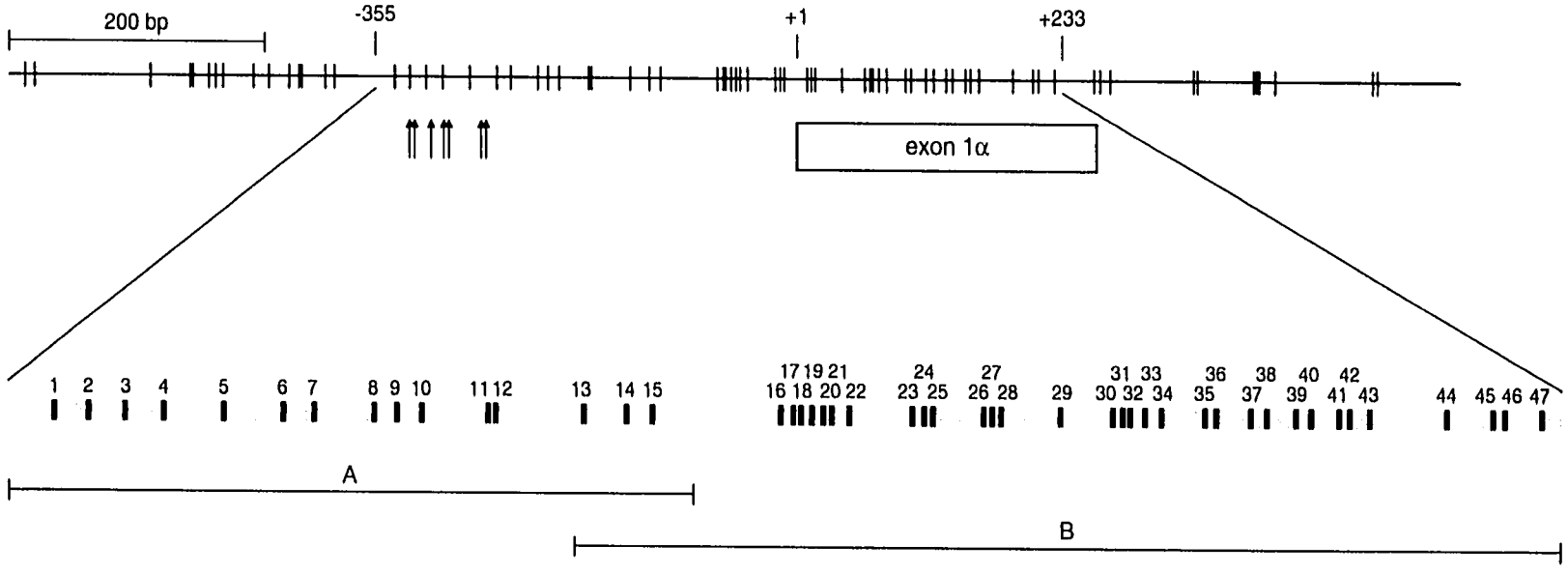
200 bp
-355
+1
+233
exon 1α
1 2 3 4 5 6 7 8 9 10 11 12 13 14 15
16 17 18 19 20 21 22
23 24 25
26 27 28
29
30 31 32 33 34
35 36
37 38
39 40
41 42 43
44
45 46 47
A
B

Figure 4.2. Development of methylation in the p16 CpG island of HMEC9. The 47 CpG sites are in numerical order according to their 5'-to-3' order in the p16 genomic sequence (-355 to +233). CpG sites are not spaced out on the x-axis according to their relative positions in the p16 genomic sequence. Percent methylation at each CpG site was calculated as the percentage of clones with a methylated cytosine at that site. Percent methylation for CpGs 13, 14 and 15 was calculated from data from clones of both PCR products A and B.

A. HMEC9 Passage 8

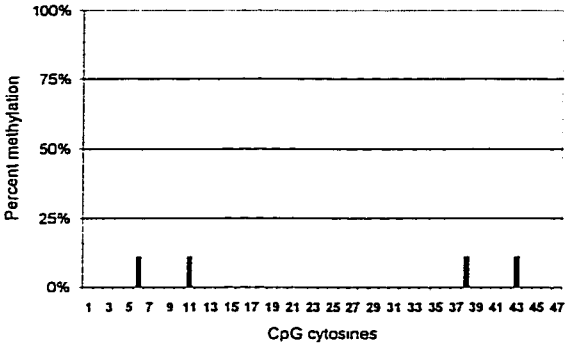

B. HMEC9 E6 Passage 16

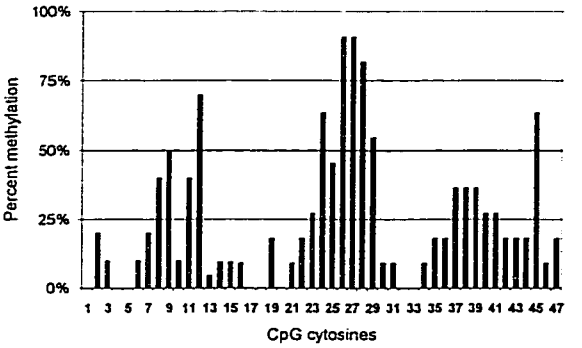

C. HMEC9 E6 Passage 29

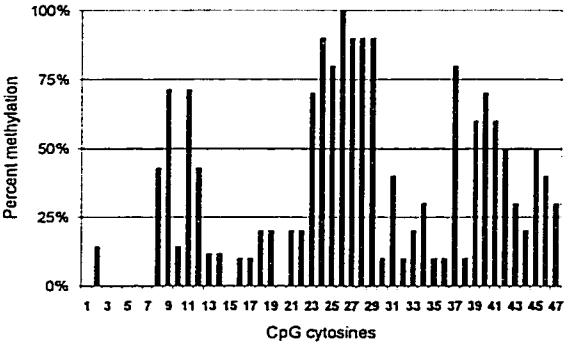

D. HMEC9 E6 Passage 42

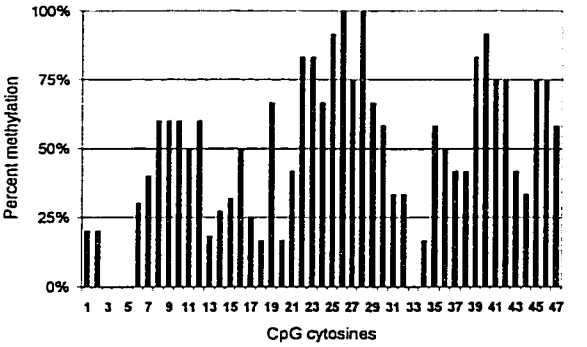

Figure 4.3. Expression of p16 in HMEC9. (A) Western analysis of p16 and p27. (B) Northern analysis of p16 with 36B4 loading control. Passage numbers are indicated above each lane. Cells were predominantly arrested at M0 by passage 8. A stable population of proliferating cells emerged by passage 14. UN, uninfected. E6 or E6/E7, infected with E6- or E6/E7-expressing retrovirus.

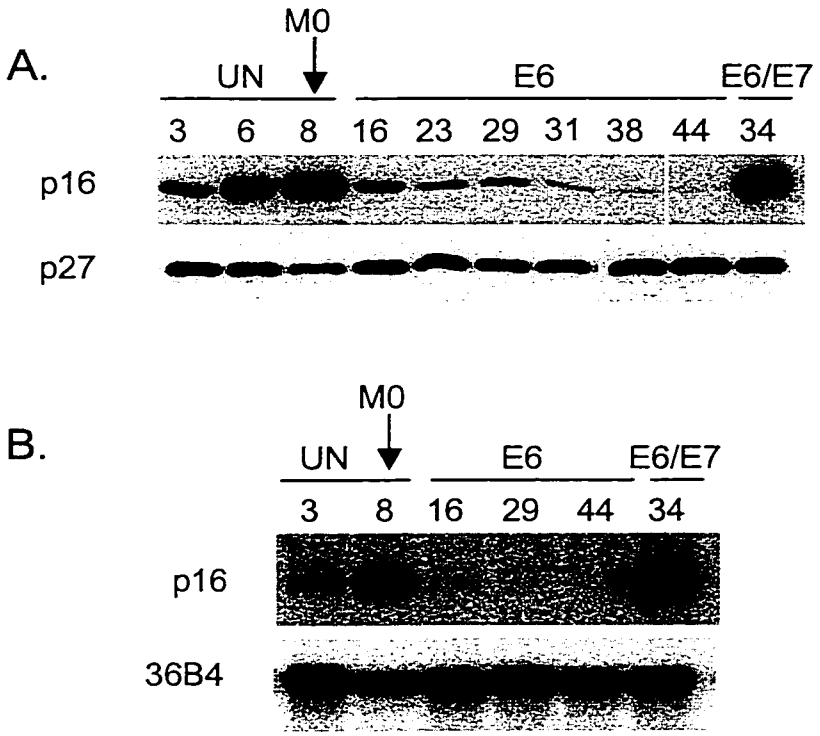
A.
M0
UN
E6
E6/E7
3 6 8 16 23 29 31 38 44 34
p16
p27
B.
M0
UN
E6
E6/E7
3 8 16 29 44 34
p16
36B4

Figure 4.4. Development of methylation in the p16 CpG island of HMEC4 and HMEC6. The 47 CpG sites are in numerical order according to their 5'-to-3' order in the p16 genomic sequence (-355 to +233). CpG sites are not spaced out on the x-axis according to their relative positions in the p16 genomic sequence. Percent methylation at each CpG site was calculated as the percentage of clones with a methylated cytosine at that site. Percent methylation for CpGs 13, 14 and 15 was calculated from data from clones of both PCR products A and B.

A. HMEC6 Passage 3

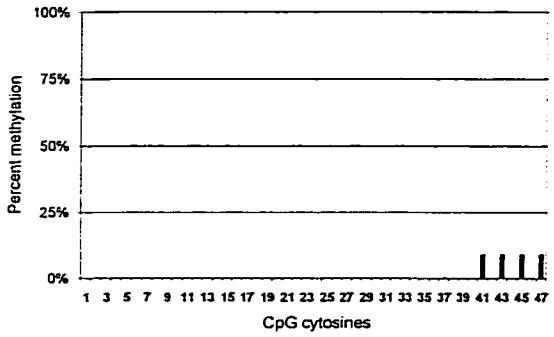

B. HMEC6 E6 Passage 12

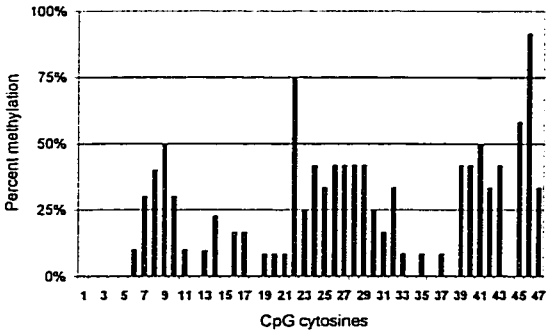

C. HMEC6 E6 Passage 25

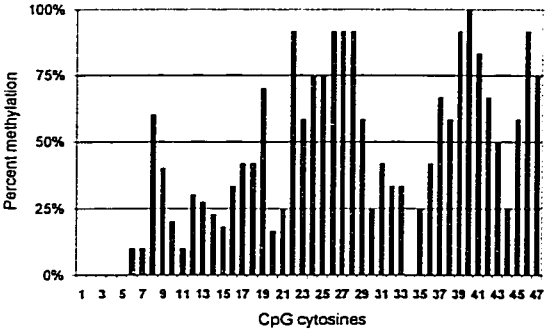

D. HMEC4 Passage 5

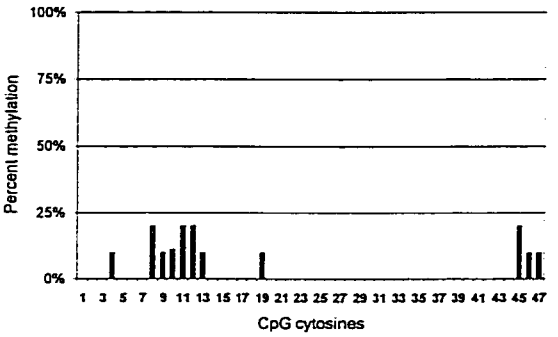

E. HMEC4 Passage 12

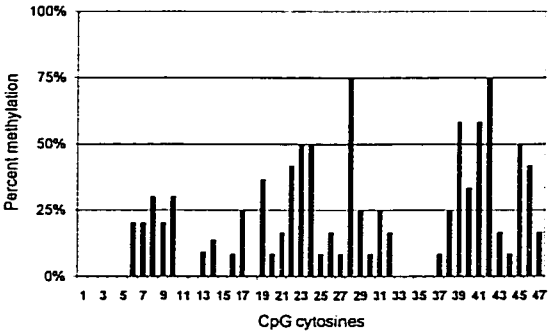

Figure 4.5. Individual epigenotypes at the p16 CpG island. The gray bar at the top of each panel represents the 588-bp region from -355 to +233 analyzed in this study. Individual epigenotypes are each represented by a gray bar with letters (A and B) and number (1 to 10, 11, and 12) on the left that represent the PCR product and clone, respectively. CpG sites on the top gray bar are numbered from 1 to 47 according to their 5'-to-3' order in the p16 genomic sequence and are spaced out according to their relative positions in the p16 genomic sequence. The methylation status of each CpG site is indicated at its relative position in the p16 genomic sequence by either a white (unmethylated) or black (methylated) box on the gray bar; an ellipse indicates ambiguous sequence information. The three preferentially methylated regions (I, II, and III) in each HMEC are based on the epigenotypes from the earliest passage after M0 (Figures 4.2B and 4.4E). The lengths of the regions were slightly different among the different HMECs.

A. HMEC4 passage 12

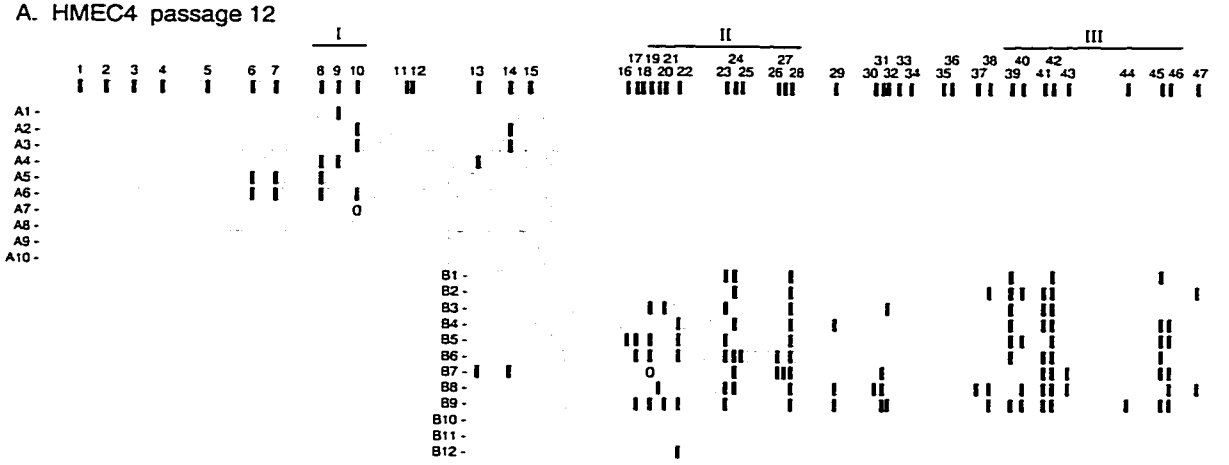

B. HMEC9 E6 passage 16

C. HMEC9 E6 passage 42

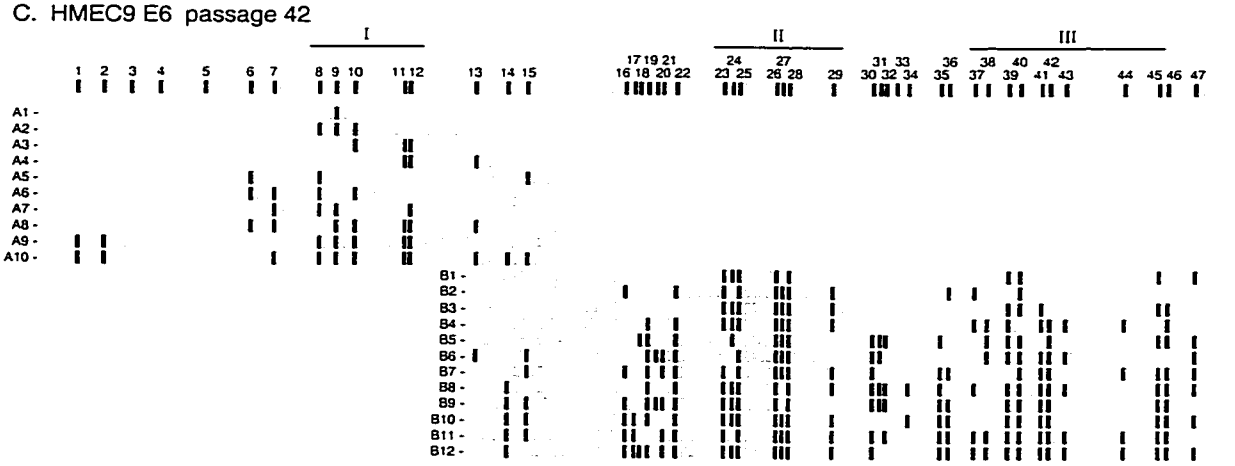

Table 4.1. Methylation in the p16 CpG island of HMECs

	N	Mean[c]	Median	Range	N	Mean[c]	Median	Range	Mean
HMEC9									
3	10	0.1 [0.0, 0.3]	0	0 - 1	10	0.5 [0.0, 1.1]	0	0 - 2	0.6
8	9	0.2 [0.0, 0.5]	0	0 - 1	9	0.2 [0.0, 0.5]	0	0 - 1	0.4
16, E6	10	2.9 [1.5, 4.3]	2	1 - 8	11	9.1 [7.0, 11.2]	9	5 - 16	11.8
29, E6	7	2.9 [1.7, 4.1]	3	1 - 5	10	13.6 [12.2, 15.0]	14	10 - 16	16.2
42, E6	10	4.6 [2.5, 6.7]	3.5	1 - 11	12	19.2 [15.4, 23.0]	20	9 - 28	23.0
32, E6/E7	10	0.0 [0.0, 0.0]	0	0	10	0.2 [0.0, 0.5]	0	0 - 1	0.2
HMEC6									
3	10	0.0 [0.0, 0.0]	0	0	11	0.4 [0.0, 0.8]	0	0 - 2	0.4
12, E6	10	2.0 [0.7, 3.3]	1	0 - 5	12	9.3 [7.2, 11.4]	8.5	6 - 17	10.9
25, E6	10	2.1 [1.1, 3.1]	2.5	0 - 4	12	19.2 [16.4, 22.0]	19	9 - 25	20.6
HMEC4									
5	10	0.9 [0.0, 2.1]	0	0 - 5	10	0.7 [0.0, 1.5]	0	0 - 3	1.5
12	10	1.5 [0.4, 2.6]	1.5	0 - 4	12	8.3 [4.7, 11.9]	8.5	0 - 17	9.5
18	9	2.9 [2.3, 3.5]	3	2 - 4	12	5.4 [3.2, 7.6]	6	1 - 11	7.7
H249	4	0.0 [0.0, 0.0]	0	0	4	0.0 [0.0, 0.0]	0	0	0.0
H1618	3	14.7 [13.3, 15.0]	15	14 - 15	4	35.0 [35.0, 35.0]	35	35	46.9

CHAPTER 5: $p16^{INK4a}$ HEMIZYGOUS CELL POPULATIONS ARISE EARLY AND EXPAND CLONALLY IN PREMALIGNANT METAPLASTIC ESOPHAGEAL (BARRETT'S) EPITHELIUM

ABSTRACT

The $p16^{INK4a}$ tumor suppressor is one of the most commonly inactivated genes in human cancer. However, it has not been possible to establish the stage at which p16 lesions occur in premalignant epithelium or their cellular phenotypic consequences in human neoplastic progression *in vivo*. We investigated p16 lesions in "mapped" endoscopic biopsy specimens of premalignant Barrett's epithelium from 276 patients who had not developed esophageal adenocarcinoma. We found 9p21 LOH in 161 of the 276 patients (58%), p16 mutation in 49 of the 276 patients (18%), and p16 methylation in 14 of the 29 evaluated patients (48%). p16 lesions were found in 22 of the 29 (76%) patients evaluated for p16 methylation, p16 mutation, and 9p21 LOH, and this prevalence did not change with increasing histologic grade of Barrett's epithelium, suggesting that p16 abnormalities are the earliest known somatic genetic/epigenetic lesions in the neoplastic progression of Barrett's esophagus. We found a high prevalence of p16 hemizygous cell populations in Barrett's epithelium. These cell populations evolved second lesions, giving rise to p16 nullizygous cell populations in many patients. Both p16 hemizygous and p16 nullizygous cell populations were strongly associated with long segments of

Barrett's epithelium and expanded clonally over extensive regions up to 12 cm in length, suggesting that p16 haplo-insufficiency is permissive for clonal expansion.

INTRODUCTION

p16 genetic lesions are one of the most common abnormalities in human cancer. In addition, p16 abnormalities have been detected in the premalignant epithelium surrounding a variety of malignancies, suggesting that they arise before the development of cancer (Barrett et al., 1996; Belinsky et al., 1998; Muto et al., 2000; Tsutsumi et al., 1998). We previously demonstrated in a retrospective study that the progenitor of neoplastic cell lineages in premalignant Barrett's epithelium had p16 lesions (Barrett et al., 1999). However, the stage at which p16 lesions arise in premalignant epithelium prior to the development of cancer has not yet been determined.

p16 is a cyclin-dependent kinase inhibitor that binds specifically to the cyclin D-dependent kinases, CDK4 and CDK6, and inhibits the ability of these CDKs to phosphorylate the retinoblastoma protein (pRb), leading to an accumulation of hypophosphorylated pRb and replicative arrest in the G1 phase of the cell cycle (Koh et al., 1995; Lukas et al., 1995). p16 transcriptional expression is induced as primary mammalian cells reach the end of their proliferative lifespan, known as senescence, or as a result of an oncogenic stimulus, such as ras or E1A, that triggers a premature senescence (Alcorta et al., 1996; Foster et al., 1998; Hara et al., 1996; Reznikoff et al., 1996; Serrano et al., 1997). p16 inactivation in primary human and mouse cells in culture results in an extension of their lifespan and in combination with telomerase activity,

cause cell immortalization (Carnero et al., 2000; Dickson et al., 2000; Foster et al., 1998; Kiyono et al., 1998). However, the phenotypic consequences of p16 lesions in neoplastic progression *in vivo* remains unknown.

p16, like most of the identified tumor suppressor genes, has been found to have two inactivated alleles in human malignancy (Cairns et al., 1995; Caldas et al., 1994; Knudson, 1971). We previously found that most (24/32; 75%) patients with esophageal adenocarcinoma had 9p21 LOH and that most of these patients with 9p21 LOH (17/24; 71%) had either CpG island methylation (12/24; 50%) or mutation (5/24; 21%) of the remaining p16 allele (Barrett et al., 1996; Barrett et al., 1999; Wong et al., 1997). However, 29% (7/24) of patients had 9p21 LOH without p16 methylation or mutation, suggesting that another tumor suppressor gene in the 9p21 region was targeted for inactivation or that p16 or another gene on 9p21 was haplo-insufficient for tumor suppression.

The premalignant epithelium that gives rise to esophageal adenocarcinoma is a metaplastic columnar epithelium called Barrett's esophagus that replaces the normal stratified squamous epithelium of the esophagus and develops in approximately 10% of patients with chronic gastroesophageal reflux disease (Lagergren et al., 1999; Phillips and Wong, 1991; Winters et al., 1987). Because patients with Barrett's esophagus frequently present at an early stage due to symptoms of gastroesophageal reflux, such as heartburn, and endoscopic biopsy surveillance is recommended for early detection of esophageal adenocarcinoma, tissue samples at various premalignant stages are available for analysis and the somatic events that occur during the progression to cancer can be investigated (Levine et al., 1993; Neshat et al., 1994). The following three-tier histological grading

has been used to stage the premalignant Barrett's epithelium, in order of increasing severity: metaplasia negative for dysplasia, indefinite for dysplasia/low-grade dysplasia, and high-grade dysplasia (Reid et al., 1988; Sampliner, 1998).

In this study, we investigated p16 inactivation in "mapped" endoscopic biopsy specimens of Barrett's epithelium from the baseline endoscopy of 276 patients who had not developed cancer. We demonstrate that p16 methylation, p16 mutation, and 9p21 LOH were highly prevalent at all of the histological stages including metaplasia negative for dysplasia and are the earliest known somatic genetic/epigenetic lesions in the neoplastic progression of Barrett's esophagus. Both p16 nullizygous and p16 hemizygous cell populations were found at a high prevalence, were strongly associated with long segments of Barrett's epithelium, and had the ability to clonally expand over extensive regions of Barrett's epithelium.

MATERIALS AND METHODS

Patient Tissue Samples. We evaluated flow-sorted samples from multiple biopsies of Barrett's epithelium from 276 patients who had Barrett's esophagus but did not have cancer. Biopsies were acquired at 2-cm intervals of the entire Barrett's segment in each patient during endoscopic surveillance using mapping protocols as described previously (Levine et al., 1993; Reid et al., 2000; Reid et al., 1988). Normal gastric tissue served as a constitutive control for each patient. Patients were counseled regarding the risks and benefits of endoscopic surveillance and informed of potential alternatives, including surgery for high-grade dysplasia. The Barrett's Esophagus Study was approved by the

Human Subjects Review Boards at the University of Washington and the Fred Hutchinson Cancer Research Center.

Flow Cytometric Sorting and DNA Extraction. Barrett's epithelial cell populations were purified from biopsies acquired at 2-cm intervals of the Barrett's segment by sorting diploid G1, 4N, and aneuploid cell populations using multiparameter Ki67/DNA-content flow sorting by a Coulter Elite ESP cell sorter as described previously (Paulson et al., 1999). Ki67 is an antibody that identifies a proliferation-associated nuclear antigen expressed in late G1, S, and mitosis, but not G0 (Gerdes et al., 1984; Gerdes et al., 1983). Biopsies were minced and sheared in NST buffer (146 mM NaCl, 10 mM Tris-HCl, pH 7.5, 1 mM $CaCl_2$, 0.5 mM $MgSO_4$, 21 mM $MgCl_2$, 0.05% bovine serum albumin, 0.2% Nonidet P40 (Sigma)). The suspension was centrifuged at 2000 r.p.m. for 10 min. at 4°C to isolate nuclei, resuspended in NST buffer with 10% normal goat serum (Caltag), then divided and incubated with Ki67-RPE (3.75 μg/ml) and IgG1-RPE isotype antibodies (Dako), respectively. Samples were centrifuged again as above and resuspended in NST buffer with 10% normal goat serum and 4,6-diamindino-2-phenylindole (DAPI; 10 μg/ml; Boehringer). With the use of multiparameter Ki67/DNA-content flow sorting, a minimum of two of the following flow-purified fractions were generated per biopsy specimen: Ki67-negative cells with a 2N DNA content (G0), Ki67-positive cells with a 2N DNA content (G1), cells with a 4N DNA content, and aneuploid cells. DNA from the flow-sorted Barrett's samples and the gastric samples were extracted as described previously (Paulson et al., 1999).

DNA Methylation Analysis. Extracted genomic DNA from flow-purified samples obtained at 2-cm intervals in the Barrett's segment were evaluated for methylation of the p16, p15, and $p14^{ARF}$ CpG islands using bisulfite treatment as described previously (Wong et al., 1997; Wong et al., 1999). Bisulfite converts unmethylated cytosines to uracils but does not alter methylated cytosines. Human genomic DNA treated *in vitro* with Sss I methyltransferase (New England Biolabs, Beverly, MA) was used as the methylated control for all three CpG islands. Each extracted genomic DNA sample (~15 ng; 2000 cells) was first denatured in 0.3 M NaOH for 20 min at 42°C, and then treated with a 3.8 M sodium bisulfite, 1.0 mM hydroquinone solution (pH 5.0) for 8 h at 55°C. The bisulfite-treated DNA was purified by reverse phase extraction using Empore SDB-XC disk cartridges (3M, St. Paul, MN), then desulfonated in 0.3 M NaOH for 20 min at 37°C, and purified by ethanol precipitation. Each purified bisulfite-treated DNA sample was divided into two PCR reactions: 1) primer-extension preamplification (PEP), which amplifies the entire genome at least 60 fold using a degenerate 15-mer, and 2) p16-specific PCR. The primer sequences for the p16-specific PCR were 5'-GTA GGT GGG GAG GAG TTT AG-3' (sense) and 5'-TCC AAT TCC CCT ACA AAC TTC-3' (antisense). The p16-specific PCR reaction used 1.75 mM $MgCl_2$, 200 μM dNTPs, 10 pmol of each primer, GeneAmp PCR buffer (Applied Biosystems, Foster City, CA), and 2.5 units of AmpliTaq Gold enzyme (Applied Biosystems).

Methylation of the p16, p15 and $p14^{ARF}$ CpG islands was assessed by methylation-specific PCR, which distinguishes unmethylated and methylated alleles based on the sequence changes after bisulfite treatment of DNA (Herman et al., 1996). Methylation-

specific PCR of the p16 CpG island was performed from either the PEP products or the p16-specific PCR products. The primer sequences designed for the p16 CpG island spanned seven CpG cytosines (bold and italicized). The primer sequences of p16 for the unmethylated reaction were 5'-TAG AGT AGG TAG ***T***GG G***T***G G***T***-3' (sense) and 5'-CTC C***A***A CC***A*** TAA CTA TTC ***A***AT AC***A***-3' (antisense), and the primer sequences of p16 for the methylated reaction were 5'-TAG AGT AGG TAG ***C***GG G***C***G G***C***-3' (sense) and 5'-TCC ***G***AC C***G***T AAC TAT TC***G*** ATA C***G*** 3' (antisense). The annealing temperature for both reactions was 59.5°C. Methylation-specific PCR of the p15 and $p14^{ARF}$ CpG islands were performed off of the PEP products. The primer sequences for p15 and $p14^{ARF}$ and the reaction conditions were as described previously (Esteller et al., 2000). All reactions used 1.5 mM $MgCl_2$, 200 μM dNTPs, 10 pmol of each primer, GeneAmp PCR buffer (Applied Biosystems), and 2.5 units of AmpliTaq Gold enzyme (Applied Biosystems). Methylation-specific PCR products were loaded onto 2.5% agarose gels, stained with ethidium bromide, and visualized under UV illumination.

Methylation of each individual CpG cytosine in the p16 CpG island was assessed by directly sequencing PCR products of bisulfite-treated DNA. Two nested PCR reactions were performed from each p16-specific PCR product. The primer sequences for the 5' end of the p16 CpG island were 5'-<u>CAG GAA ACA GCT ATG ACC</u> GTA GGT GGG GAG GAG TTT AGT T-3' and 5'-<u>TGT AAA ACG ACG GCC AGT</u> TCT AAT AAC CAA CCA ACC CCT CC-3', which were tailed with the M13 reverse and forward primer sequences, respectively (underlined). The primer sequences for the 3' end of the p16 CpG island were 5'-<u>CAG GAA ACA GCT ATG ACC</u> GAG GGG TTG

GTT GGT TAT TAG-3' and 5'-TGT AAA ACG ACG GCC AGT TCC AAT TCC CCT ACA AAC TTC-3', which were also tailed with the M13 sequences (underlined). The annealing temperatures were 64°C and 60°C, respectively. Both nested PCR reactions used 1.5 mM $MgCl_2$, 200 μM dNTPs, 10 pmol of each primer, GeneAmp PCR buffer (Applied Biosystems), and 1.25 units of AmpliTaq Gold DNA polymerase (Applied Biosystems). The nested PCR products were purified using Microcon 100 (Amicon), and then sequenced with M13 forward primers using BigDye Terminator cycle sequencing (Applied Biosystems). The sequencing reactions were run on an Applied Biosystems Incorporated 377 DNA sequencer.

DNA Sequencing Analysis. Extracted genomic DNA from flow-purified samples obtained at 2-cm intervals in the Barrett's segment were evaluated for p16 mutations by DNA sequencing. Wild-type sequences were confirmed using normal gastric tissue from each patient. Genomic DNA extracted from approximately 1000 cells was whole-genome-amplified by PEP, as described previously (Paulson et al., 1999). Exon 2 of the p16 gene was amplified by PCR from an aliquot of the PEP product using the following primer sequences: 5'-GGA AAT TGG AAA CTG GAA GC-3' and 5'-TCT GAG CTT TGG AAG CTC T-3'. The reaction conditions were 2.0 mM $MgCl_2$, 200 μM dNTPs, 14 pmol of each primer, 5% DMSO, GeneAmp PCR buffer (Applied Biosystems), 1.25 units of AmpliTaq Gold DNA polymerase (Applied Biosystems), and an annealing temperature of 66°C. The p16 exon 2 PCR products were sequenced using BigDye

Terminator cycle sequencing (Applied Biosystems). The sequencing reactions were run on an ABI 377 DNA sequencer.

Microsatellite Analysis. Extracted genomic DNA from flow-purified samples obtained at 2-cm intervals in the Barrett's segment were evaluated for 9p21 and 17p LOH using polymorphic microsatellite markers as described previously (Paulson et al., 1999). Locus-specific primers were labeled with FAM, TET, or HEX phosphoramidite dyes from Research Genetics (Huntsville, AL), and included GATA62F03 (9p23), D9S935 (9p23), D9S925 (9p22.3), D9S932 (9p21.3-22.1), D9S1121 (9p21.3), D9S1118 (9p21), D17S1298 (17p13.3), D17S1537 (17p13.2), TP53 (17p13.1) pentanucleotide repeat, TP53 (17p13.1) dinucleotide, D17S786 (17p13.1), D17S974 (17p12), D17S1303 (17p12), and D17S1288 (17p11). PCR products were run on an ABI 373 or an ABI 377 DNA sequencer and analyzed by Genescan and Genotyper software (Applied Biosystems), as described previously (Paulson et al., 1999).

Statistical Analysis. The Wilcoxon ranksum test was used to compare the mean segment lengths of Barrett's epithelium in patients with p16 lesions and patients without p16 lesions. The same test was also used to compare the mean segment lengths of patients that only had cell populations with a single p16 abnormality and patients that had samples with two p16 lesions.

RESULTS

We determined the prevalence of p16 methylation, p16 mutation, and 9p21 LOH at baseline endoscopy in 276 patients who had Barrett's esophagus but had not developed cancer. Biopsies from each 2 cm interval of the Barrett's segment of individual patients were evaluated for 9p21 LOH by microsatellite analysis (n = 276), for p16 mutation by genomic sequencing (n = 276), and for p16 methylation by bisulfite treatment and sequencing (n = 29). We found 9p21 LOH in 161 of the 276 patients (58%), p16 mutation in 49 of the 276 patients (18%), and p16 methylation in 14 of the 29 patients (48%). In total, p16 abnormalities were found in 22 of the 29 patients (76%) evaluated for all three abnormalities (9p21 LOH, p16 mutation, and p16 methylation). Thus, p16 abnormalities are highly selected lesions in premalignant Barrett's epithelium.

The 276 patients were composed of a spectrum of histologic stages of neoplastic progression: 78 had a maximum histologic stage of metaplasia negative for dysplasia, 144 had indefinite for dysplasia/low-grade dysplasia, and 54 had high-grade dysplasia. The prevalence of p16 abnormalities did not change with increasing histologic stage of neoplastic progression (Figure 5.1). We found p16 abnormalities in 70%, 86%, and 75% of patients with a maximum diagnosis of metaplasia, indefinite for dysplasia/low-grade dysplasia, and high-grade dysplasia, respectively. In addition, the prevalence of each of the p16 abnormalities (p16 methylation, p16 mutation, and 9p21 LOH, was approximately the same regardless of the histologic grade (Figure 5.1). Thus, p16 abnormalities are characteristic of Barrett's metaplasia and are the earliest known somatic lesions in the neoplastic progression of Barrett's esophagus.

In a previous study with a different set of patients who had a maximum diagnosis of high grade dysplasia or cancer, we found p16 methylation in eight of 21 patients (38%) and p16 mutation in 11 of 43 patients (26%), but did not detect p15 methylation or p15 mutation in any of 21 or 12 patients evaluated, respectively (Wong et al. and Barrett et al.). In addition, we did not detect $p14^{ARF}$ methylation in any of 16 patients evaluated (unpublished data). However, because methylation is potentially reversible (i.e. methylation could be acquired at early stages and then lost at later stages), we determined the prevalence of methylation at the p15 and $p14^{ARF}$ CpG islands by methylation-specific PCR in biopsies at 2 cm intervals from 43 of the 276 patients who had not developed cancer. Only three of the 43 patients (7%) had p15 methylation and only two (5%) had $p14^{ARF}$ methylation, whereas 21 (49%) had p16 methylation by methylation-specific PCR (Table 5.1). Thus, in contrast to p16-specific abnormalities (methylation and mutation) which are present at all histologic stages, p15- and $p14^{ARF}$-specific abnormalities do not appear to be strongly selected at any stage of neoplastic progression in Barrett's esophagus.

To determine the extent to which cells with p16 abnormalities are associated with expansion of the Barrett's epithelium *in vivo*, we investigated the relationship between p16 lesions and the length of the Barrett's segment in individual patients. Of the 29 patients evaluated for p16 methylation, p16 mutation, and 9p21 LOH, 22 (76%) had at least one p16 abnormality. These 22 patients had a mean segment length of Barrett's epithelium of 9.3 cm, whereas the 7 patients without p16 abnormalities had a mean segment length of only 2.9 cm ($p = 0.003$) (Figure 5.2). Only 1 of the 22 patients with

p16 abnormalities had a Barrett's segment length of less than 3 cm, whereas 5 of the 7 patients without p16 abnormalities had a segment length less than 3 cm. These data suggest that disruption of p16 function enables proliferative expansion of Barrett's epithelium within the esophagus.

p16 is considered a classic tumor suppressor gene that has both alleles inactivated in human malignancy. Consistent with this hypothesis, we found examples of clonal expansion of cell populations with lesions in both p16 alleles. For example, we found a clonal cell population with the same 9p21 LOH pattern and the identical p16 mutation that had expanded to occupy 12 cm of a patient's Barrett's segment (Figure 5.3a). In another patient, a clonal cell population with the same 9p21 LOH pattern and the same p16 methylation pattern occupied the entire 8 cm segment (Figure 5.3a). Thus, p16 nullizygous cell populations appear to have a growth advantage to clonally expand within Barrett's epithelium.

However, we found that p16 hemizygous cell populations were more prevalent than p16 nullizygous populations and like the nullizygous cell populations, had the ability to clonally expand within the Barrett's epithelium. Of the 67 biopsy samples from the 29 patients evaluated for all three p16 lesions, only 17 (25%) had two lesions, whereas 35 (52%) had only one (Table 5.2). Because of the lack of a polymorphism in the p16 CpG island in the cases that only had p16 methylation, we were unable to determine whether they had monoallelic or biallelic methylation. Nevertheless, there were not only patients with only p16 methylation but also patients that only had 9p21 LOH and patients that only had a single p16 mutation. For example, a patient had a clonal p16 hemizygous cell population with only 9p21 LOH that occupied a Barrett's segment of 7 cm, while a

second patient had a clonal hemizygous cell population with the identical p16 mutation that expanded to 10 cm (Figure 5.3b). Similarly, we found another patient with a cell population with only p16 methylation that had expanded to 12 cm (Figure 5.3b). The mean segment length of patients that only had cell populations with a single p16 abnormality was 8.4 cm, which was slightly less than that of patients that had samples with two p16 lesions (9.9 cm), but the difference was not significant ($p = 0.38$). We also found patients with two distinct p16 hemizygous populations occupying different regions of their esophagus. For example, we found a patient with a cell population with 9p21 LOH adjacent to a cell population with p16 mutation that together occupied a 12 cm Barrett's segment; a patient with a methylated p16 cell population next to a cell population with 9p21 LOH that together occupied an 11 cm segment; as well as patients with mutant p16 cells adjacent to methylated p16 cells that can occupy a 9 cm segment (Figure 5.3c). Thus, p16 hemizygous cell populations are prevalent and have the ability to expand to occupy extensive regions of the esophagus.

Some patients (8/29; 28%) had both p16 hemizygous and p16 nullizygous cell populations, and in all of these cases, the p16 lesion in the hemizygous population was shared by the nullizygous population, suggesting that the hemizygous population gave rise to the adjacent nullizygous population (Table 5.2). For example, we found a patient that had a clonal p16 hemizygous population with 9p21 LOH adjacent to a nullizygous population with the same 9p21 LOH pattern and a mutation of the remaining p16 allele (Figure 5.3d). In another patient, a clonal p16 hemizygous population with 9p21 LOH was adjacent to a nullizygous population with the same 9p21 LOH pattern and methylation of the remaining p16 allele (Figure 5.3d). In a third patient, a p16

hemizygous population with p16 methylation was adjacent to a p16 nullizygous population with methylation and 9p21 LOH (Figure 5.3d). Thus, p16 hemizygous cell populations often give rise to p16 nullizygous cell populations and the premalignant Barrett's epithelium are frequently composed of a mosaic of p16 hemizygous and p16 nullizygous clones.

We previously found that cell populations with both p16 and p53 abnormalities are the common progenitors of the different lineages that can give rise to cancer in Barrett's esophagus. Thus, we investigated how these progenitor cells arise amidst p16 hemizygous and p16 nullizygous clonal populations in Barrett's epithelium. We evaluated the same Barrett's biopsy samples at the 2 cm intervals in 272 of the 276 patients for 17p LOH using microsatellite analysis. 17p LOH was found in 49 (18%) of the 272 patients that were informative for the microsatellite markers. We found a patient that had a cell population with only p16 methylation adjacent to a population that had the p16 methylation and 17p LOH (Figure 5.3e, left), as well as a patient that had a p16 hemizygous cell population with 9p21 LOH and 17p LOH adjacent to a cell population that developed methylation on the remaining p16 allele (Figure 5.3e, middle). In addition, we found a patient who had a p16 nullizygous cell population with 9p21 LOH and p16 methylation adjacent to a population that also acquired 17p LOH (Figure 5.3e, right). Thus, p16 hemizygous and p16 nullizygous cell populations can give rise to neoplastic progenitor cells by acquiring p53 lesions.

DISCUSSION

We have shown here that abnormalities of the p16 gene, including methylation, mutation, and LOH, are the earliest known somatic events in Barrett's epithelium. We demonstrated that p16 abnormalities are highly prevalent in patients without cancer. p16 lesions were found in approximately 75% of patients with Barrett's esophagus at all histologic grades, including the earliest grade, metaplasia negative for dysplasia. A previous study also found p16 methylation in patients that had dysplasia but not cancer (Klump et al., 1998). These results are consistent with other studies that found p16 abnormalities in premalignant epithelium surrounding esophageal, bladder, and lung cancers (Belinsky et al., 1998; Muto et al., 2000; Tsutsumi et al., 1998). Thus, early acquisition of p16 lesions may be a common step in the development of many human epithelial tumors.

p15- and $p14^{ARF}$–specific methylation, in contrast, were rare regardless of histologic grade, suggesting that p15 and $p14^{ARF}$ are not strongly selected for inactivation during the progression of this cancer. Both p15 and $p14^{ARF}$ are located in the frequently deleted 9p21 region along with p16 and have been considered candidate tumor suppressor genes based on their ability to inhibit cell proliferation (Hannon and Beach, 1994; Quelle et al., 1995). p15 has been shown to be inactivated by CpG island methylation in the absence of p16 methylation in gliomas and leukemias, and $p14^{ARF}$ was specifically methylated in a subset of primary colorectal carcinomas (Esteller et al., 2000; Herman et al., 1996; Robertson and Jones, 1998). However, unlike p16, neither deletions nor point mutations specific for p15 or $p14^{ARF}$ have been reported in primary human tumors (Jen et

al., 1994; Kamb et al., 1994; Stone et al., 1995; Washimi et al., 1995). Although mutations in the shared exon 2 that affect both p16 and $p14^{ARF}$ have been found, such mutations do not appear to disrupt $p14^{ARF}$ function (Quelle et al., 1997). Thus, the low frequency of p15- and $p14^{ARF}$-specific lesions in Barrett's esophagus and esophageal adenocarcinoma suggests that p16 is specifically targeted by lesions in the 9p21 region in Barrett's epithelium.

Previous studies in primary human and mouse cell cultures have demonstrated that p16 inactivation lengthens the cell replicative life span (Carnero et al., 2000; Dickson et al., 2000; Foster et al., 1998; Kiyono et al., 1998). However, the cellular phenotype of p16 inactivation during human neoplastic progression *in vivo* had not been previously investigated. Normal esophageal epithelium was previously found to be polyclonal using X-inactivation as a clonal marker (Thomas et al., 1988). In contrast, we previously found that cell populations with 9p21 LOH tended to spread to large regions of esophageal mucosa (Galipeau et al., 1999). In this study, using p16 mutations and 9p21 LOH patterns as clonal markers, we found that p16 hemizygous and p16 nullizygous cell populations expanded clonally to occupy large areas of Barrett's mucosa, typically the entire Barrett's segment. Thus, consistent with having an extended cellular replicative lifespan, p16 abnormal cell clones appeared to have a growth advantage that allowed them to expand laterally within the esophageal epithelium.

In addition, patients with p16 lesions had longer Barrett's segments than those without any p16 abnormalities, suggesting that the clonal expansion of p16 hemizygous and p16 nullizygous cells lengthens the Barrett's epithelium. Although many patients

had a Barrett's epithelium that was composed of a mosaic of p16 hemizygous and/or p16 nullizygous clones, this mosaic was composed of only one or at most three clonal lineages of p16 abnormal clones in each of these patients. Our results suggest that the expansion of the Barrett's epithelium is a result of clonal proliferation rather than the polyclonal regeneration of acid reflux-damaged mucosa, and are consistent with a clonal neoplastic evolution.

Clonal hemizygous p16 cell populations were capable of extensive expansion within the Barrett's segment, suggesting that inactivation of a single p16 allele is sufficient to provide a selective proliferative advantage (i.e. p16 is haplo-insufficient). Consistent with these results, a previous study in primary human cell culture found that partial down-regulation of p16 expression is sufficient for lifespan extension (Foster et al., 1998; Wong et al., 1999). Cells that acquire a single p16 lesion may have a decrease in the senescence-induced p16 expression levels that is sufficient for continued proliferation. Another cyclin-dependent kinase inhibitor, $p27^{Kip1}$, has previously been shown to be haplo-insufficient for tumor suppression (Fero et al., 1998). However, unlike p27, loss of both copies of p16 is common in primary human tumors (Cairns et al., 1995; Caldas et al., 1994; Wong et al., 1997). We previously found that the majority of patients with esophageal adenocarcinoma that had 9p21 LOH also had either methylation or mutation of the remaining p16 allele (Barrett et al., 1999; Wong et al., 1997). In this study, p16 hemizygous cell populations were found to give rise to p16 nullizygous cell populations in several patients. These results suggest that p16 has selected phenotypes for the loss of a single allele as well as for the loss of both alleles. We did not observe a significant phenotypic difference in clonal expansion between p16 hemizygous and p16

nullizygous cell populations. Further studies will be needed to determine the selective advantage of losing both copies of p16 and whether some cancers develop without the loss of the second p16 copy.

A previous retrospective study in patients who had developed esophageal carcinoma found that cancer can evolve along many different cell lineages, acquiring many different genetic and ploidy abnormalities (Barrett et al., 1999). However, these cancers shared a common diploid progenitor cell population that had acquired both p16 and p53 abnormalities in the premalignant epithelium surrounding the cancer, suggesting that p16 and p53 lesions in combination are critical events that set the stage for the complex neoplastic evolution (Barrett et al., 1999). Consistent with our previous finding that 9p21 LOH was typically acquired before 17p LOH, we demonstrated here that the clonally expanded p16 hemizygous and p16 nullizygous cell clones acquired 17p LOH in several patients, suggesting that neoplastic cell lineages are evolving in these patients (Galipeau et al., 1999). Prospective analysis of follow-up endoscopies will be needed to determine how these p16 hemizygous and p16 nullizygous clones evolve over time, in some cases, to give rise to cancer.

In summary, we demonstrated that p16 lesions (p16 methylation, p16 mutation, and 9p21 LOH) are the earliest known somatic genetic/epigenetic abnormalities in the neoplastic progression of Barrett's esophagus. In contrast, p15 and $p14^{ARF}$ lesions are not strongly selected events at any stage of this disease. Premalignant Barrett's epithelium was composed of p16 hemizygous and p16 nullizygous cell populations, both of which were strongly associated with extensive Barrett's segments and had the ability to clonally expand over large regions of Barrett's epithelium.

Figure 5.1. Prevalence of p16 Lesions in Patients with Barrett's Esophagus Relative to Histologic Grade. "MET" refers to patients with a maximum diagnosis of metaplasia negative for dysplasia. "IND/LGD" refers to patients with a maximum diagnosis of indefinite for dysplasia/low-grade dysplasia. "HGD" refers to patients with a maximum diagnosis of high-grade dysplasia.

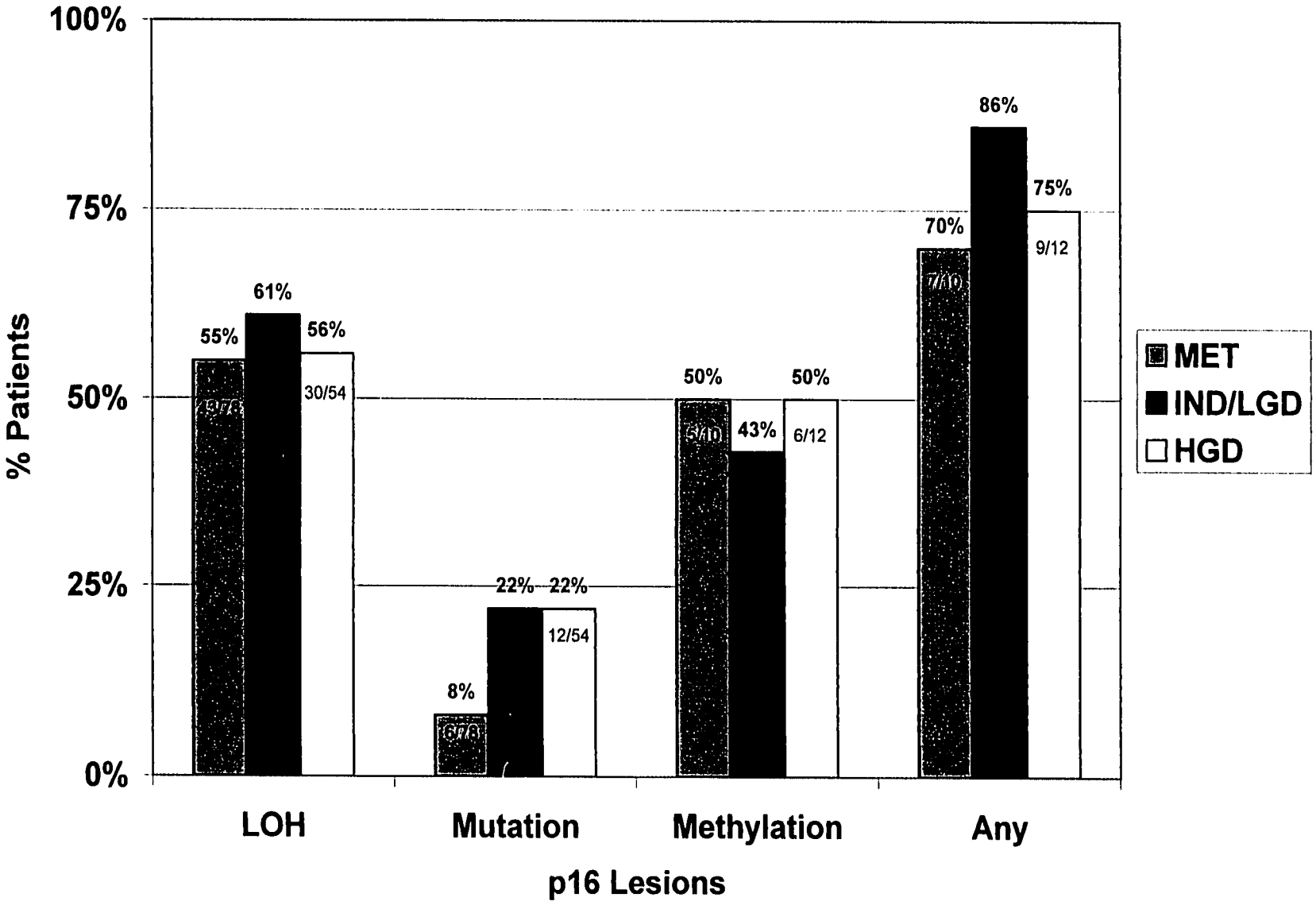
100%
75%
50%
25%
0%
% Patients
55%
61%
56%
30/54
8%
22%
22%
12/54
50%
43%
6/12
70%
86%
75%
9/12
MET
IND/LGD
HGD
LOH
Mutation
Methylation
Any
p16 Lesions

Figure 5.2. p16 Abnormalities and Barrett's Segment Length in Patients Without Cancer. Each "X" indicates an individual patient. The mean segment length for patients with no p16 abnormalities and patients with at least one p16 abnormality is indicated below the graph as well as within the graph by bars.

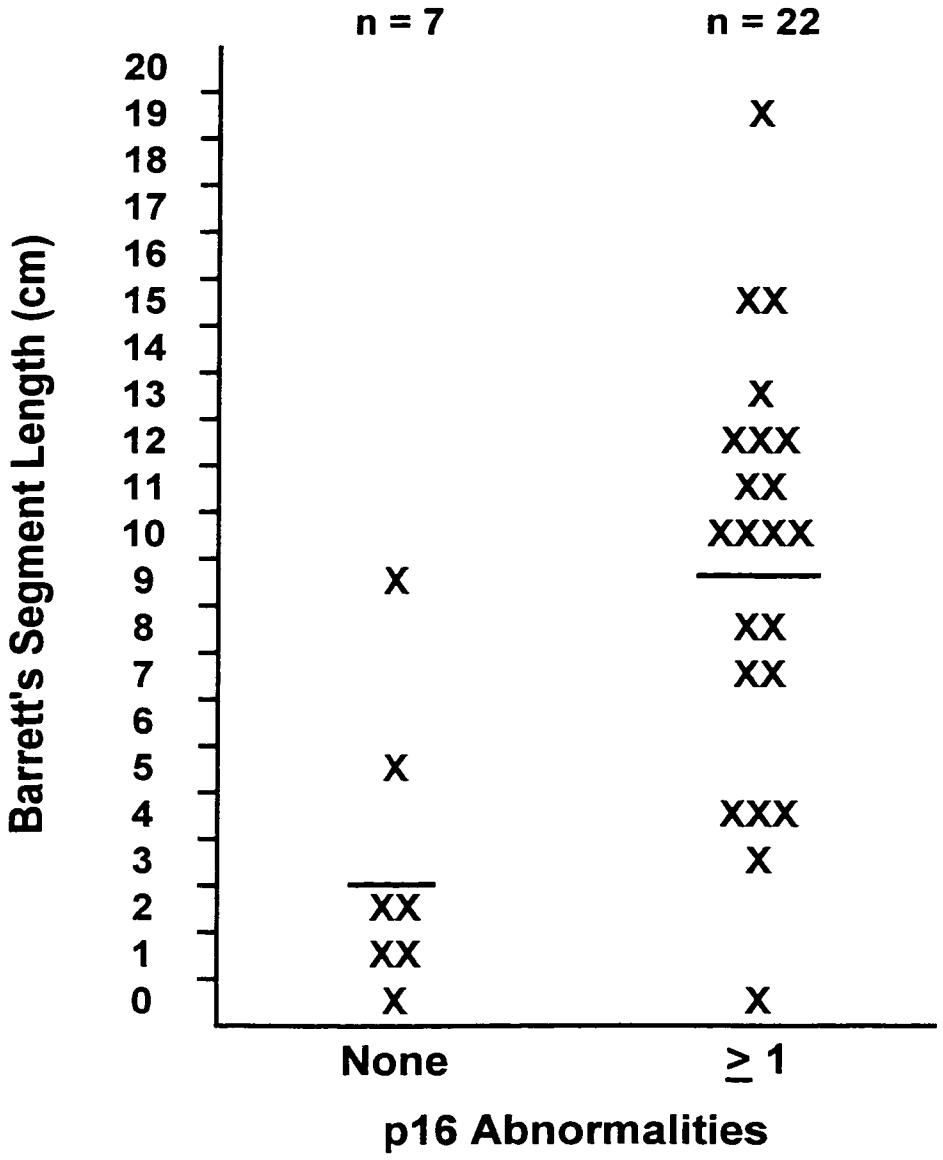
n = 7
n = 22
Barrett's Segment Length (cm)
20
19
18
17
16
15
14
13
12
11
10
9
8
7
6
5
4
3
2
1
0
X
XX
XX
X
X
XXX
XX
XXXX
XX
XX
X
XXX
X
X
None
≥ 1
p16 Abnormalities
mean = 2.9
mean = 9.3

Figure 5.3a. p16 Lesions in the Premalignant Barrett's Epithelium From "Mapped" Endoscopic Biopsies in Patients Without Cancer. Each diagram represents the esophagus of an individual patient. The length of the segment of Barrett's epithelium in each patient is indicated below the diagram. Each circle represents a single "mapped" endoscopic biopsy that was analyzed for 9p21 LOH, p16 mutation, and p16 methylation. "LOH" is an abbreviation for 9p21 LOH. "Mut" is an abbreviation for p16 mutation. "Meth" is an abbreviation for p16 methylation. The diagram on the left depicts a patient that had a p16 nullizygous clonal cell population with 9p21 LOH and a p16 mutation (H83Y) in five biopsies across a 12 cm Barrett's segment. The diagram on the right depicts a patient that had a p16 nullizygous clonal cell population with 9p21 LOH and p16 methylation in four biopsies across an 8 cm Barrett's segment. Identical 9p21 LOH patterns showed the same allelic losses at all six microsatellite markers evaluated.

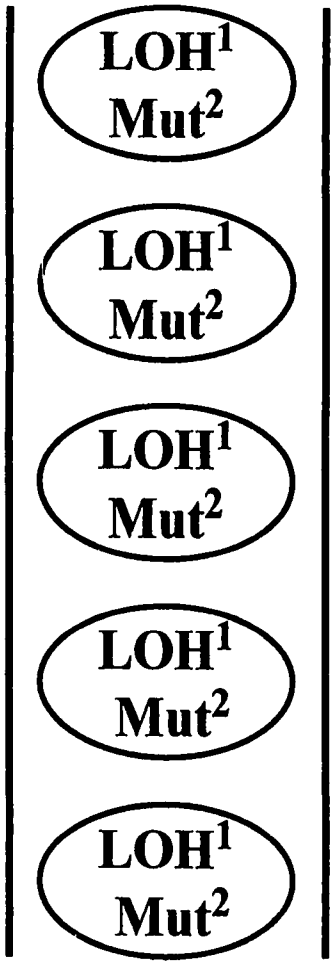

12 cm

[1] Identical LOH pattern

[2] H83Y

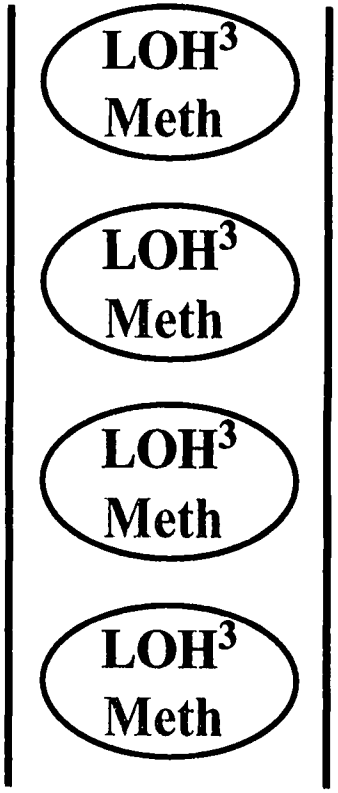

8 cm

[3] Identical LOH pattern

Figure 5.3b. p16 Lesions in the Premalignant Barrett's Epithelium From "Mapped" Endoscopic Biopsies in Patients Without Cancer. Each diagram represents the esophagus of an individual patient. The length of the segment of Barrett's epithelium in each patient is indicated below the diagram. Each circle represents a single "mapped" endoscopic biopsy that was analyzed for 9p21 LOH, p16 mutation, and p16 methylation. "LOH" is an abbreviation for 9p21 LOH. "Mut" is an abbreviation for p16 mutation. "Meth" is an abbreviation for p16 methylation. The diagram on the left depicts a patient that had a clonal cell population with 9p21 LOH but no p16 mutation or p16 methylation in four biopsies across a 7 cm Barrett's segment. The diagram in the middle depicts a patient that had a clonal cell population with a p16 mutation (R80X) but no 9p21 LOH or p16 methylation across a 10 cm Barrett's segment (p16 methylation analysis results were only available from two of the five biopsies from this patient). The diagram on the right depicts a patient that had a cell population with p16 methylation but no 9p21 LOH or p16 mutation in five biopsies across a 12 cm Barrett's segment. Identical 9p21 LOH patterns showed the same allelic losses at all six microsatellite markers evaluated.

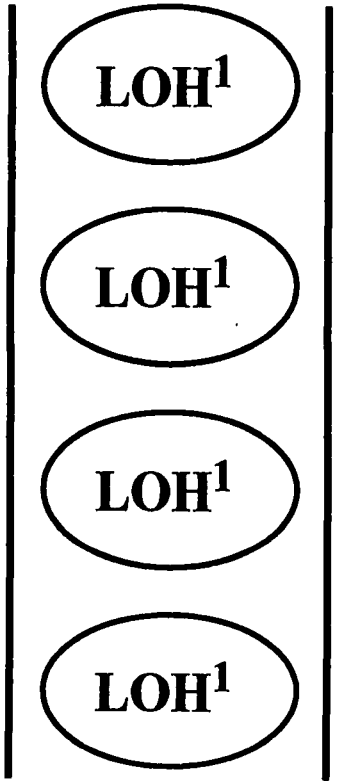

7 cm

[1] Identical LOH pattern

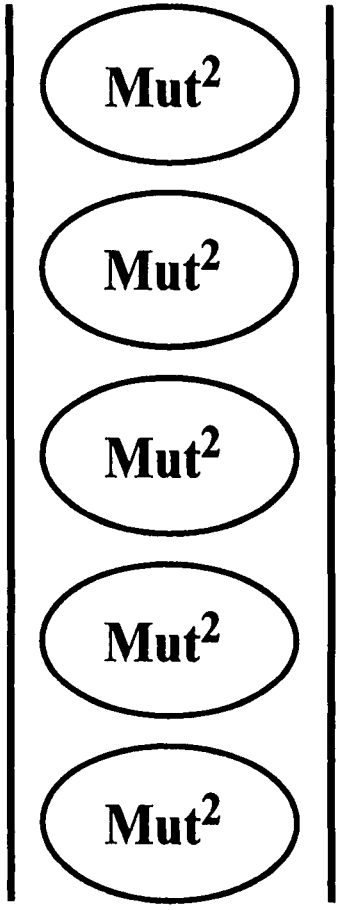

10 cm

[2] R80X

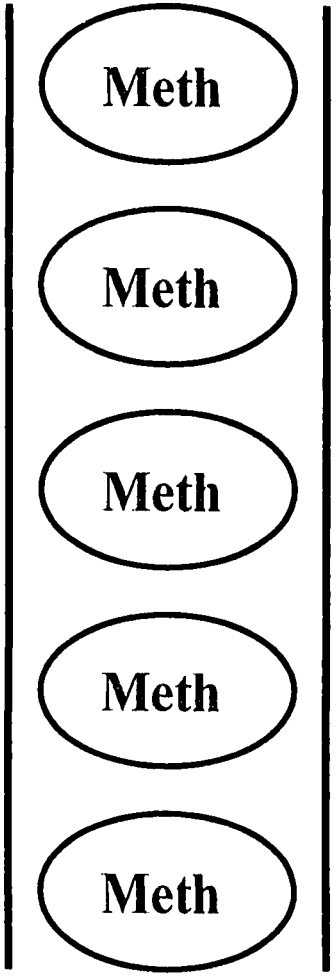

12 cm

Figure 5.3c. p16 Lesions in the Premalignant Barrett's Epithelium From "Mapped" Endoscopic Biopsies in Patients Without Cancer. Each diagram represents the esophagus of an individual patient. The length of the segment of Barrett's epithelium in each patient is indicated below the diagram. Each circle represents a single "mapped" endoscopic biopsy that was analyzed for 9p21 LOH, p16 mutation, and p16 methylation. "LOH" is an abbreviation for 9p21 LOH. "Mut" is an abbreviation for p16 mutation. "Meth" is an abbreviation for p16 methylation. "wt" is an abbreviation for wild-type p16 or no p16 lesion. The diagram on the left depicts a patient with a 12 cm Barrett's segment that had a p16 hemizygous clonal cell population with 9p21 LOH at one biopsy level adjacent to another p16 hemizygous clonal cell population with p16 mutation (A68T) at three biopsy levels. The diagram in the middle depicts a patient with an 11 cm Barrett's segment that had a cell population with only p16 methylation at two biopsy levels adjacent to another p16 hemizygous clonal cell population with 9p21 LOH at two biopsy levels. The diagram on the right depicts a patient with a 9 cm Barrett's segment that had a cell population with only p16 methylation at three biopsy levels adjacent to a cell population with a p16 mutation (H123Y) at a single biopsy level. Identical 9p21 LOH patterns showed the same allelic losses at all six microsatellite markers evaluated.

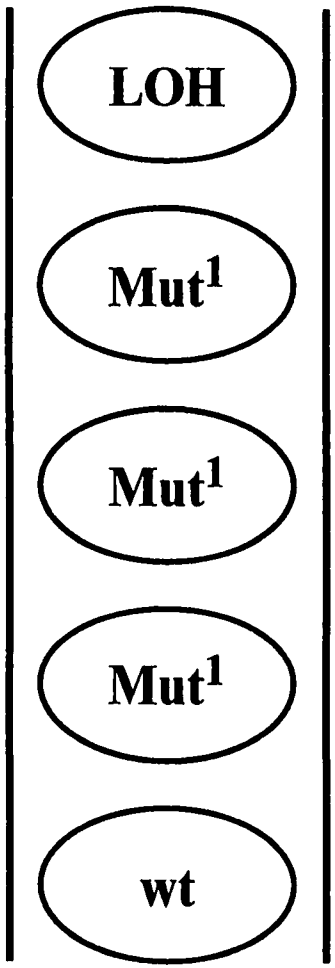

12 cm

[1] A68T

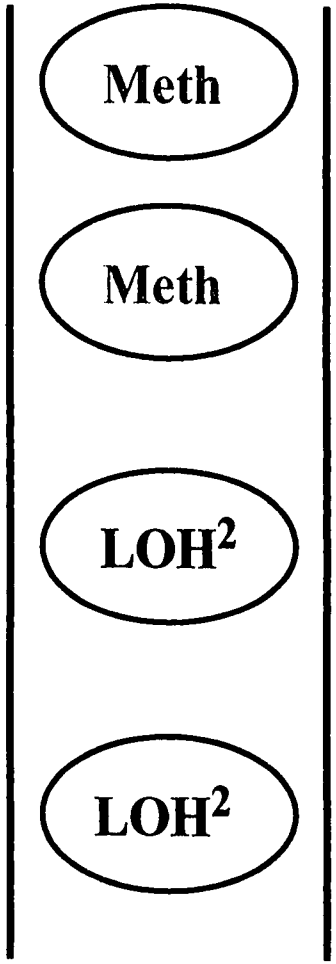

11 cm

[2] Identical LOH pattern

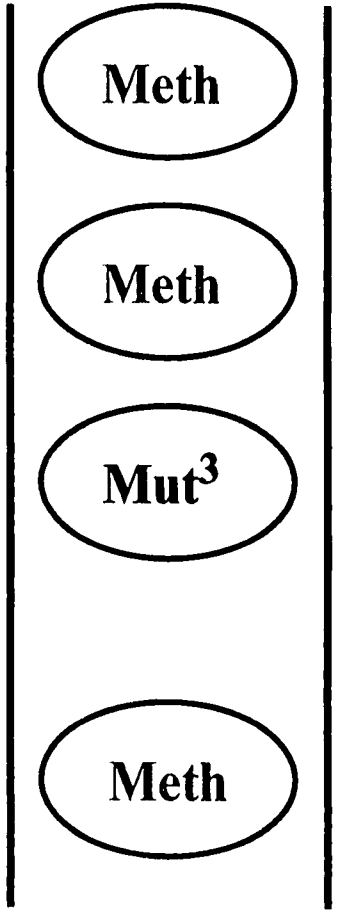

9 cm

[3] H123Y

Figure 5.3d. p16 Lesions in the Premalignant Barrett's Epithelium From "Mapped" Endoscopic Biopsies in Patients Without Cancer. Each diagram represents the esophagus of an individual patient. The length of the segment of Barrett's epithelium in each patient is indicated below the diagram. Each circle represents a single "mapped" endoscopic biopsy that was analyzed for 9p21 LOH, p16 mutation, and p16 methylation. "LOH" is an abbreviation for 9p21 LOH. "Mut" is an abbreviation for p16 mutation. "Meth" is an abbreviation for p16 methylation. "wt" is an abbreviation for wild-type p16 or no p16 lesion. The diagram on the left depicts a patient with a 10 cm Barrett's segment that had a p16 hemizygous clonal cell population with 9p21 LOH at two biopsy levels adjacent to a p16 nullizygous clonal cell population with the same 9p21 LOH pattern and a p16 mutation (L130M). The diagram in the middle depicts a patient with a 10 cm Barrett's segment that had a p16 hemizygous clonal cell population with 9p21 LOH at three biopsy levels adjacent to a p16 nullizygous clonal cell population with the same 9p21 LOH pattern and p16 methylation. The diagram on the right depicts a patient with a 4 cm Barrett's segment that had a cell population with only p16 methylation adjacent to a cell population with p16 methylation and 9p21 LOH. Identical 9p21 LOH patterns showed the same allelic losses at all six microsatellite markers evaluated.

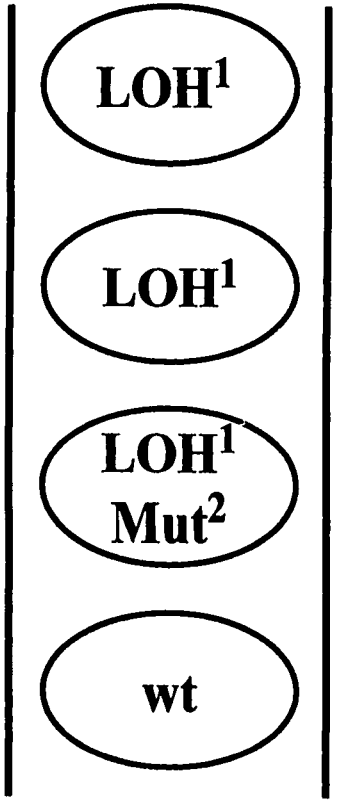

10 cm

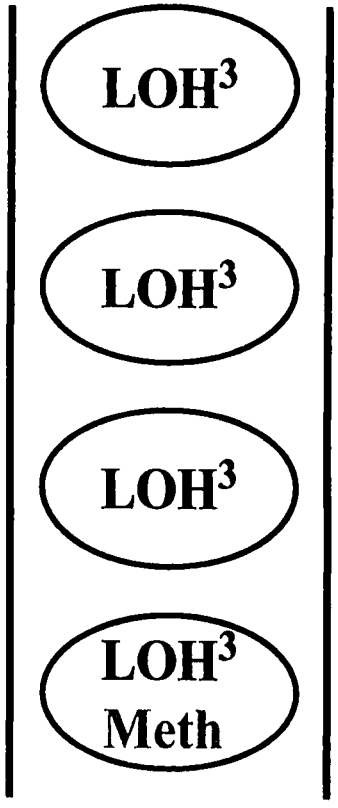

10 cm

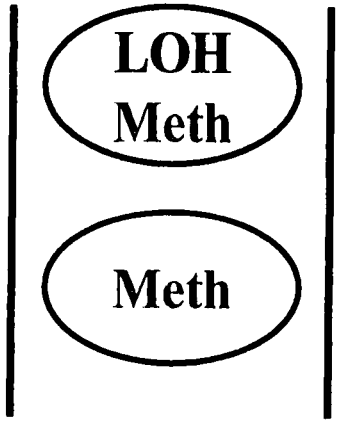

4 cm

[1] Identical LOH pattern

[2] L130M

[3] Identical LOH pattern

Figure 5.3e. p16 Lesions in the Premalignant Barrett's Epithelium From "Mapped" Endoscopic Biopsies in Patients Without Cancer. Each diagram represents the esophagus of an individual patient. The length of the segment of Barrett's epithelium in each patient is indicated below the diagram. Each circle represents a single "mapped" endoscopic biopsy that was analyzed for 9p21 LOH, p16 mutation, p16 methylation, and 17p LOH. "9p LOH" is an abbreviation for 9p21 LOH. "p16 Meth" is an abbreviation for p16 methylation. The diagram on the left depicts a patient with an 11 cm Barrett's segment that had a cell population with only p16 methylation, a cell population with p16 methylation and 17p LOH, and another cell population with only 9p21 LOH. The diagram in the middle depicts a patient with a 15 cm Barrett's segment that had a p16 hemizygous clonal cell population with 9p21 LOH and 17p LOH at four biopsy levels adjacent to a p16 nullizygous clonal cell population with 9p21 LOH, p16 methylation, and 17p LOH. The diagram on the right depicts a patient with an 11 cm Barrett's segment that had a p16 nullizygous clonal cell population with 9p21 LOH and p16 methylation adjacent to a p16 nullizygous clonal cell population with the same 9p21 LOH pattern and p16 methylation as well as 17p LOH. Identical 9p21 LOH and 17p LOH patterns showed the same allelic losses at all six and eight microsatellite markers evaluated, respectively.

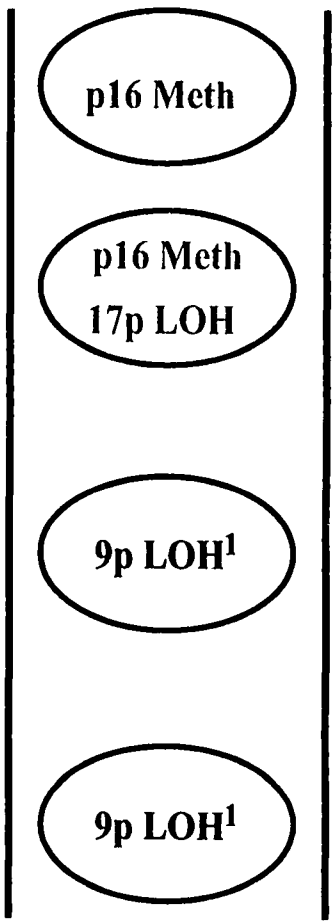

11 cm

[1] Identical LOH pattern

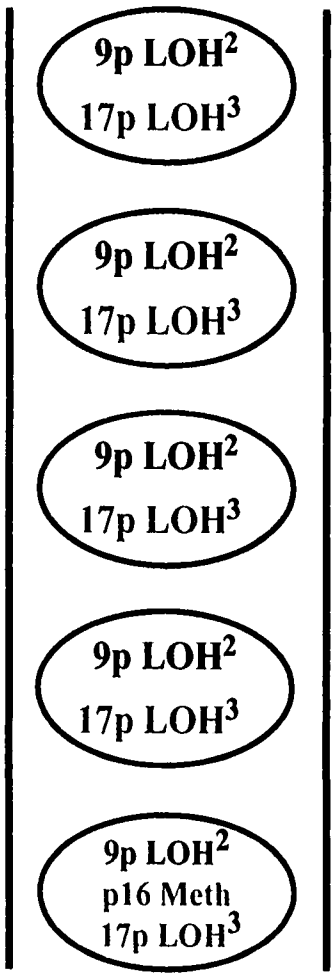

15 cm

[2] Identical LOH pattern

[3] Identical LOH pattern

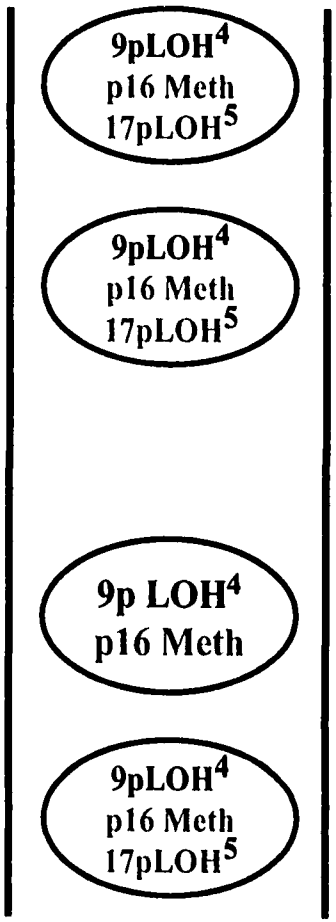

11 cm

[4] Identical LOH pattern

[5] Identical LOH pattern

Table 5.1. Prevalence of p15, $p14^{ARF}$, and p16 Methylation in Barrett's Esophagus in Patients Without Cancer

	Prevalence by Patient	Prevalence by Biopsy
p15 Methylation	3/43 (7%)	3/105 (3%)
$p14^{ARF}$ Methylation	2/43 (5%)	4/113 (4%)
p16 Methylation	21/43 (49%)	67/156 (43%)

Table 5.2. Number of p16 Lesions in Barrett's Esophagus in Patients Without Cancer

Number of p16 Lesions Per Biopsy Sample	Prevalence By Biopsy	Prevalence By Patient
Two	17/67 (25%)	5/29 (17%)
One	35/67 (52%)	9/29 (31%)
Both	N/A	8/29 (28%)
None	13/67 (19%)	7/29 (24%)

BIBLIOGRAPHY

Alcorta, D. A., Xiong, Y., Phelps, D., Hannon, G., Beach, D., and Barrett, J. C. (1996). Involvement of the cyclin-dependent kinase inhibitor p16 (INK4a) in replicative senescence of normal human fibroblasts. Proc Natl Acad Sci U S A *93*, 13742-7.

An, H. X., Niederacher, D., Picard, F., van Roeyen, C., Bender, H. G., and Beckmann, M. W. (1996). Frequent allele loss on 9p21-22 defines a smallest common region in the vicinity of the CDKN2 gene in sporadic breast cancer. Genes Chromosomes Cancer *17*, 14-20.

Antequera, F., and Bird, A. (1993). Number of CpG islands and genes in human and mouse. Proc Natl Acad Sci U S A *90*, 11995-9.

Band, V., De Caprio, J. A., Delmolino, L., Kulesa, V., and Sager, R. (1991). Loss of p53 protein in human papillomavirus type 16 E6-immortalized human mammary epithelial cells. J Virol *65*, 6671-6.

Band, V., and Sager, R. (1989). Distinctive traits of normal and tumor-derived human mammary epithelial cells expressed in a medium that supports long-term growth of both cell types. Proc Natl Acad Sci U S A *86*, 1249-53.

Banks, L., Edmonds, C., and Vousden, K. H. (1990). Ability of the HPV16 E7 protein to bind RB and induce DNA synthesis is not sufficient for efficient transforming activity in NIH3T3 cells. Oncogene *5*, 1383-9.

Barrett, M. T., Galipeau, P. C., Sanchez, C. A., Emond, M. J., and Reid, B. J. (1996). Determination of the frequency of loss of heterozygosity in esophageal adenocarcinoma by cell sorting, whole genome amplification and microsatellite polymorphisms. Oncogene *12*, 1873-8.

Barrett, M. T., Reid, B. J., and Joslyn, G. (1995). Genotypic analysis of multiple loci in somatic cells by whole genome amplification. Nucleic Acids Res *23*, 3488-92.

Barrett, M. T., Sanchez, C. A., Galipeau, P. C., Neshat, K., Emond, M., and Reid, B. J. (1996). Allelic loss of 9p21 and mutation of the CDKN2/p16 gene develop as early lesions during neoplastic progression in Barrett's esophagus. Oncogene *13*, 1867-73.

Barrett, M. T., Sanchez, C. A., Prevo, L. J., Wong, D. J., Galipeau, P. C., Paulson, T. G., Rabinovitch, P. S., and Reid, B. J. (1999). Evolution of neoplastic cell lineages in Barrett oesophagus. Nat Genet *22*, 106-9.

Barrett, M. T., Schutte, M., Kern, S. E., and Reid, B. J. (1996). Allelic loss and mutational analysis of the DPC4 gene in esophageal adenocarcinoma. Cancer Res *56*, 4351-3.

Baylin, S. B., Herman, J. G., Graff, J. R., Vertino, P. M., and Issa, J. P. (1998). Alterations in DNA methylation: a fundamental aspect of neoplasia. Adv Cancer Res *72*, 141-96.

Bedi, G. C., Westra, W. H., Gabrielson, E., Koch, W., and Sidransky, D. (1996). Multiple head and neck tumors: evidence for a common clonal origin. Cancer Res *56*, 2484-7.

Belinsky, S. A., Nikula, K. J., Palmisano, W. A., Michels, R., Saccomanno, G., Gabrielson, E., Baylin, S. B., and Herman, J. G. (1998). Aberrant methylation of p16(INK4a) is an early event in lung cancer and a potential biomarker for early diagnosis. Proc Natl Acad Sci U S A *95*, 11891-6.

Bestor, T. (1987). Supercoiling-dependent sequence specificity of mammalian DNA methyltransferase. Nucleic Acids Res *15*, 3835-43.

Bestor, T. H. (1992). Activation of mammalian DNA methyltransferase by cleavage of a Zn binding regulatory domain. Embo J *11*, 2611-7.

Bhattacharya, S. K., Ramchandani, S., Cervoni, N., and Szyf, M. (1999). A mammalian protein with specific demethylase activity for mCpG DNA [see comments]. Nature *397*, 579-83.

Bird, A. P. (1986). CpG-rich islands and the function of DNA methylation. Nature *321*, 209-13.

Bird, A. P. (1993). Functions for DNA methylation in vertebrates. Cold Spring Harb Symp Quant Biol *58*, 281-5.

Bird, A. P., and Wolffe, A. P. (1999). Methylation-induced repression--belts, braces, and chromatin. Cell *99*, 451-4.

Blount, P. L., Galipeau, P. C., Sanchez, C. A., Neshat, K., Levine, D. S., Yin, J., Suzuki, H., Abraham, J. M., Meltzer, S. J., and Reid, B. J. (1994). 17p allelic losses in diploid cells of patients with Barrett's esophagus who develop aneuploidy. Cancer Res *54*, 2292-5.

Blount, P. L., Meltzer, S. J., Yin, J., Huang, Y., Krasna, M. J., and Reid, B. J. (1993). Clonal ordering of 17p and 5q allelic losses in Barrett dysplasia and adenocarcinoma. Proc Natl Acad Sci U S A *90*, 3221-5.

Boland, C. R., Sato, J., Appelman, H. D., Bresalier, R. S., and Feinberg, A. P. (1995). Microallelotyping defines the sequence and tempo of allelic losses at tumour suppressor gene loci during colorectal cancer progression. Nat Med *1*, 902-9.

Bolden, A. H., Nalin, C. M., Ward, C. A., Poonian, M. S., and Weissbach, A. (1986). Primary DNA sequence determines sites of maintenance and de novo methylation by mammalian DNA methyltransferases. Mol Cell Biol *6*, 1135-40.

Boyes, J., and Bird, A. (1992). Repression of genes by DNA methylation depends on CpG density and promoter strength: evidence for involvement of a methyl-CpG binding protein. Embo J *11*, 327-33.

Brandeis, M., Frank, D., Keshet, I., Siegfried, Z., Mendelsohn, M., Nemes, A., Temper, V., Razin, A., and Cedar, H. (1994). Sp1 elements protect a CpG island from de novo methylation. Nature *371*, 435-8.

Bremner, R., Cohen, B. L., Sopta, M., Hamel, P. A., Ingles, C. J., Gallie, B. L., and Phillips, R. A. (1995). Direct transcriptional repression by pRB and its reversal by specific cyclins. Mol Cell Biol *15*, 3256-65.

Brenner, A. J., and Aldaz, C. M. (1995). Chromosome 9p allelic loss and p16/CDKN2 in breast cancer and evidence of p16 inactivation in immortal breast epithelial cells. Cancer Res *55*, 2892-5.

Brenner, A. J., Stampfer, M. R., and Aldaz, C. M. (1998). Increased p16 expression with first senescence arrest in human mammary epithelial cells and extended growth capacity with p16 inactivation. Oncogene *17*, 199-205.

Cairns, P., Mao, L., Merlo, A., Lee, D. J., Schwab, D., Eby, Y., Tokino, K., van der Riet, P., Blaugrund, J. E., and Sidransky, D. (1994). Rates of p16 (MTS1) mutations in primary tumors with 9p loss [letter; comment]. Science *265*, 415-7.

Cairns, P., Polascik, T. J., Eby, Y., Tokino, K., Califano, J., Merlo, A., Mao, L., Herath, J., Jenkins, R., Westra, W., and et al. (1995). Frequency of homozygous deletion at p16/CDKN2 in primary human tumours. Nat Genet *11*, 210-2.

Caldas, C., Hahn, S. A., da Costa, L. T., Redston, M. S., Schutte, M., Seymour, A. B., Weinstein, C. L., Hruban, R. H., Yeo, C. J., and Kern, S. E. (1994). Frequent somatic mutations and homozygous deletions of the p16 (MTS1) gene in pancreatic adenocarcinoma [published erratum appears in Nat Genet 1994 Dec;8(4):410]. Nat Genet *8*, 27-32.

Califano, J., van der Riet, P., Westra, W., Nawroz, H., Clayman, G., Piantadosi, S., Corio, R., Lee, D., Greenberg, B., Koch, W., and Sidransky, D. (1996). Genetic

progression model for head and neck cancer: implications for field cancerization. Cancer Res *56*, 2488-92.

Carnero, A., Hudson, J. D., Price, C. M., and Beach, D. H. (2000). p16INK4A and p19ARF act in overlapping pathways in cellular immortalization [see comments]. Nat Cell Biol *2*, 148-55.

Carotti, D., Funiciello, S., Palitti, F., and Strom, R. (1998). Influence of pre-existing methylation on the de novo activity of eukaryotic DNA methyltransferase. Biochemistry *37*, 1101-8.

Carotti, D., Palitti, F., Lavia, P., and Strom, R. (1989). In vitro methylation of CpG-rich islands. Nucleic Acids Res *17*, 9219-29.

Chaillet, J. R., Vogt, T. F., Beier, D. R., and Leder, P. (1991). Parental-specific methylation of an imprinted transgene is established during gametogenesis and progressively changes during embryogenesis. Cell *66*, 77-83.

Chen, R. Z., Pettersson, U., Beard, C., Jackson-Grusby, L., and Jaenisch, R. (1998). DNA hypomethylation leads to elevated mutation rates. Nature *395*, 89-93.

Chuang, L. S., Ian, H. I., Koh, T. W., Ng, H. H., Xu, G., and Li, B. F. (1997). Human DNA-(cytosine-5) methyltransferase-PCNA complex as a target for p21WAF1. Science *277*, 1996-2000.

Clark, S. J., Harrison, J., and Frommer, M. (1995). CpNpG methylation in mammalian cells. Nat Genet *10*, 20-7.

Comb, M., and Goodman, H. M. (1990). CpG methylation inhibits proenkephalin gene expression and binding of the transcription factor AP-2. Nucleic Acids Res *18*, 3975-82.

Correa, P., Haenszel, W., Cuello, C., Zavala, D., Fontham, E., Zarama, G., Tannenbaum, S., Collazos, T., and Ruiz, B. (1990). Gastric precancerous process in a high risk population: cohort follow- up. Cancer Res *50*, 4737-40.

Costello, J. F., Berger, M. S., Huang, H. S., and Cavenee, W. K. (1996). Silencing of p16/CDKN2 expression in human gliomas by methylation and chromatin condensation. Cancer Res *56*, 2405-10.

Davies, R., Hicks, R., Crook, T., Morris, J., and Vousden, K. (1993). Human papillomavirus type 16 E7 associates with a histone H1 kinase and with p107 through sequences necessary for transformation. J Virol *67*, 2521-8.

Demers, G. W., Espling, E., Harry, J. B., Etscheid, B. G., and Galloway, D. A. (1996). Abrogation of growth arrest signals by human papillomavirus type 16 E7 is mediated by sequences required for transformation. J Virol *70*, 6862-9.

Dickson, M. A., Hahn, W. C., Ino, Y., Ronfard, V., Wu, J. Y., Weinberg, R. A., Louis, D. N., Li, F. P., and Rheinwald, J. G. (2000). Human keratinocytes that express hTERT and also bypass a p16(INK4a)-enforced mechanism that limits life span become immortal yet retain normal growth and differentiation characteristics. Mol Cell Biol *20*, 1436-47.

Dimri, G. P., and Campisi, J. (1994). Molecular and cell biology of replicative senescence. Cold Spring Harb Symp Quant Biol *59*, 67-73.

Duro, D., Bernard, O., Della Valle, V., Berger, R., and Larsen, C. J. (1995). A new type of p16INK4/MTS1 gene transcript expressed in B-cell malignancies. Oncogene *11*, 21-9.

Dyson, N., Howley, P. M., Munger, K., and Harlow, E. (1989). The human papilloma virus-16 E7 oncoprotein is able to bind to the retinoblastoma gene product. Science *243*, 934-7.

Eide, T. J. (1986). Risk of colorectal cancer in adenoma-bearing individuals within a defined population. Int J Cancer *38*, 173-6.

Erlich, H. A. (1992). PCR technology : principles and applications for DNA amplification (New York: W.H. Freeman & Co.).

Esteller, M., Tortola, S., Toyota, M., Capella, G., Peinado, M. A., Baylin, S. B., and Herman, J. G. (2000). Hypermethylation-associated inactivation of p14(ARF) is independent of p16(INK4a) methylation and p53 mutational status. Cancer Res *60*, 129-33.

Fearon, E. R., and Vogelstein, B. (1990). A genetic model for colorectal tumorigenesis. Cell *61*, 759-67.

Ferguson-Smith, A. C., Sasaki, H., Cattanach, B. M., and Surani, M. A. (1993). Parental-origin-specific epigenetic modification of the mouse H19 gene. Nature *362*, 751-5.

Fero, M. L., Randel, E., Gurley, K. E., Roberts, J. M., and Kemp, C. J. (1998). The murine gene p27Kip1 is haplo-insufficient for tumour suppression. Nature *396*, 177-80.

Foster, S. A., and Galloway, D. A. (1996). Human papillomavirus type 16 E7 alleviates a proliferation block in early passage human mammary epithelial cells. Oncogene *12*, 1773-9.

Foster, S. A., Wong, D. J., Barrett, M. T., and Galloway, D. A. (1998). Inactivation of p16 in human mammary epithelial cells by CpG island methylation. Mol Cell Biol *18*, 1793-801.

Franklin, W. A., Gazdar, A. F., Haney, J., Wistuba, II, La Rosa, F. G., Kennedy, T., Ritchey, D. M., and Miller, Y. E. (1997). Widely dispersed p53 mutation in respiratory epithelium. A novel mechanism for field carcinogenesis [published erratum appears in J Clin Invest 1997 Nov 15;100(10):2639]. J Clin Invest *100*, 2133-7.

Frommer, M., McDonald, L. E., Millar, D. S., Collis, C. M., Watt, F., Grigg, G. W., Molloy, P. L., and Paul, C. L. (1992). A genomic sequencing protocol that yields a positive display of 5- methylcytosine residues in individual DNA strands. Proc Natl Acad Sci U S A *89*, 1827-31.

Funk, J. O., Waga, S., Harry, J. B., Espling, E., Stillman, B., and Galloway, D. A. (1997). Inhibition of CDK activity and PCNA-dependent DNA replication by p21 is blocked by interaction with the HPV-16 E7 oncoprotein. Genes Dev *11*, 2090-100.

Galipeau, P. C., Cowan, D. S., Sanchez, C. A., Barrett, M. T., Emond, M. J., Levine, D. S., Rabinovitch, P. S., and Reid, B. J. (1996). 17p (p53) allelic losses, 4N (G2/tetraploid) populations, and progression to aneuploidy in Barrett's esophagus. Proc Natl Acad Sci U S A *93*, 7081-4.

Galipeau, P. C., Prevo, L. J., Sanchez, C. A., Longton, G. M., and Reid, B. J. (1999). Clonal expansion and loss of heterozygosity at chromosomes 9p and 17p in premalignant esophageal (Barrett's) tissue. J Natl Cancer Inst *91*, 2087-95.

Garrett, L. R., Perez-Reyes, N., Smith, P. P., and McDougall, J. K. (1993). Interaction of HPV-18 and nitrosomethylurea in the induction of squamous cell carcinoma. Carcinogenesis *14*, 329-32.

Gazdar, A. F., Bader, S., Hung, J., Kishimoto, Y., Sekido, Y., Sugio, K., Virmani, A., Fleming, J., Carbone, D. P., and Minna, J. D. (1994). Molecular genetic changes found in human lung cancer and its precursor lesions. Cold Spring Harb Symp Quant Biol *59*, 565-72.

Gerdes, J., Lemke, H., Baisch, H., Wacker, H. H., Schwab, U., and Stein, H. (1984). Cell cycle analysis of a cell proliferation-associated human nuclear antigen defined by the monoclonal antibody Ki-67. J Immunol *133*, 1710-5.

Gerdes, J., Schwab, U., Lemke, H., and Stein, H. (1983). Production of a mouse monoclonal antibody reactive with a human nuclear antigen associated with cell proliferation. Int J Cancer *31*, 13-20.

Glisin, V., Crkvenjakov, R., and Byus, C. (1974). Ribonucleic acid isolated by cesium chloride centrifugation. Biochemistry *13*, 2633-7.

Goelz, S. E., Vogelstein, B., Hamilton, S. R., and Feinberg, A. P. (1985). Hypomethylation of DNA from benign and malignant human colon neoplasms. Science *228*, 187-90.

Gonzalez-Zulueta, M., Bender, C. M., Yang, A. S., Nguyen, T., Beart, R. W., Van Tornout, J. M., and Jones, P. A. (1995). Methylation of the 5' CpG island of the p16/CDKN2 tumor suppressor gene in normal and transformed human tissues correlates with gene silencing. Cancer Res *55*, 4531-5.

Gonzalgo, M. L., Hayashida, T., Bender, C. M., Pao, M. M., Tsai, Y. C., Gonzales, F. A., Nguyen, H. D., Nguyen, T. T., and Jones, P. A. (1998). The role of DNA methylation in expression of the p19/p16 locus in human bladder cancer cell lines. Cancer Res *58*, 1245-52.

Gonzalgo, M. L., and Jones, P. A. (1997). Rapid quantitation of methylation differences at specific sites using methylation-sensitive single nucleotide primer extension (Ms-SNuPE). Nucleic Acids Res *25*, 2529-31.

Halbert, C. L., Demers, G. W., and Galloway, D. A. (1991). The E7 gene of human papillomavirus type 16 is sufficient for immortalization of human epithelial cells. J Virol *65*, 473-8.

Hamilton, S. R., Smith, R. R., and Cameron, J. L. (1988). Prevalence and characteristics of Barrett esophagus in patients with adenocarcinoma of the esophagus or esophagogastric junction. Hum Pathol *19*, 942-8.

Hannon, G. J., and Beach, D. (1994). p15INK4B is a potential effector of TGF-beta-induced cell cycle arrest [see comments]. Nature *371*, 257-61.

Hara, E., Smith, R., Parry, D., Tahara, H., Stone, S., and Peters, G. (1996). Regulation of p16CDKN2 expression and its implications for cell immortalization and senescence. Mol Cell Biol *16*, 859-67.

Harbour, J. W., Luo, R. X., Dei Santi, A., Postigo, A. A., and Dean, D. C. (1999). Cdk phosphorylation triggers sequential intramolecular interactions that progressively block Rb functions as cells move through G1. Cell *98*, 859-69.

Hawley-Nelson, P., Vousden, K. H., Hubbert, N. L., Lowy, D. R., and Schiller, J. T. (1989). HPV16 E6 and E7 proteins cooperate to immortalize human foreskin keratinocytes. Embo J *8*, 3905-10.

Hayflick, L. (1976). The cell biology of human aging. N Engl J Med *295*, 1302-8.

Hayflick, L. (1965). The limited in vitro lifetime of human diploid cell strains. Exp Cell Res *37*, 614-36.

Herman, J. G., Graff, J. R., Myohanen, S., Nelkin, B. D., and Baylin, S. B. (1996). Methylation-specific PCR: a novel PCR assay for methylation status of CpG islands. Proc Natl Acad Sci U S A *93*, 9821-6.

Herman, J. G., Jen, J., Merlo, A., and Baylin, S. B. (1996). Hypermethylation-associated inactivation indicates a tumor suppressor role for p15INK4B. Cancer Res *56*, 722-7.

Herman, J. G., Merlo, A., Mao, L., Lapidus, R. G., Issa, J. P., Davidson, N. E., Sidransky, D., and Baylin, S. B. (1995). Inactivation of the CDKN2/p16/MTS1 gene is frequently associated with aberrant DNA methylation in all common human cancers. Cancer Res *55*, 4525-30.

Hornstra, I. K., and Yang, T. P. (1994). High-resolution methylation analysis of the human hypoxanthine phosphoribosyltransferase gene 5' region on the active and inactive X chromosomes: correlation with binding sites for transcription factors. Mol Cell Biol *14*, 1419-30.

Howlett, S. K., and Reik, W. (1991). Methylation levels of maternal and paternal genomes during preimplantation development. Development *113*, 119-27.

Hsieh, C. L. (1994). Dependence of transcriptional repression on CpG methylation density. Mol Cell Biol *14*, 5487-94.

Hurlin, P. J., Kaur, P., Smith, P. P., Perez-Reyes, N., Blanton, R. A., and McDougall, J. K. (1991). Progression of human papillomavirus type 18-immortalized human keratinocytes to a malignant phenotype. Proc Natl Acad Sci U S A *88*, 570-4.

Huschtscha, L. I., Noble, J. R., Neumann, A. A., Moy, E. L., Barry, P., Melki, J. R., Clark, S. J., and Reddel, R. R. (1998). Loss of p16INK4 expression by methylation is associated with lifespan extension of human mammary epithelial cells [In Process Citation]. Cancer Res *58*, 3508-12.

Hussussian, C. J., Struewing, J. P., Goldstein, A. M., Higgins, P. A., Ally, D. S., Sheahan, M. D., Clark, W. H., Jr., Tucker, M. A., and Dracopoli, N. C. (1994). Germline p16 mutations in familial melanoma [see comments]. Nat Genet *8*, 15-21.

Iguchi-Ariga, S. M., and Schaffner, W. (1989). CpG methylation of the cAMP-responsive enhancer/promoter sequence TGACGTCA abolishes specific factor binding as well as transcriptional activation. Genes Dev *3*, 612-9.

Jen, J., Harper, J. W., Bigner, S. H., Bigner, D. D., Papadopoulos, N., Markowitz, S., Willson, J. K., Kinzler, K. W., and Vogelstein, B. (1994). Deletion of p16 and p15 genes in brain tumors. Cancer Res *54*, 6353-8.

Jewers, R. J., Hildebrandt, P., Ludlow, J. W., Kell, B., and McCance, D. J. (1992). Regions of human papillomavirus type 16 E7 oncoprotein required for immortalization of human keratinocytes. J Virol *66*, 1329-35.

Jones, P. A. (1996). DNA methylation errors and cancer. Cancer Res *56*, 2463-7.

Jones, P. A., and Laird, P. W. (1999). Cancer epigenetics comes of age. Nat Genet *21*, 163-7.

Kafri, T., Ariel, M., Brandeis, M., Shemer, R., Urven, L., McCarrey, J., Cedar, H., and Razin, A. (1992). Developmental pattern of gene-specific DNA methylation in the mouse embryo and germ line. Genes Dev *6*, 705-14.

Kamb, A., Gruis, N. A., Weaver-Feldhaus, J., Liu, Q., Harshman, K., Tavtigian, S. V., Stockert, E., Day, R. S., 3rd, Johnson, B. E., and Skolnick, M. H. (1994). A cell cycle regulator potentially involved in genesis of many tumor types [see comments]. Science *264*, 436-40.

Kamijo, T., Zindy, F., Roussel, M. F., Quelle, D. E., Downing, J. R., Ashmun, R. A., Grosveld, G., and Sherr, C. J. (1997). Tumor suppression at the mouse INK4a locus mediated by the alternative reading frame product p19ARF. Cell *91*, 649-59.

Kass, S. U., Goddard, J. P., and Adams, R. L. (1993). Inactive chromatin spreads from a focus of methylation. Mol Cell Biol *13*, 7372-9.

Kiyono, T., Foster, S. A., Koop, J. I., McDougall, J. K., Galloway, D. A., and Klingelhutz, A. J. (1998). Both Rb/p16INK4a inactivation and telomerase activity are required to immortalize human epithelial cells [see comments]. Nature *396*, 84-8.

Klingelhutz, A. J., Smith, P. P., Garrett, L. R., and McDougall, J. K. (1993). Alteration of the DCC tumor-suppressor gene in tumorigenic HPV-18 immortalized human keratinocytes transformed by nitrosomethylurea. Oncogene *8*, 95-9.

Klump, B., Hsieh, C. J., Holzmann, K., Gregor, M., and Porschen, R. (1998). Hypermethylation of the CDKN2/p16 promoter during neoplastic progression in Barrett's esophagus. Gastroenterology *115*, 1381-6.

Knoepfler, P. S., and Eisenman, R. N. (1999). Sin meets NuRD and other tails of repression. Cell *99*, 447-50.

Knudson, A. G., Jr. (1971). Mutation and cancer: statistical study of retinoblastoma. Proc Natl Acad Sci U S A *68*, 820-3.

Koh, J., Enders, G. H., Dynlacht, B. D., and Harlow, E. (1995). Tumour-derived p16 alleles encoding proteins defective in cell-cycle inhibition. Nature *375*, 506-10.

Kuukasjarvi, T., Karhu, R., Tanner, M., Kahkonen, M., Schaffer, A., Nupponen, N., Pennanen, S., Kallioniemi, A., Kallioniemi, O. P., and Isola, J. (1997). Genetic heterogeneity and clonal evolution underlying development of asynchronous metastasis in human breast cancer. Cancer Res *57*, 1597-604.

Laborda, J. (1991). 36B4 cDNA used as an estradiol-independent mRNA control is the cDNA for human acidic ribosomal phosphoprotein PO. Nucleic Acids Res *19*, 3998.

Lagergren, J., Bergstrom, R., Lindgren, A., and Nyren, O. (1999). Symptomatic gastroesophageal reflux as a risk factor for esophageal adenocarcinoma [see comments]. N Engl J Med *340*, 825-31.

Larsen, F., Gundersen, G., Lopez, R., and Prydz, H. (1992). CpG islands as gene markers in the human genome. Genomics *13*, 1095-107.

Lei, H., Oh, S. P., Okano, M., Juttermann, R., Goss, K. A., Jaenisch, R., and Li, E. (1996). De novo DNA cytosine methyltransferase activities in mouse embryonic stem cells. Development *122*, 3195-205.

Leonhardt, H., Page, A. W., Weier, H. U., and Bestor, T. H. (1992). A targeting sequence directs DNA methyltransferase to sites of DNA replication in mammalian nuclei. Cell *71*, 865-73.

Levine, D. S., Haggitt, R. C., Blount, P. L., Rabinovitch, P. S., Rusch, V. W., and Reid, B. J. (1993). An endoscopic biopsy protocol can differentiate high-grade dysplasia from early adenocarcinoma in Barrett's esophagus [see comments]. Gastroenterology *105*, 40-50.

Levine, D. S., Rabinovitch, P. S., Haggitt, R. C., Blount, P. L., Dean, P. J., Rubin, C. E., and Reid, B. J. (1991). Distribution of aneuploid cell populations in ulcerative colitis with dysplasia or cancer. Gastroenterology *101*, 1198-210.

Li, E., Bestor, T. H., and Jaenisch, R. (1992). Targeted mutation of the DNA methyltransferase gene results in embryonic lethality. Cell *69*, 915-26.

Loughran, O., Malliri, A., Owens, D., Gallimore, P. H., Stanley, M. A., Ozanne, B., Frame, M. C., and Parkinson, E. K. (1996). Association of CDKN2A/p16INK4A with human head and neck keratinocyte replicative senescence: relationship of dysfunction to immortality and neoplasia. Oncogene *13*, 561-8.

Ludlow, J. W., Shon, J., Pipas, J. M., Livingston, D. M., and DeCaprio, J. A. (1990). The retinoblastoma susceptibility gene product undergoes cell cycle-dependent dephosphorylation and binding to and release from SV40 large T. Cell *60*, 387-96.

Lukas, J., Parry, D., Aagaard, L., Mann, D. J., Bartkova, J., Strauss, M., Peters, G., and Bartek, J. (1995). Retinoblastoma-protein-dependent cell-cycle inhibition by the tumour suppressor p16. Nature *375*, 503-6.

Lundberg, A. S., and Weinberg, R. A. (1998). Functional inactivation of the retinoblastoma protein requires sequential modification by at least two distinct cyclin-cdk complexes. Mol Cell Biol *18*, 753-61.

Macleod, D., Charlton, J., Mullins, J., and Bird, A. P. (1994). Sp1 sites in the mouse aprt gene promoter are required to prevent methylation of the CpG island. Genes Dev *8*, 2282-92.

Mao, L., Lee, J. S., Kurie, J. M., Fan, Y. H., Lippman, S. M., Lee, J. J., Ro, J. Y., Broxson, A., Yu, R., Morice, R. C., Kemp, B. L., Khuri, F. R., Walsh, G. L., Hittelman, W. N., and Hong, W. K. (1997). Clonal genetic alterations in the lungs of current and former smokers [see comments]. J Natl Cancer Inst *89*, 857-62.

Mao, L., Merlo, A., Bedi, G., Shapiro, G. I., Edwards, C. D., Rollins, B. J., and Sidransky, D. (1995). A novel p16INK4A transcript. Cancer Res *55*, 2995-7.

Martin, G. M., Sprague, C. A., and Epstein, C. J. (1970). Replicative life-span of cultivated human cells. Effects of donor's age, tissue, and genotype. Lab Invest *23*, 86-92.

McDonald, L. E., and Kay, G. F. (1997). Methylation analysis using bisulfite genomic sequencing: application to small numbers of intact cells. Biotechniques *22*, 272-4.

Medema, R. H., Herrera, R. E., Lam, F., and Weinberg, R. A. (1995). Growth suppression by p16ink4 requires functional retinoblastoma protein. Proc Natl Acad Sci U S A *92*, 6289-93.

Merlo, A., Herman, J. G., Mao, L., Lee, D. J., Gabrielson, E., Burger, P. C., Baylin, S. B., and Sidransky, D. (1995). 5' CpG island methylation is associated with transcriptional silencing of the tumour suppressor p16/CDKN2/MTS1 in human cancers [see comments]. Nat Med *1*, 686-92.

Mihara, K., Cao, X. R., Yen, A., Chandler, S., Driscoll, B., Murphree, A. L., T'Ang, A., and Fung, Y. K. (1989). Cell cycle-dependent regulation of phosphorylation of the human retinoblastoma gene product. Science *246*, 1300-3.

Miller, A. D., and Rosman, G. J. (1989). Improved retroviral vectors for gene transfer and expression. Biotechniques *7*, 980-2, 984-6, 989-90.

Monk, M., Boubelik, M., and Lehnert, S. (1987). Temporal and regional changes in DNA methylation in the embryonic, extraembryonic and germ cell lineages during mouse embryo development. Development *99*, 371-82.

Munger, K., Phelps, W. C., Bubb, V., Howley, P. M., and Schlegel, R. (1989). The E6 and E7 genes of the human papillomavirus type 16 together are necessary and sufficient for transformation of primary human keratinocytes. J Virol *63*, 4417-21.

Munger, K., Werness, B. A., Dyson, N., Phelps, W. C., Harlow, E., and Howley, P. M. (1989). Complex formation of human papillomavirus E7 proteins with the retinoblastoma tumor suppressor gene product. Embo J *8*, 4099-105.

Muto, S., Horie, S., Takahashi, S., Tomita, K., and Kitamura, T. (2000). Genetic and epigenetic alterations in normal bladder epithelium in patients with metachronous bladder cancer. Cancer Res *60*, 4021-5.

Neshat, K., Sanchez, C. A., Galipeau, P. C., Blount, P. L., Levine, D. S., Joslyn, G., and Reid, B. J. (1994). p53 mutations in Barrett's adenocarcinoma and high-grade dysplasia. Gastroenterology *106*, 1589-95.

Neshat, K., Sanchez, C. A., Galipeau, P. C., Cowan, D. S., Ramel, S., Levine, D. S., and Reid, B. J. (1994). Barrett's esophagus: a model of human neoplastic progression. Cold Spring Harb Symp Quant Biol *59*, 577-83.

Noble, J. R., Rogan, E. M., Neumann, A. A., Maclean, K., Bryan, T. M., and Reddel, R. R. (1996). Association of extended in vitro proliferative potential with loss of p16INK4 expression. Oncogene *13*, 1259-68.

Nobori, T., Miura, K., Wu, D. J., Lois, A., Takabayashi, K., and Carson, D. A. (1994). Deletions of the cyclin-dependent kinase-4 inhibitor gene in multiple human cancers. Nature *368*, 753-6.

Nowell, P. C. (1976). The clonal evolution of tumor cell populations. Science *194*, 23-8.

Oberle, I., Rousseau, F., Heitz, D., Kretz, C., Devys, D., Hanauer, A., Boue, J., Bertheas, M. F., and Mandel, J. L. (1991). Instability of a 550-base pair DNA segment and abnormal methylation in fragile X syndrome. Science *252*, 1097-102.

Okano, M., Bell, D. W., Haber, D. A., and Li, E. (1999). DNA methyltransferases Dnmt3a and Dnmt3b are essential for de novo methylation and mammalian development. Cell *99*, 247-57.

Okano, M., Xie, S., and Li, E. (1998). Cloning and characterization of a family of novel mammalian DNA (cytosine-5) methyltransferases [letter]. Nat Genet *19*, 219-20.

Park, J. G., and Chapman, V. M. (1994). CpG island promoter region methylation patterns of the inactive-X- chromosome hypoxanthine phosphoribosyltransferase (Hprt) gene. Mol Cell Biol *14*, 7975-83.

Paulson, T. G., Galipeau, P. C., and Reid, B. J. (1999). Loss of heterozygosity analysis using whole genome amplification, cell sorting, and fluorescence-based PCR. Genome Res *9*, 482-91.

Petersen, S. E., Lorentzen, M., and Bichel, P. (1980). A mosaic subpopulation structure of human colorectal carcinomas demonstrated by flow cytometry. Flow Cytometry *IV*, 412-6.

Pfeifer, G. P., Steigerwald, S. D., Hansen, R. S., Gartler, S. M., and Riggs, A. D. (1990). Polymerase chain reaction-aided genomic sequencing of an X chromosome- linked CpG island: methylation patterns suggest clonal inheritance, CpG site autonomy, and an explanation of activity state stability. Proc Natl Acad Sci U S A *87*, 8252-6.

Pfeifer, G. P., Tanguay, R. L., Steigerwald, S. D., and Riggs, A. D. (1990). In vivo footprint and methylation analysis by PCR-aided genomic sequencing: comparison of active and inactive X chromosomal DNA at the CpG island and promoter of human PGK-1. Genes Dev *4*, 1277-87.

Phillips, R. W., and Wong, R. K. (1991). Barrett's esophagus. Natural history, incidence, etiology, and complications. Gastroenterol Clin North Am *20*, 791-816.

Pomerantz, J., Schreiber-Agus, N., Liegeois, N. J., Silverman, A., Alland, L., Chin, L., Potes, J., Chen, K., Orlow, I., Lee, H. W., Cordon-Cardo, C., and DePinho, R. A. (1998). The Ink4a tumor suppressor gene product, p19Arf, interacts with MDM2 and neutralizes MDM2's inhibition of p53. Cell *92*, 713-23.

Qian, X. C., and Brent, T. P. (1997). Methylation hot spots in the 5' flanking region denote silencing of the O6-methylguanine-DNA methyltransferase gene. Cancer Res *57*, 3672-7.

Quelle, D. E., Cheng, M., Ashmun, R. A., and Sherr, C. J. (1997). Cancer-associated mutations at the INK4a locus cancel cell cycle arrest by p16INK4a but not by the alternative reading frame protein p19ARF. Proc Natl Acad Sci U S A *94*, 669-73.

Quelle, D. E., Zindy, F., Ashmun, R. A., and Sherr, C. J. (1995). Alternative reading frames of the INK4a tumor suppressor gene encode two unrelated proteins capable of inducing cell cycle arrest. Cell *83*, 993-1000.

Rabinovitch, P. S., Reid, B. J., Haggitt, R. C., Norwood, T. H., and Rubin, C. E. (1989). Progression to cancer in Barrett's esophagus is associated with genomic instability. Lab Invest *60*, 65-71.

Reed, A. L., Califano, J., Cairns, P., Westra, W. H., Jones, R. M., Koch, W., Ahrendt, S., Eby, Y., Sewell, D., Nawroz, H., Bartek, J., and Sidransky, D. (1996). High frequency of p16 (CDKN2/MTS-1/INK4A) inactivation in head and neck squamous cell carcinoma. Cancer Res *56*, 3630-3.

Reid, B. J., Barrett, M. T., Galipeau, P. C., Sanchez, C. A., Neshat, K., Cowan, D. S., and Levine, D. S. (1996). Barrett's esophagus: ordering the events that lead to cancer. Eur J Cancer Prev *5 Suppl 2*, 57-65.

Reid, B. J., Blount, P. L., Rubin, C. E., Levine, D. S., Haggitt, R. C., and Rabinovitch, P. S. (1992). Flow-cytometric and histological progression to malignancy in Barrett's esophagus: prospective endoscopic surveillance of a cohort [see comments]. Gastroenterology *102*, 1212-9.

Reid, B. J., Haggitt, R. C., Rubin, C. E., and Rabinovitch, P. S. (1987). Barrett's esophagus. Correlation between flow cytometry and histology in detection of patients at risk for adenocarcinoma. Gastroenterology *93*, 1-11.

Reid, B. J., Haggitt, R. C., Rubin, C. E., Roth, G., Surawicz, C. M., Van Belle, G., Lewin, K., Weinstein, W. M., Antonioli, D. A., Goldman, H., and et al. (1988). Observer variation in the diagnosis of dysplasia in Barrett's esophagus. Hum Pathol *19*, 166-78.

Reid, B. J., Levine, D. S., Longton, G., Blount, P. L., and Rabinovitch, P. S. (2000). Predictors of progression to cancer in Barrett's esophagus: baseline histology and flow cytometry identify low- and high-risk patient subsets. Am J Gastroenterol *95*, 1669-76.

Reid, B. J., Weinstein, W. M., Lewin, K. J., Haggitt, R. C., VanDeventer, G., DenBesten, L., and Rubin, C. E. (1988). Endoscopic biopsy can detect high-grade dysplasia or early adenocarcinoma in Barrett's esophagus without grossly recognizable neoplastic lesions. Gastroenterology *94*, 81-90.

Reynisdottir, I., Polyak, K., Iavarone, A., and Massague, J. (1995). Kip/Cip and Ink4 Cdk inhibitors cooperate to induce cell cycle arrest in response to TGF-beta. Genes Dev *9*, 1831-45.

Reznikoff, C. A., Yeager, T. R., Belair, C. D., Savelieva, E., Puthenveettil, J. A., and Stadler, W. M. (1996). Elevated p16 at senescence and loss of p16 at immortalization in human papillomavirus 16 E6, but not E7, transformed human uroepithelial cells. Cancer Res *56*, 2886-90.

Riggs, A. D., and Pfeifer, G. P. (1992). X-chromosome inactivation and cell memory. Trends Genet *8*, 169-74.

Riggs, A. D., Xiong, Z., Wang, L., and LeBon, J. M. (1998). Methylation dynamics, epigenetic fidelity and X chromosome structure. Novartis Found Symp *214*, 214-25.

Robertson, K. D., and Jones, P. A. (1998). The human ARF cell cycle regulatory gene promoter is a CpG island which can be silenced by DNA methylation and down-regulated by wild-type p53. Mol Cell Biol *18*, 6457-73.

Rohme, D. (1981). Evidence for a relationship between longevity of mammalian species and life spans of normal fibroblasts in vitro and erythrocytes in vivo. Proc Natl Acad Sci U S A *78*, 5009-13.

Rozen, P., Baratz, M., Fefer, F., and Gilat, T. (1995). Low incidence of significant dysplasia in a successful endoscopic surveillance program of patients with ulcerative colitis [see comments]. Gastroenterology *108*, 1361-70.

Sampliner, R. E. (1998). Practice guidelines on the diagnosis, surveillance, and therapy of Barrett's esophagus. The Practice Parameters Committee of the American College of Gastroenterology. Am J Gastroenterol *93*, 1028-32.

Sanford, J. P., Clark, H. J., Chapman, V. M., and Rossant, J. (1987). Differences in DNA methylation during oogenesis and spermatogenesis and their persistence during early embryogenesis in the mouse. Genes Dev *1*, 1039-46.

Scheffner, M., Werness, B. A., Huibregtse, J. M., Levine, A. J., and Howley, P. M. (1990). The E6 oncoprotein encoded by human papillomavirus types 16 and 18 promotes the degradation of p53. Cell *63*, 1129-36.

Schneider, E. L., and Mitsui, Y. (1976). The relationship between in vitro cellular aging and in vivo human age. Proc Natl Acad Sci U S A *73*, 3584-8.

Schutte, M., Hruban, R. H., Geradts, J., Maynard, R., Hilgers, W., Rabindran, S. K., Moskaluk, C. A., Hahn, S. A., Schwarte-Waldhoff, I., Schmiegel, W., Baylin, S. B., Kern, S. E., and Herman, J. G. (1997). Abrogation of the Rb/p16 tumor-suppressive pathway in virtually all pancreatic carcinomas. Cancer Res *57*, 3126-30.

Serrano, M., Hannon, G. J., and Beach, D. (1993). A new regulatory motif in cell-cycle control causing specific inhibition of cyclin D/CDK4 [see comments]. Nature *366*, 704-7.

Serrano, M., Lee, H., Chin, L., Cordon-Cardo, C., Beach, D., and DePinho, R. A. (1996). Role of the INK4a locus in tumor suppression and cell mortality. Cell *85*, 27-37.

Serrano, M., Lin, A. W., McCurrach, M. E., Beach, D., and Lowe, S. W. (1997). Oncogenic ras provokes premature cell senescence associated with accumulation of p53 and p16INK4a. Cell *88*, 593-602.

Shay, J. W., Wright, W. E., Brasiskyte, D., and Van der Haegen, B. A. (1993). E6 of human papillomavirus type 16 can overcome the M1 stage of immortalization in human mammary epithelial cells but not in human fibroblasts. Oncogene *8*, 1407-13.

Sherr, C. J. (1996). Cancer cell cycles. Science *274*, 1672-7.

Sidransky, D., Mikkelsen, T., Schwechheimer, K., Rosenblum, M. L., Cavanee, W., and Vogelstein, B. (1992). Clonal expansion of p53 mutant cells is associated with brain tumour progression. Nature *355*, 846-7.

Silva, A. J., Ward, K., and White, R. (1993). Mosaic methylation in clonal tissue. Dev Biol *156*, 391-8.

Spechler, S. J. (1987). Endoscopic surveillance for patients with Barrett esophagus: does the cancer risk justify the practice? Ann Intern Med *106*, 902-4.

Stampfer, M. R. (1985). Isolation and growth of human mammary epithelial cells. J Tissue Culture Methods *9*, 107-15.

Stein, R., Gruenbaum, Y., Pollack, Y., Razin, A., and Cedar, H. (1982). Clonal inheritance of the pattern of DNA methylation in mouse cells. Proc Natl Acad Sci U S A *79*, 61-5.

Stirzaker, C., Millar, D. S., Paul, C. L., Warnecke, P. M., Harrison, J., Vincent, P. C., Frommer, M., and Clark, S. J. (1997). Extensive DNA methylation spanning the Rb promoter in retinoblastoma tumors. Cancer Res *57*, 2229-37.

Stoger, R., Kajimura, T. M., Brown, W. T., and Laird, C. D. (1997). Epigenetic variation illustrated by DNA methylation patterns of the fragile-X gene FMR1. Hum Mol Genet *6*, 1791-801.

Stoger, R., Kubicka, P., Liu, C. G., Kafri, T., Razin, A., Cedar, H., and Barlow, D. P. (1993). Maternal-specific methylation of the imprinted mouse Igf2r locus identifies the expressed locus as carrying the imprinting signal. Cell *73*, 61-71.

Stone, S., Dayananth, P., Jiang, P., Weaver-Feldhaus, J. M., Tavtigian, S. V., Cannon-Albright, L., and Kamb, A. (1995). Genomic structure, expression and mutational analysis of the P15 (MTS2) gene. Oncogene *11*, 987-91.

Stone, S., Jiang, P., Dayananth, P., Tavtigian, S. V., Katcher, H., Parry, D., Peters, G., and Kamb, A. (1995). Complex structure and regulation of the P16 (MTS1) locus. Cancer Res *55*, 2988-94.

Surani, M. A. (1998). Imprinting and the initiation of gene silencing in the germ line. Cell *93*, 309-12.

Tao, W., and Levine, A. J. (1999). P19(ARF) stabilizes p53 by blocking nucleo-cytoplasmic shuttling of Mdm2. Proc Natl Acad Sci U S A *96*, 6937-41.

Thomas, G. A., Williams, D., and Williams, E. D. (1988). The demonstration of tissue clonality by X-linked enzyme histochemistry. J Pathol *155*, 101-8.

Toth, M., Lichtenberg, U., and Doerfler, W. (1989). Genomic sequencing reveals a 5-methylcytosine-free domain in active promoters and the spreading of preimposed methylation patterns. Proc Natl Acad Sci U S A *86*, 3728-32.

Tremblay, K. D., Duran, K. L., and Bartolomei, M. S. (1997). A 5' 2-kilobase-pair region of the imprinted mouse H19 gene exhibits exclusive paternal methylation throughout development. Mol Cell Biol *17*, 4322-9.

Tremblay, K. D., Saam, J. R., Ingram, R. S., Tilghman, S. M., and Bartolomei, M. S. (1995). A paternal-specific methylation imprint marks the alleles of the mouse H19 gene. Nat Genet *9*, 407-13.

Tsutsumi, M., Tsai, Y. C., Gonzalgo, M. L., Nichols, P. W., and Jones, P. A. (1998). Early acquisition of homozygous deletions of p16/p19 during squamous cell carcinogenesis and genetic mosaicism in bladder cancer. Oncogene *17*, 3021-7.

van der Burgh, A., Dees, J., Hop, W. C., and van Blankenstein, M. (1996). Oesophageal cancer is an uncommon cause of death in patients with Barrett's oesophagus [see comments]. Gut *39*, 5-8.

Vertino, P. M., Yen, R. W., Gao, J., and Baylin, S. B. (1996). De novo methylation of CpG island sequences in human fibroblasts overexpressing DNA (cytosine-5-)-methyltransferase. Mol Cell Biol *16*, 4555-65.

Walsh, C. P., Chaillet, J. R., and Bestor, T. H. (1998). Transcription of IAP endogenous retroviruses is constrained by cytosine methylation [letter]. Nat Genet *20*, 116-7.

Wang, J. Y., Knudsen, E. S., and Welch, P. J. (1994). The retinoblastoma tumor suppressor protein. Adv Cancer Res *64*, 25-85.

Washimi, O., Nagatake, M., Osada, H., Ueda, R., Koshikawa, T., Seki, T., and Takahashi, T. (1995). In vivo occurrence of p16 (MTS1) and p15 (MTS2) alterations preferentially in non-small cell lung cancers. Cancer Res *55*, 514-7.

Watt, F., and Molloy, P. L. (1988). Cytosine methylation prevents binding to DNA of a HeLa cell transcription factor required for optimal expression of the adenovirus major late promoter. Genes Dev *2*, 1136-43.

Watts, G. S., Pieper, R. O., Costello, J. F., Peng, Y. M., Dalton, W. S., and Futscher, B. W. (1997). Methylation of discrete regions of the O6-methylguanine DNA methyltransferase (MGMT) CpG island is associated with heterochromatinization of the MGMT transcription start site and silencing of the gene. Mol Cell Biol *17*, 5612-9.

Wazer, D. E., Liu, X. L., Chu, Q., Gao, Q., and Band, V. (1995). Immortalization of distinct human mammary epithelial cell types by human papilloma virus 16 E6 or E7. Proc Natl Acad Sci U S A *92*, 3687-91.

Weber, J. D., Taylor, L. J., Roussel, M. F., Sherr, C. J., and Bar-Sagi, D. (1999). Nucleolar Arf sequesters Mdm2 and activates p53. Nat Cell Biol *1*, 20-6.

Weintraub, S. J., Chow, K. N., Luo, R. X., Zhang, S. H., He, S., and Dean, D. C. (1995). Mechanism of active transcriptional repression by the retinoblastoma protein. Nature *375*, 812-5.

Werness, B. A., Levine, A. J., and Howley, P. M. (1990). Association of human papillomavirus types 16 and 18 E6 proteins with p53. Science *248*, 76-9.

Wiest, J. S., Franklin, W. A., Otstot, J. T., Forbey, K., Varella-Garcia, M., Rao, K., Drabkin, H., Gemmill, R., Ahrent, S., Sidransky, D., Saccomanno, G., Fountain, J. W., and Anderson, M. W. (1997). Identification of a novel region of homozygous deletion on chromosome 9p in squamous cell carcinoma of the lung: the location of a putative tumor suppressor gene. Cancer Res *57*, 1-6.

Wigler, M., Levy, D., and Perucho, M. (1981). The somatic replication of DNA methylation. Cell *24*, 33-40.

Winters, C., Jr., Spurling, T. J., Chobanian, S. J., Curtis, D. J., Esposito, R. L., Hacker, J. F. d., Johnson, D. A., Cruess, D. F., Cotelingam, J. D., Gurney, M. S., and et al. (1987). Barrett's esophagus. A prevalent, occult complication of gastroesophageal reflux disease. Gastroenterology *92*, 118-24.

Wong, D. J., Barrett, M. T., Stoger, R., Emond, M. J., and Reid, B. J. (1997). p16INK4a promoter is hypermethylated at a high frequency in esophageal adenocarcinomas. Cancer Res *57*, 2619-22.

Wong, D. J., Foster, S. A., Galloway, D. A., and Reid, B. J. (1999). Progressive region-specific de novo methylation of the p16 CpG island in primary human mammary epithelial cell strains during escape from M(0) growth arrest. Mol Cell Biol *19*, 5642-51.

Wu, T. T., Watanabe, T., Heitmiller, R., Zahurak, M., Forastiere, A. A., and Hamilton, S. R. (1998). Genetic alterations in Barrett esophagus and adenocarcinomas of the esophagus and esophagogastric junction region. Am J Pathol *153*, 287-94.

Xiong, Y., Zhang, H., and Beach, D. (1993). Subunit rearrangement of the cyclin-dependent kinases is associated with cellular transformation. Genes Dev *7*, 1572-83.

Xu, L., Sgroi, D., Sterner, C. J., Beauchamp, R. L., Pinney, D. M., Keel, S., Ueki, K., Rutter, J. L., Buckler, A. J., Louis, D. N., and et al. (1994). Mutational analysis of CDKN2 (MTS1/p16ink4) in human breast carcinomas. Cancer Res *54*, 5262-4.

Yoder, J. A., Soman, N. S., Verdine, G. L., and Bestor, T. H. (1997). DNA (cytosine-5)-methyltransferases in mouse cells and tissues. Studies with a mechanism-based probe. J Mol Biol *270*, 385-95.

Yoder, J. A., Walsh, C. P., and Bestor, T. H. (1997). Cytosine methylation and the ecology of intragenomic parasites [see comments]. Trends Genet *13*, 335-40.

Zerfass-Thome, K., Zwerschke, W., Mannhardt, B., Tindle, R., Botz, J. W., and Jansen-Durr, P. (1996). Inactivation of the cdk inhibitor p27KIP1 by the human papillomavirus type 16 E7 oncoprotein. Oncogene *13*, 2323-30.

Zhang, H. S., Gavin, M., Dahiya, A., Postigo, A. A., Ma, D., Luo, R. X., Harbour, J. W., and Dean, D. C. (2000). Exit from G1 and S phase of the cell cycle is regulated by repressor complexes containing HDAC-Rb-hSWI/SNF and Rb-hSWI/SNF. Cell *101*, 79-89.

Zhang, H. S., Postigo, A. A., and Dean, D. C. (1999). Active transcriptional repression by the Rb-E2F complex mediates G1 arrest triggered by p16INK4a, TGFbeta, and contact inhibition. Cell *97*, 53-61.

Zhang, L., Cui, X., Schmitt, K., Hubert, R., Navidi, W., and Arnheim, N. (1992). Whole genome amplification from a single cell: implications for genetic analysis. Proc Natl Acad Sci U S A *89*, 5847-51.

Zhang, Y., Xiong, Y., and Yarbrough, W. G. (1998). ARF promotes MDM2 degradation and stabilizes p53: ARF-INK4a locus deletion impairs both the Rb and p53 tumor suppression pathways. Cell *92*, 725-34.

APPENDIX: DNA METHYLATION ANALYSIS FLOW CHART

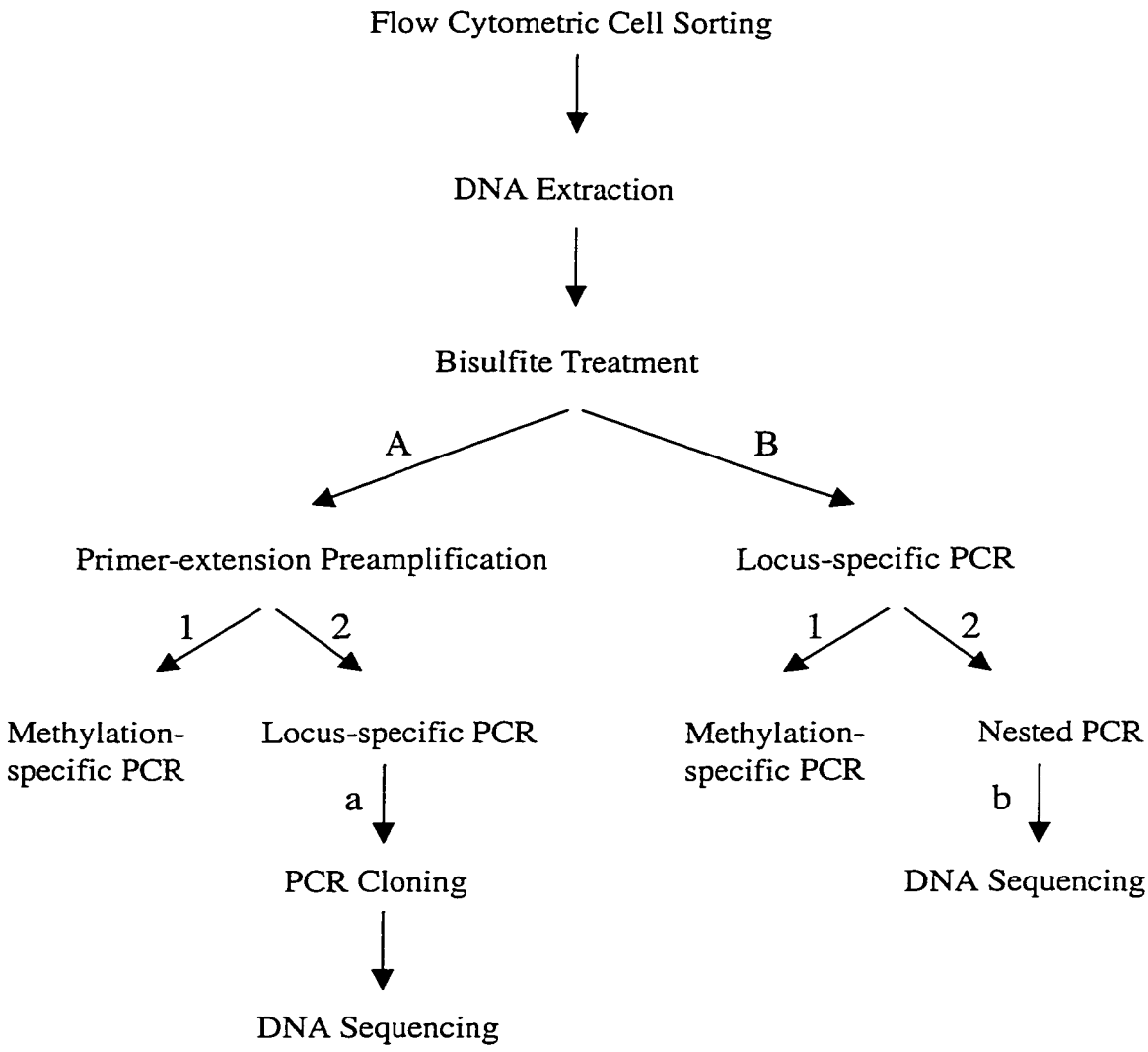

A: for analysis of multiple loci
B: for analysis of a single locus

1: for rapid methylation screening
2: for analyzing methylation at individual cytosines

a: for analyzing methylation on individual DNA strands
b: for analyzing methylation of cell population

VITA

David J. S. Wong

December 30, 1971	Born, Honolulu, HI
1994	B.S. Biochemistry, Brown University, Providence, RI
2000	Ph.D., University of Washington, Seattle, WA

PUBLICATIONS

Journal Articles

Wong, D. J., Foster, S. A., Galloway, D. A., and Reid, B. J. (1999). Progressive region-specific de novo methylation of the p16 CpG island in primary human mammary epithelial cell strains during escape from M(0) growth arrest. Mol Cell Biol 19: 5642-51.

Barrett, M. T., Sanchez, C. A., Prevo, L. J., Wong, D. J., Galipeau, P. C., Paulson, T. G., Rabinovitch, P. S., and Reid, B. J. (1999). Evolution of neoplastic cell lineages in Barrett oesophagus. Nat Genet *22*: 106-9.

Funk, J. O., Schiller, P. I., Barrett, M. T., Wong, D. J., Kind, P., and Sander, C. A. (1998). p16INK4a expression is frequently decreased and associated with 9p21 loss of heterozygosity in sporadic melanoma. J Cutan Pathol *25*, 291-6.

Foster, S. A., Wong, D. J., Barrett, M. T., and Galloway, D. A. (1998). Inactivation of p16 in human mammary epithelial cells by CpG island methylation. Mol Cell Biol *18*, 1793-801.

Trask, B. J., Friedman, C., Martin-Gallardo, A., Rowen, L., Akinbami, C., Blankenship, J., Collins, C., Giorgi, D., Iadonato, S., Johnson, F., Kuo, W.-L., Massa, H., Morrish, T., Naylor, S., Nguyen, O. T. H., Rouquier, S., Smith, T., Wong, D. J., Youngblom, J., and van den Engh, G. (1998) Members of the olfactory receptor gene family are contained in large blocks of DNA duplicated polymorphically near the ends of human chromosomes. Hum Mol Genet *7*, 13-26.

Wong, D. J., Barrett, M. T., Stoger, R., Emond, M J., and Reid, B. J. (1997). p16INK4a promoter is hypermethylated at a high frequency in esophageal adenocarcinomas. Cancer Res *57*, 2619-22.

Ang, S. L., Wierda, A., Wong, D., Stevens, K. A., Cascio, S., Rossant, J., and Zaret, K. S. (1993). The formation and maintenance of the definitive endoderm lineage in the mouse: involvement of HNF-3/forkhead proteins. Development *119*, 1301-15.

Book Chapters

Barrett, M.T., Sanchez, C.A., Prevo, L.J., Galipeau, P.C., Wong, D.J., and Reid, B.J. (1999). Early events during neoplastic progression in Barrett's esophagus. In: Molecular Pathology of Early Cancer. IOS Press, Van Diemenstratt, Amsterdam, Netherlands.